Addis Ababa University
አዲስ አበባ ዩኒቨርሲቲ
Seek Wisdom, Elevate your Intellect and Serve Humanity

COLLEGE OF NATURAL AND COMPUTATIONAL SCIENCES

SCHOOL OF EARTH-SCIENCES

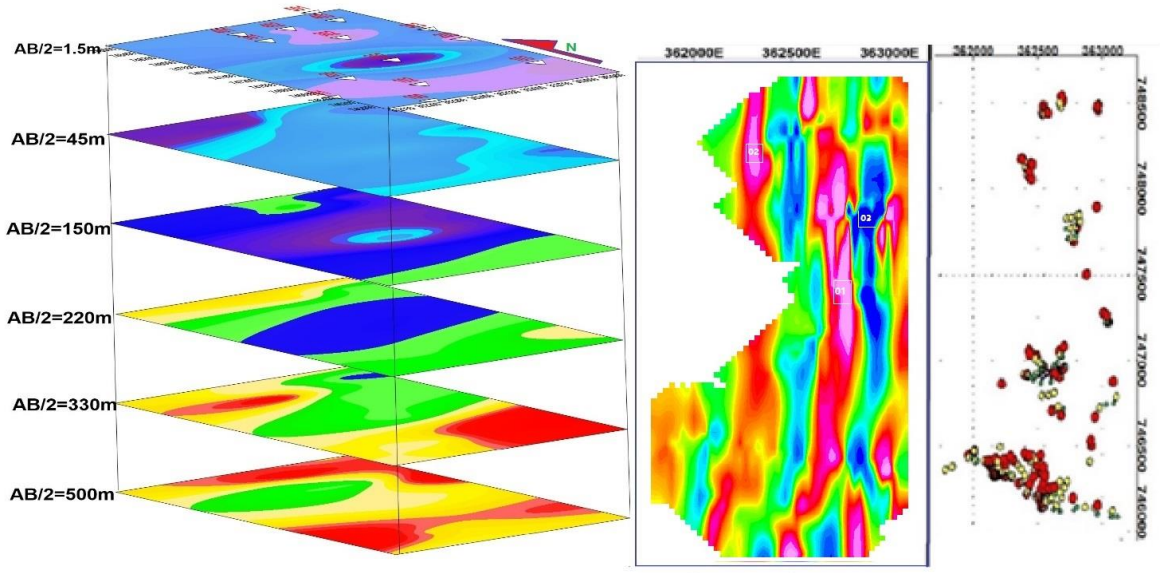

Application of Integrated Geophysical Techniques to Map Groundwater Potential Zones and Geological Structures for Irrigation purpose at 'Humbo-Larena' Plain, Wolaita Zone-Ethiopia.

A Thesis Submitted to the School of Earth Sciences of Addis Ababa University in Partial Fulfillment of the Requirements for the Degree of Master of Science in Exploration Geophysics

By

Ayalew Lemma.

Addis Ababa

May 2021

ADDIS ABABA UNIVERSITY

SCHOOL OF GRADUATE STUDIES

This is to certify that the thesis prepared by **Ayalew Lemma**, entitled **"Application of Integrated Geophysical Techniques to Map Groundwater Potential Zones and Geological Structures for Irrigation purpose at 'Humbo-Larena' Plain, Wolaita Zone-Ethiopia.",** submitted in partial fulfillment of the requirements for the degree of Master of Science in Applied Geophysics complies with the regulations of the University and meets the accepted standards concerning originality and quality.

Approved by board of examiners:

	Signature	Date
Dr. Balemwal Atnafu	_____	_____
(Head, School of Earth Sciences)		
Prof. Tigistu Haile	_____	_____
(Advisor)		
Dr. Abera Alemu	_____	_____
(Internal examiner)		
Dr. Tilahun Azagegn	_____	_____
(External examiner)		

DECLARATION

I, the undersigned, hereby declare that the thesis entitled **"Application of Integrated Geophysical Techniques to Map Groundwater Potential Zones and Geological Structures for Irrigation purpose at 'Humbo-Larena' Plain, Wolaita Zone-Ethiopia.",** is my original work carried out under the supervision of Professor Tigistu Haile. The thesis has not been presented to any university or institution for the award of any degree or diploma and all sources of materials used for the thesis are duly acknowledged.

Name of the Candidate	Signature	Date
Ayalew Lemma	_____	_____

This is to certify that the above declaration made by the candidate is correct to the best of our knowledge and it has been submitted for examination with our approval as university advisor.

Name (Advisor)	Signature	Date
Prof. Tigistu Haile	_____	_____

Abstract

Combined geophysical techniques, i.e. electrical resistivity and magnetic methods, were carried out on an area of volcanic and volcano-sedimentary rocks in “Larena-Plain” at the western margin of the Southern Main Ethiopian Rift (SMER), as part of groundwater resource investigation to be used for irrigation purposes. The depth and extent of the potential groundwater aquifer were examined and mapped using the electrical resistivity (VES) technique, and the geological structures and lithological contacts responsible for groundwater flow and accumulation were revealed and mapped by using the magnetic method. Fourteen VES points were carried out over five profile lines and more than 240 magnetic data point readings distributed along the VES lines and at random points were collected and processed using different software. Additionally, apriori information/data from nearby boreholes were combined with the geophysical results for constraining the interpretation of the results.

According to the investigation outputs, there are two-stage aquifers in the study area: a deeper fractured ignimbrite and volcanoclastic-sediment aquifer covered by the shallow weathered ignimbrite aquifer. The depth to these aquifers and their distribution over the area are mapped. From thew combined results, the geological structures in the area mapped with the survey are generally aligned in NNE-SSW orientation. In addition to locating preferential areas of borehole sinking for groundwater exploitation, the study provides useful information that can be used to develop a much broader understanding of the nature of groundwater resource in the area and their relationship with the local geology.

Keywords: Electrical resistivity, Magnetic survey, Groundwater potential, aquifers, irrigation

Acknowledgment

Any attempt at any level would not be satisfactorily completed without the support and help of many people.

Foremost, I would like to express my sincere gratitude to my advisor Professor Tigistu Haile for the continuous support of my MSc. study and research, for his patience, motivation, enthusiasm and immense knowledge. His guidance helped me all along from the fieldwork to the completion of the research.

Besides my advisor, I would like to thank my instructors Dr. Abera Alemu and Professor Tilahun Mammo for their support, encouragement, insightful comments and provision of reliable knowledge and information during my study and writing of this thesis.

I would like to thank Wolaita Sodo University for permission to work on the project site and Wolaita Zone water, mines and energy department that supported by providing the water well data and other relevant information of the study area.

I am extremely grateful to my parents for their love, prayers, caring and sacrifices for educating and preparing me for my future. My Special thanks go to Dr. Abrham Asha for his constant encouragement and genuine support throughout this research work. Finally, my thanks go to my friends and classmates for the keen interest shown to complete this thesis successfully.

Table of Contents

LIST OF FIGURES

LIST OF TABLES

Acronyms

AFMAG----------Audio-Frequency Magnetic

AS----------Analytic Signal

CSA----------Central Statistical Agency

CST----------Constant Separation Traversing

EMA---------- Ethiopian Mapping Agency

EM----------Electromagnetic

Hp----------High Pass Filter

IGRF---------- International Geomagnetic Reference Field

IP----------Induced Polarization

ITCZ---------- Inter-Tropical Convergence Zone

LP---------- Low Pass Filter

m.s.l----------Mean Sea Level

MER----------Main Ethiopian Rift.

RTP----------Reduced to Pole

SP----------Self-Potential

TDR----------Tilt Derivative

TDEM----------Time Domain Electromagnetic Methods

TMA----------Total Magnetic Anomaly

UC----------Upward Continuation

VES---------- Vertical Electrical Sounding

W.H.O---------World Health Organization

CHAPTER ONE

1. INTRODUCTION

1.1 Background

Water is the most important substance for the existence of life, though it is recognized to be ordinary. "Water is life" is such a common expression that we use it almost as a cliché. However, this phrase is probably one of the most powerfully true messages the whole creation bears witness to.

Any developmental activity relies on the available water sources, whether it is surface or groundwater, also giving more concern to its quality and quantity. In areas where there is no sufficient surface water for the entire developmental activities, the search for water takes a new approach to the next alternative- the groundwater. Groundwater plays a vital role in the development of arid and semiarid zones, sometimes supporting vast agricultural and industrial enterprises that could not otherwise exist (Haile Arefayne and Semir Abdi, 2016).

Access to clean water is a human right and a basic requirement for economic development. The safest kind of water supply is the use of groundwater. Since groundwater originates from surface water that has been purified while it percolates down through geologic formation, it normally has natural protection against pollution by the covering layers and hence only minor water treatment is required. However, detailed knowledge about the extent, hydraulic properties, and vulnerability of groundwater reservoirs is necessary to enable sustainable use of the resources (Kirsch, 2006).

Nowadays, both developing and developed countries utilize groundwater for their economic activities in urban as well as in rural areas. So, the demands for groundwater have been increased due to population growth, severe limitations on the availability and/or accessibility of surface water and continuous degradation of surface water in terms of its quality. Therefore, the demand for groundwater will increase in the coming times too (Taylor and Francis, 2008). However, it is important to take into consideration the difficulty of groundwater exploration/assessment in hard rock terrain in which groundwater potential is dependent and is related to the thickness of fractured and fissured zones of such rocks. Like in many countries, groundwater plays an important role in Ethiopia as a major source of water for domestic, industries, agriculture and livestock use.

Based on World-Meter (2020) elaboration of the latest United Nations and world-Bank World Population Prospect data (2020), the current population of Ethiopia is more than 110 million. The report of the Central Statistical Agency (CSA) of Ethiopia (CSA, 2012) indicated a population of over 87 million; growing at a rate of over 2.9% per annum. Similarly, the population of Wolaita zone- the project area of this thesis work- was over 5.4 million as CSA report in July 2012. Agriculture is the livelihood for more than 90% of the population in rural areas in Ethiopia and this is expected to be true for the area of the current study.

According to the International Monetary Fund (IMF) World Economic Outlook Database (2020) report, Ethiopia is one of the seven fastest-growing countries in the world for the last decade, while it is also being reported that in Human Development-Index Report (HDR, 2019) Ethiopia is at a lower level. Thus, it is wise to analyze areas where Ethiopia is performing well or badly. This enables the country to target and prioritize areas that need immediate intervention. For the assessment of food insecurity, for example, the World Food Program (WFP) indicated identifying the target groups, their number, their location and the reason for food insecurity to enable the stakeholders to design appropriate interventions (WFP, 2014, 2019). To overcome food insecurity problem, the government of Ethiopia in collaboration with international donors have been formulating and implementing different strategies such as increasing the level and stability of production, increasing food reserve and distributing of subsidizing basic food items, increasing job creation opportunity, increasing private sector investment, improving the wage for a government employee, improving income, improving productivity and other market and non-market transfer and strengthening disaster prevention and preparedness capabilities through adequate early warning systems to attain food self-sufficiency and reduce food aid dependency. But still, food insecurity remains the main problem in the country and the need for food aid is increasing (Bogale et al., 2014; WFP, 2014, 2019; HDR, 2019). According to the United Nations (UN) Sustainable Development Cooperation Framework (2020-2025) signed between the Government of Ethiopia and the United Nations in Ethiopia, and also the UN-2030 Sustainable Development Goals (SDG) agenda, high attention should be given to food and agriculture to meet the goal of 2030 SDG agenda (UN, 2020).

Similar to other food-insecure areas of the country, Wolaita zone in general and Humbo-Larena and the surrounding rural kebeles in particular, is well known for its increase in the rural population, particularly in the last 30 years. This has resulted in population pressure

(Adugna Enyew and Wagayehu Bekele, 2011). Irrigation development, particularly the small holders have significant importance to raise production and productivity to achieve food self-sufficiency and ensure food security at the household level (MoANRM,2011; Svizzero, 2016).

Since modern agricultural practices are among the main activities planned by the Zonal government of Wolaita for food security and sustainable development, the Humbo-Larena and the surrounding rural kebeles are also some of those places that have been given better attention. Wolaita Sodo University is also projecting a community service to overcome the food insecurity problem in different parts in collaboration with different stakeholders, governmental and non-governmental organizations. So, the Humbo-Larena and the surrounding rural kebeles will be identified as major developmental corridors of the Zone and it will be the future hope for the rest of the region as well.

As a result, water supply is the key issue for the achievement of the goal set by the government as well as the University. In the study area specifically, and Wolaita zone in general, low agricultural productivity resulted due to natural and human-induced factors; especially climate change and technological factors (Samuel Tessema et al., 2017; Bagnara, 2017; Almaz Balta et al., 2015).

The surface water resource potential of the country in general remains the main source of irrigation water supply for small-scale irrigation development. But, in areas where surface water resource is limited and rainfall is inadequate to ensure crop production of high-value crops, the development of groundwater resource is considered as potential sources for supplementary means of irrigation (MoANRM, 2011). Although there are some deep wells drilled in the area for domestic purposes, there is no means of using the groundwater for irrigation purposes other than the ones available in small water harvesting ponds.

Therefore, the target of this research work will be to use groundwater for irrigation purposes through having the objective to identify potential well sites and to know the overall groundwater conditions of the study area using integrated surface geophysical survey methods. More specifically, the study will aim at understand the nature, number and type of aquifers within the study area to identify the potential well sites that could balance the water demand and supply for irrigation. This endeavour is believed to boost agricultural production and income of the farming population and it will benefit first of all the ‘Humbo-Larena’

community and can be an optimistic project for the other related environments and thereby help the local population attain improved food security.

1.2 Description of the Study Area

1.2.1 Location and Accessibility

The study area- Larena Plain- is located in Wolaita Zone; Southern Ethiopia at the western margin of the Southern Main Ethiopian Rift (SMER). The administrative center of the Wolaita Zone is Sodo town, which lies geographically at 37°45'54.29"E 6°51'26.21"N and at elevation ranging from 1850m to 2250m above mean sea level (amsl). Wolaita is administratively bordered on the south by Gamo and Gofa zones, on the west by the Omo River which limits it from Dawro zone, on the northwest by Kambata-Tambaro, on the north by Hadiya zone, on the northeast by the Oromia Region, on the east by the Bilate River which limits it from Sidama Region and on the southeast by the Lake Abaya which limits it from Oromia Region (Figure 1.1).

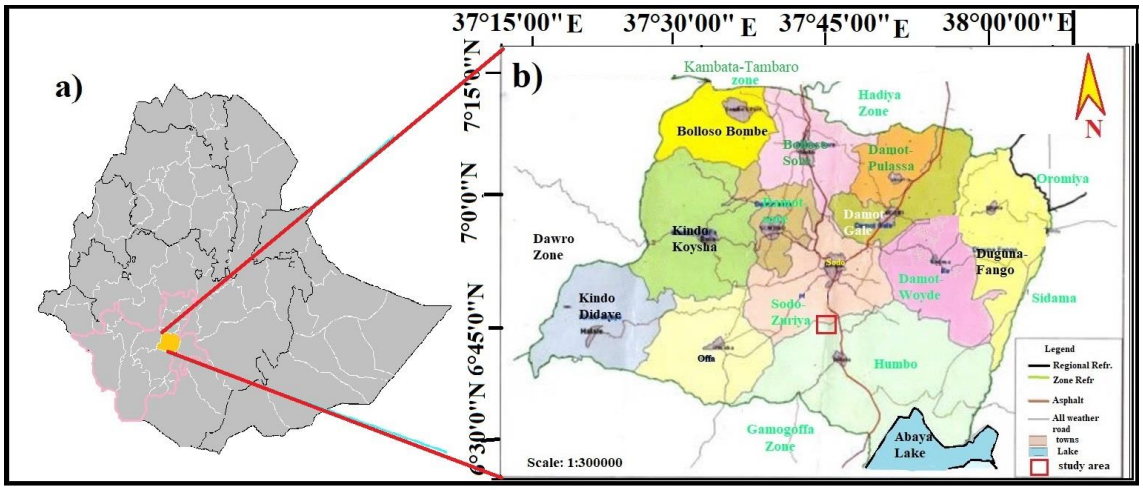

Figure 1.1: a) Regions of Ethiopia b) Administrative map of wolaita zone and Location of study Area modified from different sources.

The study area "Larena plain" is found partly in Sodo Zuriya and partly in Humbo Woredas, which are part of the sixteen Woredas in Wolaita Zone. Geographically, the area lies at a latitude and longitude of 6°45'13.22"N and 37°45'17.12"E respectively, and an elevation about 1780m amsl. It is found at a distance of 390 km (to the south) from Addis Ababa via the Addis Ababa-Shashemene-Wolaita Sodo root, or 336km (to the south) from Addis Ababa via the Addis Ababa-Hosana-Wolaita Sodo route. It is 10 km to the South of Sodo town

which is the seat of Wolaita Zone administration. It is accessible by an asphalt concrete road and a short detour following an all-weather dry road.

1.2.2 Physiography, Climate and Drainage

Physiography: Wolaita area is topographically composed of low lands of Humbo, Fango-Gelchecha area, and parts of Boloso-Bombe and Boloso-Sore to the highland of Damot-mountain. Generally, a rugged, undulating mountain, hills, plateaus, plains, gorges that extend up and down to low land of Humbo - Fango -Gelchecha area and the different parts of the zone are dominated by flatlands, plains and midlands.

Climate and rainfall: The climatic zones are traditionally subdivided into five elevation classes. The elevation less than 800m is categorized as Desert climatic zone (Bereha, in Amharic), from 800m up to 1500m is categorized as Tropical (Kola), from 1500 up to 2300m is categorized as Subtropical (Weynadega), from 2300m up to 3300m is categorized as Temperate (Dega), and areas with elevation greater than 3300 m are categorized as Alpine (Kur) (Daniel, 1977). The elevation of the study area ranges from about 1730m up to 1880m. Accordingly, the climate zone of the study area is classified into subtropical (1500-2300m). According to the prevailing weather conditions, this zone receives maximum rainfall from July to September and it ranges from 801-1600 mm while the average temperature varies from a minimum of 15.1 ^{0} c to maximum of 31 ^{0} c. Wolaita zone is categorized under rift valley and, in terms of agroecology, the area is 14% highland (Dega), 56% is midland (Weinadega), and 30% lowland (Kola). The altitude ranges from lowest at the foot of Omo river at 501m above m.s.l. to highest 2950m above m.s.l at the peak of Damota mountain. Climate plays a great role in influencing moisture contents of sub-grade and sub-base soil parameters such as rainfall, temperature, relative humidity, evapotranspiration, and wind speed, which are very important to evaluate the sub-base soil are soaked by infiltration water or increased groundwater table.

The rainfall pattern in wolaita area is bimodal, that is because Ethiopia is situated under the influence of the Inter-Tropical Convergence Zone (ITCZ). When the ITCZ just moves from South to North the small rains prevail "Belg" (March-April). When the ITCZ zone is beyond the Northern boundary heavy rain ("Kiremt"-Rainy summer) prevails. The rainfall levels on average of 1300mm/year and frequently reaching values as high as 1800-2000mm/year, around the mountainous areas like Damot. Based on the altitude and temperature, Ethiopia Mapping Agency (EMA) classified five climatic zones. Table 2.1 shows the classification of

climate zone based on Altitude and Temperature presented by the Ethiopian Mapping Agency (1981) in the National Atlas of Ethiopia.

Table 2.1 Classification of the climatic zone (from National Atlas of Ethiopia, 1981),

No	Altitude (a.m.s.l.)	Temperature (°C)	Climate Zone
1	Below 500	30-40	Desert (Bereha)
2	500-1500	About 30	Tropical (Kolla)
3	1500-2300	15-20	Sub-Tropical (WeinaDega)
4	2300 -3300	10-15	Temperate (Dega)
5	3300 & above	10 or less	Alpine (Kur)

Based on the classification in Table 2.1, Wolaita has three climatic zones such as Tropical/Kolla (Humbo, Bele, Bedesa, Bombe areas, etc), Sub Tropical /WeinaDega (the plateau areas of the Zone), and Temperate/Dega (Mount Damot and other mountainous areas).

Drainage: Wolaita zone mainly comprises two basin systems- the Omo and Bilate basins. The Omo drainage system is controlled by geological structures. In the zone, most of the streams and/or rivers originate from Mount Damot and some streams flow towards the Rift valley basin (Bilate basin) and then to Lake Abaya, and some others flow towards the Omo River Basin and then to the Omo man-made Lake. On the other hand, the Bilate River basin flows from the Gurage Mountains in the north towards the south into Lake Abaya. There are a number of perennial rivers such as Bilate, Hamasa and Bisare Gelana that flow into Lake Abaya as well. Generally, many small streams drain towards Lake Abaya along with Bilate river whose tributaries drain large volume of water from the highlands of the catchment. The increase downstream of the river water could be influenced by the corresponding low rainfall, high evapotranspiration, relatively slow drainage, and thermal springs that join the river downstream. The drainage density is high in the plateau and escarpment areas and very low on the rift floor.

1.2.3 Land Use and Land Cover

A large area of the land of Wolaita is intensively cultivated. These areas are used to grow cereal crops such as teff, false banana (Enset) and cash crops such as coffee, ginger and others. The growth of vegetation, whether natural or cultivated, depends on the availability of favorable soil conditions and sufficient soil moisture.

Generally, the vegetation cover is decreasing from time to time and now it is in a very dangerous condition. The main causes for the destruction of forests in the study area are: cleaning for farmlands (largely), cutting and using woods for furniture and fuel at the household level (less) and overgrazing (least). This is due to having a high population density in the Zone that has been increasing from time to time. Hence due to the lack of farmland, nature competition is increasing.

1.3 Statement of the Problem

The largest amount of water on Earth (97.2 %) is contained in the oceans and seas as saline or salty water, but only a small amount (2.8%) exists as freshwater on land. This freshwater found on land is distributed as ice caps and glaciers (76.43 %) which is inaccessible, groundwater and soil moisture (21.96 %), freshwater lakes (0.32%) and a very small portion of it as streams in channels (0.004%). The amount of freshwater that is available for domestic, industrial and agricultural purposes is very limited as compared to the total volume of water on planet Earth (Fetter, 2001).

However, it is found that the availability and accessibility of quality water (freshwater) resources has always been the primary concern of societies all over the world. The problem of obtaining an adequate supply of water is generally becoming more acute due to the ever-increasing population, climate change and industrialization. More specifically, Ethiopia is being substantially affected by climate change, whose impact is to be seen in marked seasonal variations of climatic, hydrometric parameters and the El-Nino effect which results in drought for millions of people (MoANRM, 2011).

The study area is situated in Southern Ethiopia and the fast-growing population incorporated with climate change in the area demanded the assessment of the groundwater potential for different purposes. When one considers the study area (the 'Humbo-Larena plain') groundwater resource, the geological situation and the structural setting of the area being at the western edge of the Main Ethiopian Rift (MER) coupled with the low lying and flat nature of the area favor the accumulation of a considerable groundwater resource within it. Moreover, because the study area is located in the lowest plain of south Damota watersheds (the highest point ground over the area and probably Wolaita zone), the flow of groundwater is towards it due to the watershed of the rest of the environment. Over this potential groundwater rich area, so far, the extraction and development of this resource have been done for domestic activities. Further, agriculture is the livelihood of rural communities in the study area. Failure to obtain an adequate supply of water has rendered that almost all of the

agricultural activities be done only in the rainy season within limited land which is not balanced with the fast-growing population. Consequently, the productive age group of the population is migrating to the cities and towns. From the pilot social assessment conducted over the general area of Wolaita zone (Bagnara, 2017), it is understood that the community needs to work on their land on multi harvesting scheme per year if there would be enough water and mechanized technology for agricultural activities. Furthermore, due to population growth, the need for water for domestic and agricultural activities has increased, so that for the sake of food security and also to increase productivity in the area Wolaita-Sodo University is doing research-based community service in different parts. Consequently, the rural kebeles surrounding the study area are those areas that need immediate intervention to enhance the agricultural sector performance. As a result, it is very essential to use groundwater, because of the inaccessibility of surface water around the area and also the quality problem that normally arise with it due to its location in relation to the many acidic centers of the Ethiopian Rift that are normally influence the groundwater quality over the general area.

Therefore, the principal objective of the study will focus on the assessment of the groundwater potential of the study area, determine the location of preferred borehole sites and the depth at which the aquifers are located by using electrical resistivity and magnetic methods of prospecting. This will be utilized for the welfare of society.

1.4 Research Motivation

The cost of drilling for water supply boreholes almost demands that the risk of drilling a poorly yielding borehole should be lessened through the proper use of geophysics. Geophysics can be used to screen potential drilling locations and remarkably decrease the risk of drilling in unproductive areas. In this respect, geophysics is cost-effective and its proper application always increases the success of drilling.

In any groundwater project, drilling for groundwater is simply costly so that it affects the benefit of the project found from the result. In addition, there is the question to what depth should a borehole be sunk to get the potential zone of groundwater. Such a project which has the probability of failure and incurs a huge cost needs proper investigation for the accurate identification of potential groundwater zones and their depth to reduce the expected risks and cost of the project. Using the appropriate geophysical methods of prospecting does greatly reduces the risks involved. Furthermore, in areas that depend heavily on groundwater (like in

the area under study), groundwater models are often used to simulate subsurface flow for a more quantitative hydrogeological analysis of the effect of proposed water supply boreholes and planning purposes. These groundwater models are usually limited in accuracy by the hydrogeological data available. Geophysics can provide additional data to improve the accuracy of groundwater models for hydrogeologists (Tenalem Ayenew et al., 2008). What makes geophysical techniques even more attractive is that the techniques have proved to be efficient tools in groundwater exploration and the steep technological growth of the last 15 years in geophysics, due mainly to advances in microprocessors and associated numerical modeling solutions, have greatly affected this field of geophysics. Not only has geophysics been used in the direct detection of the presence of water but also in the estimation of aquifer size and properties, groundwater quality and movement, mapping saline water intrusions and buried valleys even in areas of complex geology (Kirsch, 2006).

In the Ethiopian context and especially in the study area, the prevailing complex nature of the geology and the groundwater system makes a detailed and systematic geophysical study, the appropriate alternative, as conventional hydrological approach so far has proved its inability to exhaustively deal with the problem alone (Bagnara, 2017). In this research, therefore, ground-based geophysical methods including existing borehole data were used to study the potential zone of groundwater and to identify linear geologic features of the study area. The actual work involved dedicated geophysical fieldwork to collect VES and magnetic data with a view to outlining the subsurface electrical properties and magnetic anomaly of the area.

1.5 Objectives of the study

1.5.1 General objective

The main objective of the study is the assessment of the groundwater potential and determine the location of preferred borehole sites and the depth at which the aquifers are located over the Humbo Larena area, Wolaita Zone of South Ethiopia.

1.5.2 Specific Objectives

- To identify the major subsurface geological units and structures in the area by integrating magnetic and electrical resistivity and map possible water-saturated horizons and structures that control movement of groundwater.
- To infer areas of maximum groundwater reservoir potential and propose site/s to drill a borehole /boreholes/ with sufficient and sustainable yield of groundwater.

- To determine the depth of the groundwater table and to locate potential drilling sites for the extraction of groundwater.

1.6 Material and Methodology:

1.6.1 Materials

To achieve the objectives of this research work, the following materials were used.

I. Geophysical Equipment:

- Earth Resistivity Meter (PASI-16 GL), P100-3 Energizer and associated accessories
- Earth Magnetometer (EM2), proton magnetometer working in total field mode.

II. Digital materials:

Software components: WINRESIST, Ipi2win, SURFER-13, AutoCAD-2007, GEOSOFT (Oasis-Montaj_V-7.0.1), ArcGIS 10.7 were used to process and enhance both VES and magnetic data. Both field data were initially inserted into the computer using an Excel spreadsheet and this program was used at the initial data correction and processing stage.

III. Auxiliary materials:

Topographic map of scale 1:50,000, geological map of the study area and field equipment: such as GPS, communication radios, digital camera and writing pads for field note, were used.

1.6.2 Methodology

To achieve the objectives of this research; the methods are classified as pre-field work, during-field work and post-fieldwork tasks. These included reviewing different previous works and literature on geophysical works (related to groundwater exploration and identification of geological structures), and also geological and hydro-geological literature on the study area that the researcher could put hands on. Two geophysical methods were employed, i.e. VES and Magnetic Methods of prospecting. Data from both methods were collected over selected profiles well distributed over all the study areas as well as over random points (for the magnetic data) designed to cover the study area as much as possible. Both VES and magnetic data were analyzed using the appropriate software listed in section 1.6.1.

Pre-fieldwork

Existing data and materials were collected from different sources and were used in the surveying and analysis parts of the research work. These are:

- Hydrogeological maps and logs, which are very crucial for geophysical interpretation
- Borehole data (location coordinates, depth, year drilled, pumping test data, etc.)

During-field work

During fieldwork, different activities (geophysical investigations) were undertaken to achieve the objectives;

- Making traverses in the different direction of the study area to identify the subsurface stratification and geological structures to better define the possible aquifer system and estimate the aquifer parameters, such as porosity and permeability, which are key issues that determine the occurrence and the depth of the groundwater table.
- Assessing the water sources, i.e the existing boreholes available in and around the area.
- Acquiring Vertical Electrical Sounding (VES) data by taking measurements with the Earth Resistivity Meter at different selected locations /sounding points/ of the study area. The VES procedure primarily assumes that the subsurface has horizontal stratigraphy. The potential electrodes remain constant at some stations; the measurements are taken with gradually increasing distances of the current electrodes. When the distance between current probes is increased, also increased depth at which the current penetrates below the surface of the ground, i.e. increasing the depth of investigation. Hence, the vertical electrical drilling- as the VES technique is commonly called- can identify the resistivity of different horizontal strata below the investigation points.
- Acquiring total field magnetic data by using the MP-2 proton magnetometer
- Taking additional relevant information, such as GPS data for the sounding point and magnetic data location, photos and notes, say the proximity of the magnetic measurement to magnetic noises like power lines, houses, etc.

Data Analysis and Reporting (post-fieldwork)

The collected primary data from the field and secondary data acquired from different sources were integrated to get reliable and more accurate subsurface information. The activities performed at this stage are as follows:

- Processing and analyzing the primary geophysical raw data by using ArcGIS/global mapper to plot location map of the study area and to show VES data points, magnetic data, and previously drilled borehole location. Follow this with the use of WINRESIST, Ip2win to analyze the VES data. In addition to these, Oasis Montaj (V-7.0.1), SURFER-13, Paint, and Microsoft Excel were used to facilitate the interpretation of magnetic data.

- Determining the vertical resistivity distributions below the center of the array– the sounding point. The data are usually plotted as depth against resistivity so that the resistivities of different depths were analyzed and interpreted.
- Interpreting each resistivity stratification through comparison with different geological and hydrogeological logs.
- Converting of the processed data to resistivity model curves to reveal the subsurface model with apparent resistivity value and thicknesses of each model layer,
- Producing the geoelectrical map based on information from geological, hydrological, and geophysical inventory gathered in the fields as well as from different sources to deduce hydrogeological logs of the site.
- Locating the appropriate borehole drilling site/s and possibly the depth to the water table.
- Finally, the report writing was based on geological, hydrological, and geophysical information gathered from the field as well as from different sources.

  The above component stages of the thesis work are summarized in the flow chart given in Figure 1.2.

1.7 Basic Research Questions and Hypothesis

1.7.1. Basic Research Questions

- How to identify the groundwater table of the area?
- How to map the saturated zone of the area?
- How to identify weak zones of the area?
- How to map the location of geological structures- faults and fractures?
- Where to locate the drilling point?

1.7.2. Research Hypothesis

- The potential of groundwater bearing horizons, their depth and geologic structures can be obtained by measuring the electrical and magnetic properties of the subsurface.

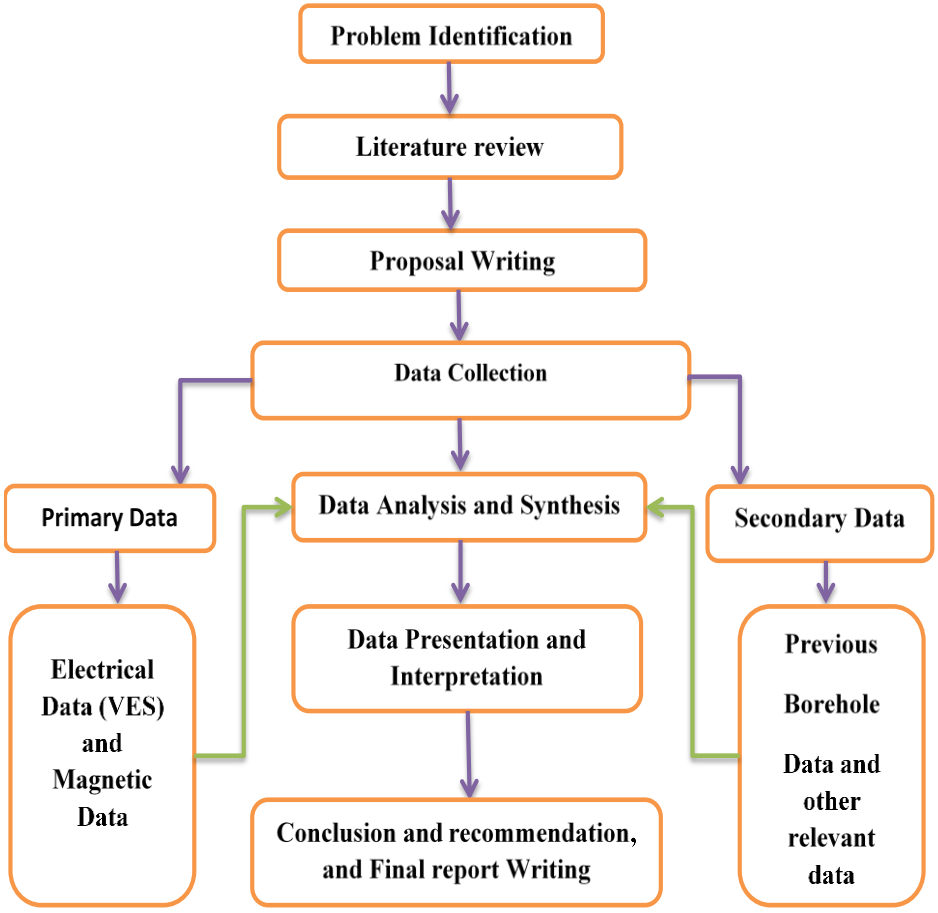

Figure 1.2: Flow Chart model of the project.

1.8 Expected outcome and Significance of the study

The main expected outcome of the research and its significance/contribution to the scientific community and/or the wider public are listed below;

- generates two geophysical survey results (Electrical and Magnetic surveys) that reveal the subsurface conditions related to groundwater potential zones (Gives Spatial variations of the subsurface resistivity and magnetic anomaly map)
- develops an understanding of the geological structure of the area and its implication to groundwater resources, and a simplified model for a selected portion of the area.
- For the sustainable source of water in the Humbo-Larena and surrounding community.
- As input to review and see the applicability of the subject matters and enhances the researcher's ability to geophysical instruments and software.
- It gives a better understanding of subsurface layers.

- fills the existing gap of detailed information and its usage in the geophysical methods in the country.
- As a reference for other researchers who may study the area in the future and contributes some data set for the ongoing study of exploration of groundwater in the country.
- The result of the research will be published and it will give a better recognition for the scientific community.

1.9 Limitation of the Study

Like any other research works, this study has also faced several limitations in this research. The main obstacles were:

- Severe financial and necessary field materials like transport and geophysical instrument,
- Inaccessibility of software for analysis and interpretation of geophysical data,
- Non-availability of previous geophysical work on the area, and
- The time-bound set for the thesis work is coupled with field constraints (transport and instruments).

1.10 Literature Review: State of Knowledge on Research

Many researchers study the compounded problems of food insecurity generally in wolaita and specifically in the study area; such as climate variability conditions, rapid population growth, low productivity (that lead to low monthly income), lack of improved agricultural technologies, and land degradation, that can increase the frequency and severity of drought, death of livestock, decline in crop yields, and food and water shortages for both human and animals, so that these indicate food insecurity and challenge for adaptation to climate change in the study area (Samuel Tessema et al, 2017; Bagnara, 2017; Almaz Balta et al., 2015). The researchers recommended different mitigation measurements other than adaptation strategies that the farmers have been using to climate change impact. Irrigation is one of those mitigation measurements that should be applied to improve the livelihood of the farmers.

The few communities in Wolaita that have irrigation infrastructure do not experience these challenges in any significant way. Such communities have three or four yields per year instead of one or two yields per year. As a result of increased and consistent yields, seasonal food insecurity had largely been overcome. Households experienced an increase in their

income from improved yield and from the ability to plant new crops, particularly vegetables (Bagnara, 2017).

Except for geological and hydrogeological investigations that have been done so far in the study area to explore groundwater for domestic use, there is no experience of using the groundwater for irrigation. Little previous work has been done on the detailed subsurface structure study using geophysical methods. Since Surface water resource is limited/inaccessible and rainfall is inadequate to ensure crop production of high-value crops, the development of groundwater resource will be considered as a potential source for supplementary means of irrigation.

Therefore, this research work is selected to explore and map the groundwater potential zone in the study area to use for irrigation purposes.

There are different approaches for assessing and mapping groundwater potential and geological structures used by many researchers. The geological and hydrogeological methods use topographical, hydrogeological and structural maps; incorporating lithological samples from different outcrops, boreholes, well completion data and pumping test data (Sikakwe, 2018; Suleyman, 2017; Oha et al., 2011).

The existence of groundwater is also evaluated and mapped by other authors using GIS and Remote-Sensing (RS) methods (they call it Multi-Criteria Design Analysis-MCDA) by considering the lithology, drainage density, lineament density, geomorphology, land use and land cover, soil, and slope of a given catchment in combination with topographic maps and satellite images (Ayele et al., 2014; Fathy, 2012; Sedhuraman et al., 2014). The thematic map of each parameter is produced by using the Geographical Information System (GIS) and Remote Sensing (RS) data techniques and topographic maps to map the thematic layers; which affect the occurrence, flow, quantity, and quality of groundwater (Sedhuraman et al., 2014; Haleh et al., 2014).

Although the exploration and mapping of groundwater potential are done by different researchers using the above Geological, Hydrogeological, GIS, and Remote Sensing methods, they include several drawbacks; they lack depth information, samples may not be representative, outcrops may not be present in all area (most areas are hidden by soil and forest). The only sub-surface information can be achieved from core samples, but it is very difficult to say a given core sample is representative of the whole study area (e.g. at

catchment scale); and also, it is not cost-effective and even it is not possible to drill a bore in the whole study area to have all the information. A correlation could be done, but we are not sure about the local condition between the two borehole sites.

Therefore, searching for the physical property of sub-surface geological materials is most favorable and it is crucial using Geophysical methods; such as Electrical, Seismic, Magnetic, Gravity...etc. (Sandberga et al., 2002). Using Geophysical methods, it is possible to i) model the subsurface Hydrogeology, and ii) know the different Hydrogeological properties (i.e., porosity, permeability, hydraulic conductivity, transmissivity, ...etc) and geological structures of an aquifer. And, also the Geophysical methods are non-destructive while providing depth information, cost-effective and are representative of the whole area. However, since they provide indirect information, this may be subjected to greater uncertainties compared to core samples and outcrops. So, often interpreted in combination with geological logs, and hydrogeological results (Mohamed and Sharharin, 2013; Sandberga, et al., 2002; Tibebe, 2006).

Nowadays, many authors described the advantage of the electrical resistivity method in the exploration of groundwater by interpreting the results concerning aquifer porosity, hydraulic conductivity, transmissivity, and groundwater contamination zone (Jackson et al., 1978; Yadav. and Abolfazli, 1998; Troisi, et al., 2000; Kossinski. and Kelly, 1981). Other authors even explored the existence of water in the lower continental crust by modeling the Magneto-Telluric (MT), and Seismic-Reflection results (Hyndman. and Shearer, 1998).

The delineation of geological structures and geological identification, characterization, and monitoring of groundwater flow path is done using Magnetic, Terrain Conductivity Measurement, Ground Penetrating Radar (GPR), Electrical Resistivity Tomography (ERT), and Self Potential (SP) methods (Sandberga et al., 2002; Tibebe, 2006).

Electrical Resistivity and magnetic methods are the two methods out of the different Geophysical methods that were focused on this research work. Electrical resistivity surveying is a widely used geophysical tool to assess the groundwater potential used for the determination of the thickness and resistivity of layered media (Ahmad, 2017; Tibebe, 2006; Yadav and Abolfazli, 1998) and it is the best method in locating a site for boreholes. Also, by using this method it is possible to delineate and map underground leachate zonation (Mepaiyeda, et al., 2019). The magnetic profiles are best to determine basement depth,

expected geological structures, and thickness of sedimentary succession that could include some basins suitable for groundwater accumulation as groundwater aquifers.

The interpretations of both methods are based on anomalies considering the background geology. Using geological, Hydrogeological, and some geophysical exploration several water wells drilled in and around the study area. Using the lithological logs of different boreholes, the potential layer, and the soil profiles were classified. Based on the evaluation of the logs, identification of the different formations was made. Accordingly, the main formations are the upper thin clay layer up to 5m, the slightly to highly weathered and/or fractured ignimbrite which extends to 210m depth, volcaniclastic sediments and volcanic sand that lies stratigraphically below the ignimbrite formations having varying thickness of up to 10m, and fresh ignimbrite. Based on the lithological log of the study area the main formations of the aquifer are weathered and/or fractured ignimbrite and volcanoclastic-sediments. From the Shochoro-pesho water well completion report, a physio-chemical analysis of the water sample from the borehole indicates that all chemical constituents lie within the range of permissible limits as to W.H.O standard. Therefore, the shape of the resistivity log curves depends mainly on the degree of fracturing and the presence or absence of water.

1.11 Organization of the thesis

This thesis is organized into six chapters. The first chapter is the introductory part which deals with the general background, the objectives, methods followed by the research and previous works. The second chapter describes the location, geology and hydrogeology of the study area. In the third chapter, the general theoretical background on the theories of the geophysical methods followed by the research works are included. Acquisition and processing of field data are discussed in the fourth chapter. The fifth chapter is all about the discussion and interpretation of the processed data. Finally, the conclusion points of the research work and recommendation ideas based on the result of the research are put under the sixth chapter.

CHAPTER TWO

2. GEOLOGY AND STRUCTURAL SETTING

2.1 Geology of Wolaita Area

2.1.1 Regional Geology

Ethiopia has a complex geological history represented in three major geological terrains, late Palaeozoic, Mesozoic and Cenozoic. Continental and marine sediments occur mainly in the eastern part of Ethiopia (GSE, 1996). Also, Cenozoic volcanic and sedimentary rocks occur, including those of the East African Rift Valley transecting the country from south to north. The Main Ethiopian Rift (MER) has a complex structural pattern composed of southern, central and northern segments (Bonini et al., 2005).

Since Wolaita area is typically occurring in the western margin of the Southern Main Ethiopian Rift (SMER), the geologic units of Wolaita area are associated with the main rifting events of the Main Ethiopian Rift (MER). It consists of mainly volcanic and volcano-sedimentary rocks. These rock units are subdivided into **(i)** Plateau Flood Basalt (the Tertiary Basaltic Sequence), **(ii)** Pliocene, Peralcaline Pantelleritic ignimbrites (Nazret Pyroclastics), **(iii)** Damota Volcano (Silicic Volcanic complex), **(iv)** Complex Pleistocene Sequence**, (v)** Quaternary Peralcaline Lava flows, Domes, and pyroclastic deposits and **(vi)** Holocene Lacustrine sediments (Figure 2.1).

i. Plateau Flood Basalt (the Tertiary Basaltic Sequence)

The large area of Ethiopia's land mass is covered by the Tertiary Basaltic Sequence and generally, the sequence is termed as Plateau Flood Basalt or Trap-Series (Mohr and Zanettin, 1988; Abbate et al., 2015)**.** The first volcanic activity in Ethiopia is represented by this sequence which is related to Tertiary rifting in Ethiopia, although the volcanic phase designates the main rifting event earlier than this (Abbate et al., 2015; Bonini et al., 2005). According to Zanettin et al., (1978), the mildly Alkaline basalt flows cover the areas around Sodo-to-Arbaminch and are exposed at the northern termination of Chencha-escarpment, and the sequence is estimated about 30-36Ma in age.

ii. Pliocene Peralcaline Pantelleritic Ignimbrites (Nazret Pyroclastics):

This unit covers large parts of the western plateau of North-West of Lake Abaya. The time correlation of these rocks is with Nazret pyroclastic of the North and Central MER (Abbate et

al., 2015). It is believed that the beginning of the rifting in MER is an eruption of a high volume of acidic pyroclastic deposits of the Nazret unit (Bonini et al., 2005).

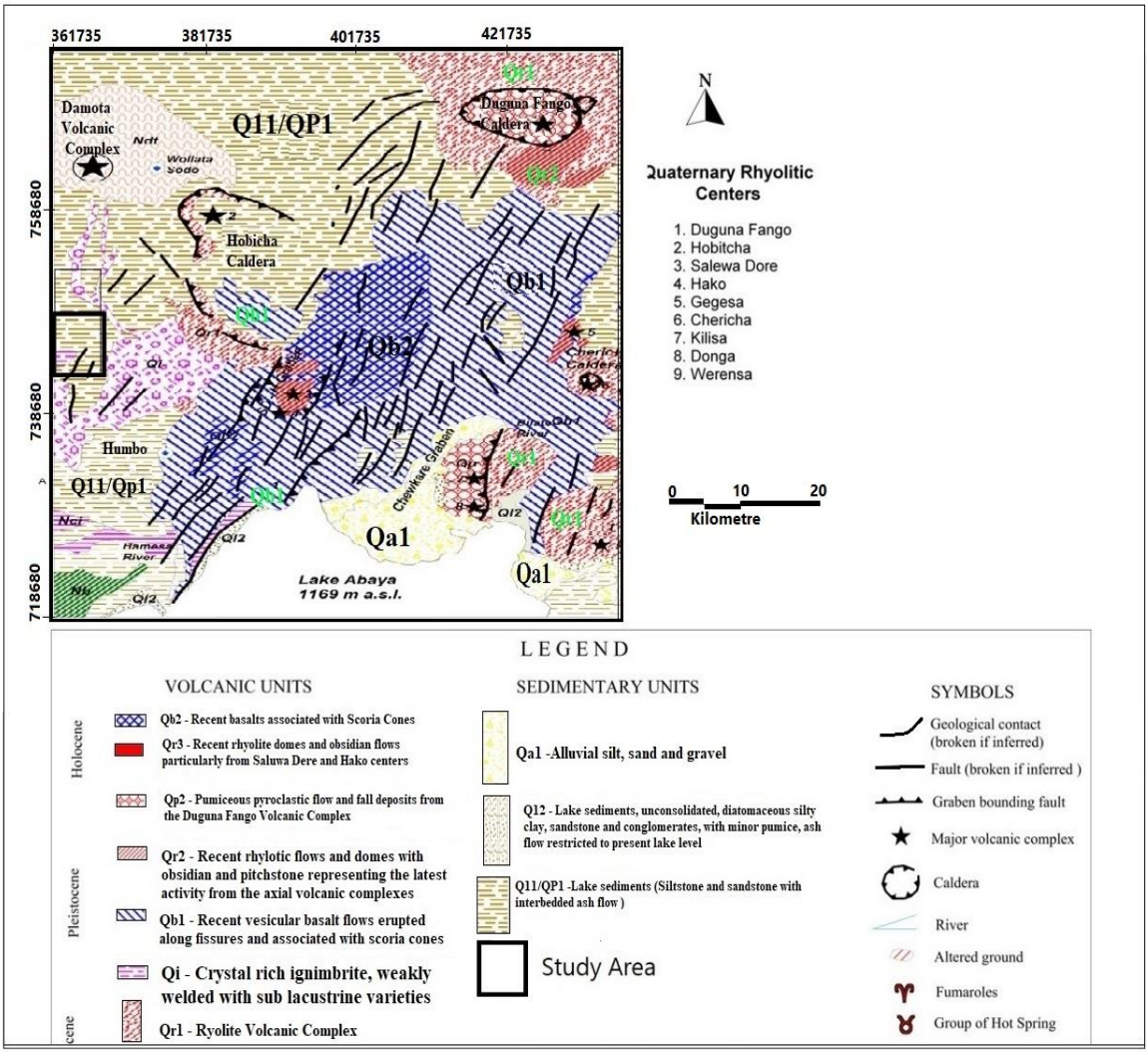

Figure 2.1: Regional Geological Map of the Central and Eastern Part of Wolaita (Adopted from Tadiwos Chernet, 2011).

iii. Damota Volcano (Silicic Volcanic complex):

This group locally overlies the Nazret group (Nazret pyroclastic rocks) and it is ~1000m higher from the surrounding rift escarpments. The trachyte lava flows from the Damota volcano are of late Pliocene (~2.9Ma) in age (Woldegebriel et al., 1990). From its morphological characteristic, Tadewos Chernet (2011) suggested the activity might have continued into the Quaternary. Making a fair equivalent, the Pliocene activity at Damota has been related to a phase of rift margin volcanism associated with the transverse fault, roughly E-W of the Goba-Bonga structure (Abbate et al., 2015).

iv. Complex Pleistocene Sequence

These sequences cover the Pliocene units and are made of alluvial and rare lacustrine sediments with interbedded pyroclastics and rare basalt flows. A wide area north of Lake Abaya is covered by horizontally bedded yellowish-brown poorly hardened siltstone, mudstone with interbedded reworked pumice. Quaternary volcanic centers (such as Hobicha- Figure 2.1) have supplied large quantities of pyroclastic material to this ancestral lacustrine system, together with basaltic flows evident as hyaloclastite layers in some sections of this unit (Tadewos Chernet, 2011).

v. Quaternary Peralcaline Lava Flows and Domes, and Pyroclastic Deposits

These are produced from the Quaternary rhyolitic volcanic centers with earlier members intercalated with lacustrine sediments. The earliest phase of rhyolitic volcanism in the Quaternary was associated with the Hobitcha rhyolitic center- a "Horseshoe-shaped caldera" with a diameter of ~10 km that exposes large volumes of lava and pyroclastic products on its flanks and caldera rim (Tadewos Chernet, 2011). The Quaternary-recent volcanic activity is also characterized by widespread basaltic volcanism (Qb1 and Qb2 in Figure 2.1), which mostly occupies a broad area between Lake Abaya and Duguna. As in other MER sectors, basaltic lava flows, scoria, and phreato magmatic deposits- typically referred to as Wonji basalt (Abbate et al., 2015).

vi. Lacustrine sediments.

The most recent deposits in the area correspond to the Holocene lacustrine sediments related to the recent fluctuations of Lake Abaya, and to fluvial sediments deposited by the two major rivers (Bilate and Gidabo) over the Wolaita area, which have formed lacustrine-deltas of a few kilometers wide on the northern part of Lake Abaya.

2.1.2 Local Geology

The geology of the area is mainly composed of volcanic rocks that consist of ignimbrite, welded tuff, rhyolites, trachyte flows and tuff with minor basalt. Flood basalts with minor silisic-flows, pumice and pyroclastic rocks is partly covering the area. Some units are exposed in the study area and its surrounding environments, such as ignimbrite and Alluvial Silt, Sand, and Gravel. The ignimbrite unit is exposed at the eastern direction of the study area near the Hamassa river.

Ignimbrite

This unit is exposed along the Hamassa River cut in the Eastern direction of the study area (Figure 2.3) and it covers small area at south western part of the study area (Figure 2.2). Fresh

ignimbrite deposits are characterized by poorly sorted aggregates of tuff and pumice. The unit is welded tuff and a special group of pyroclastic rocks. The weathered and highly fractured ignimbrite is found in the southern part from study area towards Humbo-Taballa area, otherwise, the study area is covered with thick deposition of alluvial silt and clay.

Alluvial Silt, Sand, and Gravel

Almost all part of the study area is covered by the quaternary alluvial silt, clay, and gravel deposits (Figure 2.2). The alluvial is typically made up of a variety of materials, including fine particles of silt and clay and larger particles of sand and gravel (Figure 2.4). The alluvial deposit is the result of the deposited or cemented lithological unit or lithified alluvial material.

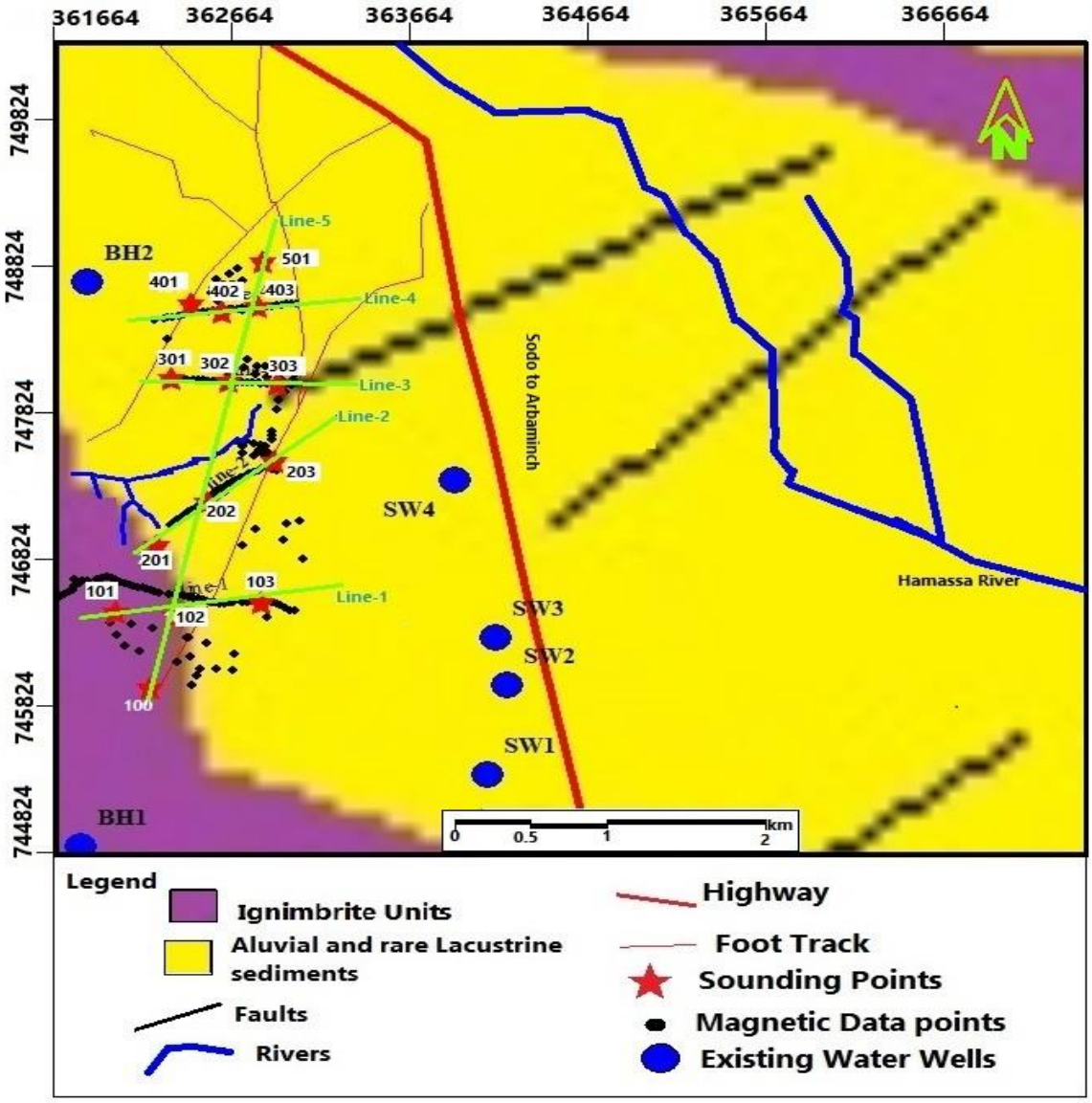

Figure 2.2: Local Geology and Data distribution over the study area.

2.2 Regional Hydrogeology

Wolaita zone has two river basins- the Bilate and Omo river basins. The Bilate basin is covered by volcanic rocks that have different hydrological properties due to differences in their texture, lithology, primary and secondary geological structures hence the geological formation that exists in this area have different water-bearing capacities (Abrham Asha, 2008).

Figure 2.3: Ignimbrite unit is exposed in the east part of the study area near the Hamassa river (terminated Quarry site).

Figure 2.4: Alluvial silt, sand, and gravel exposed at Larena-plain

In the Bilate basin, groundwater leaves the aquifer formations in the subsurface in the form of springs, pumpage from wells, evapotranspiration and outflow from this river to Lake Abaya. Many springs discharge groundwater to land surfaces from mainly along the faults and

fracture zones at higher rates in the escarpments and most are scattered along fault scarps west and north of the Soddo area across the study area alignment.

Hydrogeology of the area: According to Wolaita Zone Water, Mines, and Energy Department, the groundwater and natural spring assessment study show shallow groundwater discharge is featured by the springs on the slopes and foot of adjacent escarpments as well as by the many hand-dug wells. On other hand, in the Omo river basin, the groundwater resource is mainly focused on different springs. For example, Kindo-Koyisha and Kindo-Didaye Woredas- on the lower zones of the Omo river basin- are rich in spring resources. Fractured ignimbrite and basalts are the aquifers of these springs.

It is a well-established fact that, the occurrence of groundwater is greatly influenced by the geology, topography and climatic factors that prevailed in a given area. By the same fact, the hydrogeological condition of the study area is mainly controlled by the geology and geological structures. On the other hand, the rate of recharge is influenced by the intensity of rainfall, topography and hydraulic properties of the rock formations that outcropped in the catchment. Hydraulic properties (Permeability, Storativity and Transmissivity) of the geologic formation are dependent on both primary and secondary porosities which are created either due to shearing or fracture pore spaces in the rocks. The water-bearing formation is mainly fractured rocks of the above formations.

2.3 Structural Setting

Faults and fault zones: According to Habtamu (2014), Various different sets of brittle structures are present across the Western and eastern escarpment of Southern MER such as regional normal faults to strike-slip faults and fault zones, and extensional joints. Rare caldera related faults are associated with the evolution of individual volcanic bodies, for example Hobitcha Caldera in the northern part of Abaya Lake (Figure 2.1) and have a curved asymmetric shape, mostly parallel to the caldera rim. These faults predominantly dip steeply to moderately towards the central parts of the caldera, bearing evidence of normal kinematics. Regional faults and fault zones related to the East African Rift System significantly affect the geological framework of the area (Tesfaye et al. 2003) and are mostly parallel to the main axis of the rift and morphological escarpments. These faults dip steeply to East or West bearing well developed steeply plunging slickensides. The observed slickenside asymmetry reveals normal movement in the direction of the lineation (Figure 2.1). A subordinate set of normal faults has a W (WNW) to E (ESE) trend. Next, minor strike-slip faults with both left- and right-lateral kinematic indicators are present.

CHAPTER THREE

3. THEORY OF GEOPHYSICAL METHODS

3.1 General

In the broadest sense, the science of geophysics is the application of the principles of physics to the study of the Earth, the ocean, its surrounding atmosphere and space. Normally, however, the definition of 'geophysics' is used in a more restricted way, being applied solely to the Earth. Geophysical investigations of the interior of the Earth involve taking measurements at or near the Earth's surface that are influenced by the internal distribution of physical properties. Analysis of these measurements can reveal how the physical properties of the Earth's interior vary vertically and laterally. 'Applied geophysics' covers everything from experiments to determine the thickness of the crust, to studies of shallow structures for engineering site investigations, exploring for groundwater and for minerals and other economic resources, to try to locate narrow mine shafts or other forms of buried cavities, or the mapping of archaeological remains or locating buried pipes and cables (Kearey et al., 2002; Reynolds, 1997).

Geophysical investigations, although sometimes plagued with ambiguities and uncertainties in interpretation, provide a rapid and cost-effective means of deriving distributed information on subsurface hydrogeology (Kearey and Brooks, 1991). The use of geophysical methods for both groundwater resource mapping and water quality evaluation has increased dramatically over the last decades due to rapid advances in electronic technology and the development of numerical modeling solutions (Metwaly et al., 2009).

Applications of geophysics for groundwater exploration and resource evaluation investigations include detection of the depth to the bedrock, depth to the water table, mapping of the geological structures, depth to known aquifer thickness and its structures, etc. By obtaining the property and thickness of various lithological units from the geophysical survey at different locations, geophysical surveys are used extensively in the search for suitable groundwater potential and also to monitor types of groundwater pollution in any hydrogeological setup and locate preferred borehole site.

There is a broad division of geophysical surveying methods into those that make use of natural fields of the Earth and those that require the input into the ground of artificially

generated energy. The natural field methods utilize the gravitational, magnetic, electrical, and electromagnetic fields of the Earth, searching for local perturbations in these naturally occurring fields that may be caused by concealed geological features of economic or other interest. Artificial source methods involve the generation of local electrical or electromagnetic fields that may be used analogously to natural fields, or, in the most important single group of geophysical surveying methods, the generation of seismic waves whose propagation velocities and transmission paths through the subsurface are mapped to provide information on the distribution of geological boundaries at depth. Generally, natural field methods can provide information on Earth properties to significantly greater depths and are logistically simpler to carry out than artificial source methods. The latter, however, are capable of producing a more detailed and better-resolved picture of the subsurface geology (Kearey et al., 2002).

Though almost all geophysical survey methods have a wider scope of utilizations, there is always one physical property for which a particular method is exceptionally sensitive and as such determines its specific range of applications. However, several geophysical methods may be applied simultaneously (integrated geophysical exploration) in solving certain geological problems and such an approach greatly reduces the problem of ambiguity, which is the inherent drawback in the interpretations of results from one method, by complementing the information gap from the additional methods. Moreover, surface and drill hole geological information are of vital importance for the successful analysis and interpretation of geophysical data.

Of the number of geophysical methods that could measure variations in the physical field of the Earth and its perturbations, the electrical and magnetic methods of prospecting have found major applications in groundwater investigations. This is because; the electrical methods are the most suitable to investigate the presence of saturated zones in the subsurface while the magnetic methods, in addition to several advantages they offer, are the best tools that could map subsurface fractures detrimental for the movement of groundwater. These two methods have accordingly been used over the ‘Humbo-Larena’ plain to investigate its groundwater potential and form the main methods used in this research work. The theoretical foundations of the methods are therefore briefly discussed in the following sections.

3.2 The Electrical Method:

Electrical prospecting involves a wide range of geophysical surveying methods for the detection of subsurface effects produced by electric current flow in the ground. For each of which there is an 'operative' physical property to which the method is sensitive (Kearey et al., 2002). Using electrical methods, one may measure potentials, currents, and electromagnetic fields that may occur naturally, or are introduced artificially in the Earth. Natural electrical methods such as the Self-Potential (SP), Telluric-Current, Magnetotelluric and Audio-Frequency Magnetic (AFMAG) methods, depend on naturally occurring fields and in this respect resemble gravity and magnetic prospecting. Artificial electrical methods such as Resistivity, Equipotential line, Mise-a-la-Masse, Electromagnetic (EM), and the Induced Polarization (IP) are similar to seismic methods. Electrical methods are more frequently used in searching for metals, groundwater, archaeology and engineering problems. In this research, the method used to map the groundwater potential is the electrical resistivity surveying method.

Though, the technique of resistivity survey was developed by Conrad Schlumberger who conducted the first experiments in 1912 in the field of Normandy (Sharma, 1997), real progress in applying electrical methods to groundwater exploration began during World War II (Zohdy et al.,1990). According to Reynolds (1997), the electrical resistivity methods were developed in the early 1900s, but have become widely used since the 1970's due primarily to the availability of computers to process and analyze the data.

The resistivity method is also used in the study of horizontal and vertical discontinuities in the electrical properties of the ground, and also in the detection of three-dimensional bodies of anomalous electrical conductivity. Electrical resistivity is a fundamental and diagnostic physical property that can be determined by a wide variety of techniques, including electromagnetic induction. Thus, alternative techniques for the determination of the same property are extremely useful, as some methods are more directly applicable or practicable in some circumstances than others (Reynolds, 1997).

Electrical methods of geophysical prospecting are well established and are the most important methods for groundwater exploration (Kearey et al., 2002). The electrical resistivity method has been widely used because of theoretical, operational and interpretational ease the method provides. The advantages of electrical methods also include control over the depth of

investigation techniques, portability of the equipment, availability of a wide range of simple and elegant interpretation techniques, and related software, etc.

There are three ways in which electric current can be conducted through a rock: electrolytic, electronic (Ohmic) and dielectric conduction. In most rocks, conduction is by way of pore fluids acting as electrolytes, with the actual mineral grains contributing very little to the overall conductivity of the rock (except where those grains are themselves, good electronic conductors). At the frequencies used in electrical resistivity surveying, dielectric conduction can be disregarded (Reynolds, 1997).

There are two main modes of deployment of electrode arrays. One is for depth sounding (to determine the vertical variation of resistivity)–this is known as Vertical Electrical Sounding (VES). The other is for producing either a horizontal profile (lateral variation of resistivity) using a fixed electrode separation (called Constant Separation Traversing, CST) or both a lateral and vertical variation in resistivity, called Sub-Surface Imaging (SSI), or Electrical Resistivity Tomography, ERT (Milsom, 2003).

VES measures the vertical variation of the subsurface at a point by assuming the horizontal layer of the Earth while the profiling surveys measure the lateral variation of the subsurface by assuming the vertical layer in electrical properties of the Earth. VES survey is the technique that is widely and commonly employed for groundwater resources potential studies (Reynolds, 1997).

3.2.1 Principles of Vertical Electrical Sounding (VES) Survey

A Vertical Electrical Sounding (VES) survey method is a 1D resistivity method that provides deep information of the subsurface with minimal equipment and personnel. It is one of the oldest methods for acquiring resistivity and one of the least expensive to conduct per unit depth. The VES method can be quite versatile for reconnaissance surveying or when there are equipment limitations. The data from vertical electrical sounding are more sensitive to general electrical structure than other 1D electromagnetic method, such as Time Domain Electromagnetic Methods (TDEM), because high resistivity contrasts are better resolved with VES.

In VES, the positions of the electrodes are changed about a fixed point known as the sounding point and the measured values reflect the vertical distribution of resistivity values

on a geologic setting. The technique is extensively used in hydrogeological investigations to define horizontal zones of porous strata (Kearey et al., 2002).

Vertical Electrical Sounding consists of a symmetrical electrode array used to determine vertical variation in resistivity of the subsurface which is assumed to be consisting of horizontally stratified media. The technique is also called electrical drilling or commonly vertical electrical sounding. As shown in Figure 3.1, it is achieved by symmetrically expanding the distance between the current electrodes (AB) about the point called the sounding point ('**o**'), while keeping the potential electrodes (MN) at the same position. This exercise provides a sounding curve corresponding to the apparent resistivity versus depth. As the distance between the current electrodes is increased, so does the depth to which the current penetrates and hence the depth of investigation. Increasing the potential electrode spacing produces a 'step' in the apparent resistivity curve. It is common to obtain an overlap between the curve segments by obtaining two readings at different potential electrode spacing for two adjacent current electrode spacings (Reynolds, 1997).

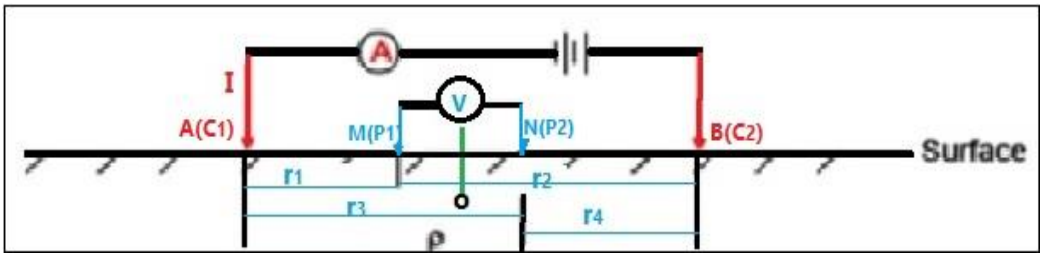

Figure 3.1: The arrangement of current and potential electrodes in a four-electrode system.

A solution for the potential field over a horizontally stratified Earth where the measurements of the type shown in Figure 3.2 can be obtained as follows. Consider a point electrode delivering a current **('+I')** located at the surface of the subsurface which consists of an infinite number of layers separated by horizontal boundary planes; where the air above has zero conductivity. The deepest layer existing to finite depth and the other layers have finite thickness $h_i = h_1, h_2, h_3 \ldots h_n$ and resistivities $\rho_i = \rho_1, \rho_2, \rho_3, \ldots, \rho_n$. Each of the layers is electrically homogeneous and isotropic (Figure 3.2).

The electrical potential field V for direct current satisfies the differential equation of Laplace, which is

$$\frac{\partial^2 V}{\partial x^2} + \frac{\partial^2 V}{\partial y^2} + \frac{\partial^2 V}{\partial z^2} = 0 \qquad (3.1)$$

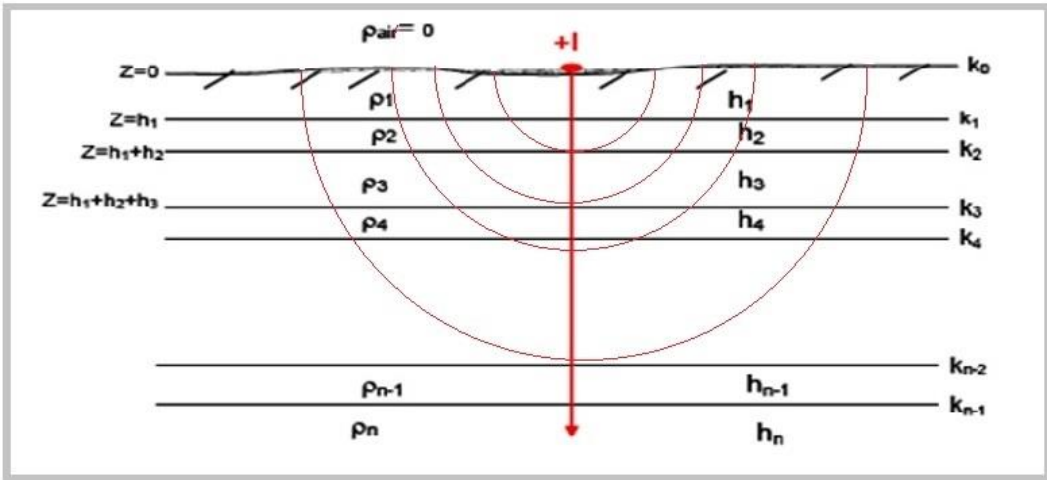

Figure 3.2: A multi-layer Earth and problem presentation for solution of the potential field (after Loke, 2001)

The potential field has a cylindrical symmetry concerning the vertical axis line through the current source. Therefore, the Laplace equation in cylindrical coordinate is most appropriate. For a solution symmetrical with the vertical axis

$$\frac{\partial V}{\partial \theta} = \frac{\partial^2 V}{\partial \theta^2} = 0$$

Therefore,

$$\frac{\partial^2 V}{\partial r^2} + \frac{1}{r}\frac{\partial V}{\partial r} + \frac{\partial^2 V}{\partial z^2} = 0 \tag{3.2}$$

The particular solution of equation (3.2) can be obtained using the method of separation of variables and can be assumed to be of the form:

$$V(r, z) = U(r)W(z) \tag{3.3}$$

Substituting equation (3.3) to (3.2) and divide throughout by the product U(r) W (z) gives

$$\frac{1}{U(r)}\frac{\partial^2 U(r)}{\partial r^2} + \frac{1}{rU(r)}\frac{\partial U(r)}{\partial r} + \frac{1}{W(z)}\frac{\partial^2 W9z)}{\partial z^2} = 0 \tag{3.4}$$

This equation is satisfied if and only if;

$$\frac{1}{U(r)}\frac{\partial^2 U(r)}{\partial r^2} + \frac{1}{rU(r)}\frac{\partial U(r)}{\partial r} = \lambda^2 \tag{3.5}$$

and

$$\frac{1}{W(z)}\frac{\partial^2 W9z)}{\partial z^2} = -\lambda^2 \tag{3.6}$$

where 'λ' is an arbitrary constant.

The solution of equation (3.6) may be given as

$$W(z) = C_1 e^{-\lambda z} \quad \text{and} \quad W(z) = C_1 e^{+\lambda z} \tag{3.7}$$

and that of equation (3.5) is given as

$$U(r) = C_3 J_0(\lambda r) \tag{3.8}$$

where J_0 is the Bessel function of order zero.

The combination of equation (3.7) and (3.8) gives the particular solution of the differential equation given by equation (3.9), which is

$$V(r,z) = C_4 e^{-\lambda z} J_0(\lambda r) \quad \text{and} \quad V(r,z) = C_4 e^{+\lambda z} J_0(\lambda r) \tag{3.9}$$

where c and λ are both constants in the last of these equations.

Since, in the theory of differential equation, every linear combination of the particular solution is also a solution, one can make λ to rough all possible values from zero to infinity and allowing the constant "c" to very independent of λ the general solution of equation (3.2) can be obtained as:

$$V(r,z) = \int_0^\infty \left[\phi(\lambda)e^{-\lambda z} + \psi(\lambda)e^{+\lambda z}\right] J_0(\lambda r)\, d\lambda \tag{3.10}$$

Here $\phi(\lambda)$ and $\psi(\lambda)$ are arbitrary functions of the boundary conditions that control the special form of these equations.

From basic theory, the potential generated by a single point source of current intensity "I" located at the surface of electrically homogeneous Earth is given by

$$V(r) = \frac{I\rho}{2\pi}\frac{1}{\sqrt{r^2 + z^2}} \tag{3.11}$$

where ρ is the resistivity of homogeneous Earth.

Equation (3.11) can be written in integral form by using the so-called Lipchitz integral (also called the Weber Integral Formula) in the theory of Bessel function as

$$\int_0^{\infty} e^{-\lambda z} J_0(\lambda r) d\lambda = \frac{1}{\sqrt{r^2 + z^2}} \tag{3.12}$$

So that equation (3.12) gives

$$V(r) = \frac{I\rho}{2\pi} \int_0^{\infty} e^{-\lambda z} J_0(\lambda r) d\lambda \tag{3.13}$$

Equation (3.13) is also a solution of equation (3.2).

Therefore, the combined solution will also, be a solution to the equation, that is

$$V(r) = \frac{I\rho}{2\pi} \int_0^{\infty} \left[e^{-\lambda z} + \Theta(\lambda) e^{-\lambda z} + \mathrm{X}(\lambda) e^{+\lambda z} \right] J_0(\lambda r) d\lambda \tag{3.14}$$

where Q (l)and C (l) are arbitrary functions.

Solutions of equation (3.14) are valid in all the layers of the subsurface. However, necessarily it is the same in different layers of the subsurface. Therefore, the potential due to a point source of current at the surface of a horizontally layered earth must in each layer satisfy,

$$V_i(r) = \frac{I\rho_i}{2\pi} \int_0^{\infty} \left[e^{-\lambda z} + \Theta_i(\lambda) e^{-\lambda z} + \mathrm{X}_i(\lambda) e^{+\lambda z} \right] J_0(\lambda r) d\lambda \tag{3.15}$$

This equation is called the Stefanescu Integral, with 'i' referring to the several layers of the subsurface.

Boundary conditions

For a potential set up by a single source of current at the surface of a horizontally stratified earth, the following boundary conditions are fulfilled.

i. At each of the boundary planes in the subsurface, the electrical potential must be the Same

$V_i = V$ **at** $h_i = z$

ii. The vertical component of the current density must be continuous on each boundary plane (the current density normal to the boundary planes …)

$(J_i)_N = (J_{i+1})_N$

$$\frac{1}{\rho_i}\frac{\partial V_i}{\partial z} = \frac{1}{\rho_{i+1}}\frac{\partial V_{i+1}}{\partial z} \tag{3.16}$$

At the surface (z=0) the vertical component of the current density J_v (and hence that of the electric field intensity) must be zero everywhere except in the infinitesimal neighborhood around the current source. In air $J_{air} = 0$ and from condition (2), the vertical component of the current density at depth zero must be zero. Near the current source the potential must not approach infinity (must remain finite) as

$$V(r) = \frac{I\rho}{2\pi}\frac{1}{\sqrt{r^2 + z^2}} \text{ at depth z = 0 when r}\rightarrow 0 \tag{3.17}$$

iii. At infinite depth, the potential must approach zero, i.e., $V \rightarrow 0$ when $Z \rightarrow \infty$

3.2.2 The Fundamental Essence of Resistivity for Groundwater Study

Although various hydrogeophysical techniques are available, electrical resistivity is a popular method because of its low cost, simple operation and efficiency in areas with high contrasting resistivity, such as between the weathered overburden and the bedrock (Telford et al., 1990). The resistivity method is used in the study of the horizontal and vertical discontinuities in the electrical properties of the ground and also in the detection of three-dimensional bodies of anomalous electrical conductivity. Electrical methods are particularly suitable for groundwater studies because hydrogeologic properties, such as porosity and permeability, can be correlated to electrical resistivity values. In geophysical inquiring different types of physical properties of rocks are often used; such as electrical resistivity or conductivity, magnetic susceptibility, thermal conductivity and density.

According to Ohm's Law, the ratio of the potential drop to the applied current (V/I) also define the resistance (R) of the cube and these two expressions can be combined to form the product of a resistance (Ω) and a distance (area/length; meters), which is defined as the resistivity (units: ohm-meters, Ω-m). The inverse of resistivity (1/ρ) is conductivity (σ), which has units of Siemens/meter (S/m) that are equivalent to mhos/meter (Ω-1 m-1) (Milsom, 2003).

The resistivity of a material is defined as the resistance offered at a particular temperature by an electrical conductor of any given material in a cube length expressed in ohm-meter (Ω m) in a metric system of measurement. It is a basic property of a material that determines how strongly it transfers or resists electrical current. A low resistivity shows a material that easily

allows electric current. For a conducting cylinder of resistance **δR,** length **δL** and cross-sectional area **δA** (Figure 3.3) the resistivity **ρ** is given by

$$\rho = \frac{\delta R - \delta A}{\delta L} \tag{3.18}$$

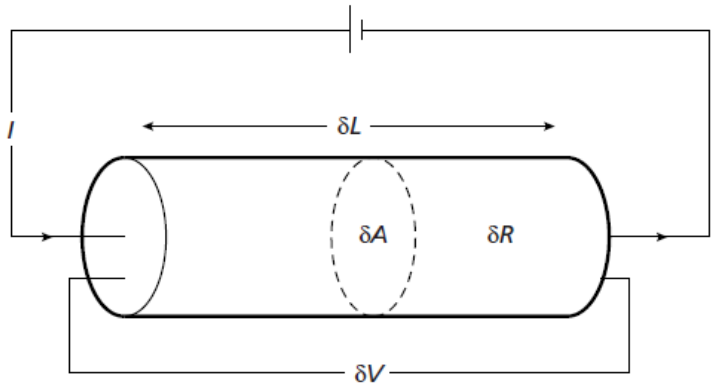

Figure 3.3: the parameters used in defining resistivity (after Kearey et al., 2002).

There is a criterion to meet when the charge moves through conducting material and to conduct electricity. With this respect, electrical conduction in most rocks is due to the movement of ions in electrolytes (Reynolds, 1997; Kearey et al., 2002).

According to the expression of Kearey and his colleagues (Kearey et al., 2002), most rocks conduct electricity by electrolytic process rather than electronic processes i.e., the availability of pore spaces (meaning porosity) of the rocks and pore fluid characteristics is the major geologic factor that affects the resistivity of rocks and Earth materials (Table 3.1). The degree of porosity, where the electrolytes of rocks and earth materials, mainly dependent on the degree of fracturing, the availability of fault, cracks, and fissure structures in the rock. Since most rock-forming minerals are poor conductors; the current that passes through the earth is then carried by the presence of pore water ions. Pure water is ionized to only a very small extent and the electrical conductivity of pore waters depends on the presence of dissolved salts, mainly sodium chloride (Milsom, 2003). Since groundwater contains dissolved salt, it is ionically conductive and enables electric current to flow through the ground. Therefore, it is possible to identify the conditions necessary for the presence or absence of water by measuring the resistivity of the sub-surface geologic material.

Table 3.1: Numerical values for various types of water (from Bernard, 2003).

Type of Water	Resistivity (Ohm-m)	Conductivity (micros/cm)	Salinity (mg/l)
Very fresh	200	50	35
Fresh	20	500	150
Salted	10	1000	700
Sea Water	0.3	30000	35000

In resistivity surveying, especially in vertical electrical sounding (VES), conduction in rocks is mainly due to pore fluids acting as electrolytes. Water in its pure form is a poor conductor but most water contains dissolved salts that facilitate the flow of current. Resistivities of rocks generally depend on the water content (porosity), the resistivity of the water, the clay content, and the content of metallic minerals (Bernard, 2003).

In the determination of the resistivity of rocks, it is better to consider some issues. The hard and fresh rocks show very high electrical resistivity due to the absence of porosity and fractures. But when these rocks are porous and fractured their resistivity depends on the resistivity of the water and the porosity of the rocks. Some rock types, such as impermeable clay layer in wet condition has low resistivity, but the water yield may not be enough for groundwater exploitation (Table 3.2). Mineral ore bodies (iron, sulfides) have very low resistivity due to their electronic conduction; usually lower or much lower than 1Ohm-m (Bernard, 2003).

Electrical current is injected into the ground by active outer electrodes and the resistance of the current is measured at various locations along the line by inner potential electrodes. A variety of testing methods (i.e., Dipole-Dipole, Schlumberger, Wenner, Gradient, etc.) can be used to collect data using different combinations of electrodes from the general arrangement shown in Figure (3.4). In this work, the Schlumberger method is employed. In this configuration, the potential electrodes are placed at the center of the electrode array with a small separation, typically less than one-fifth of the current electrode spacing. The current-electrodes separation is gradually increased during the survey while the potential electrodes remain unchanged until the measured voltage becomes too small to be detected. The Electrode spacing determines the depth of penetration. Schlumberger soundings generally have better resolution, greater probing depth, and less time-consuming field deployment compared to Wenner arrays (Reynolds, 1997).

Table 3.2: Resistivity value of common geological materials.

Earth Material	Nominal resistivity (Ωm)	Earth Material	Nominal resistivity (Ωm)
Quartz	$300 - 10^6$	Consolidated shales	20–2000
Rock salt	$30 - 10^{13}$	Conglomerates	$2 \times 10^3 - 10^4$
Anthracite	$10^{-3} - 2 \times 10^5$	Sandstones	$1 - 7.4 \times 10^8$
Granite	$300 - 1.3 \times 10^6$	Sandstones (weathered)	50-200
Granite (weathered)	30–500	Limestone	$50 - 10^7$
Basalt	$10 - 1.3 \times 10^7$	Dolomite	$350 - 5 \times 10^3$
Clays	1–100	Marls	3–70
Topsoil	250–1700	Clays	1–100
Unsaturated landfill	30–100	Slates	$600 - 4 \times 10^7$
Saturated landfill	15–30	Marble	$100 - 2.5 \times 10^8$

When a four-electrode system, with two current and two measuring electrodes, is employed with distances between them as shown in Figure 3.1; the potential difference measured between the two potential electrodes, MN (Figure 3.4) i.e. the potential at point P_1 is given by,

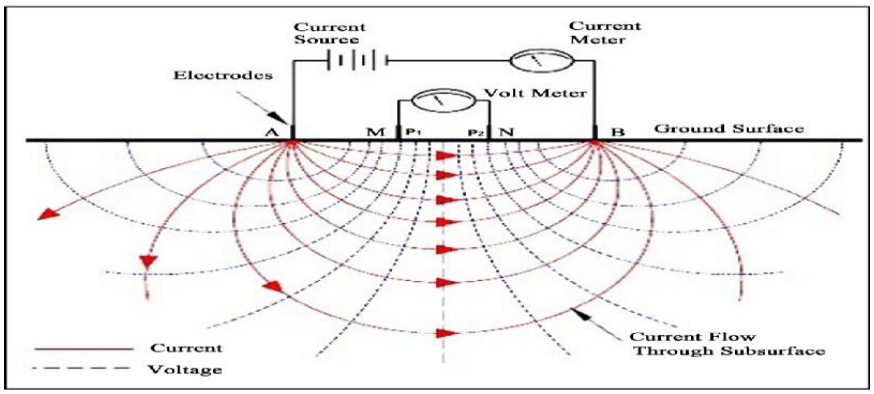

Figure 3.4: DC Resistivity measurements.

$$V_{P_1} = \frac{I\rho_a}{2\pi}\left(\frac{1}{r_1} - \frac{1}{r_2}\right) \tag{3.19}$$

and similarly, the potential at point P_2 is given by,

$$V_{P_2} = \frac{I\rho_a}{2\pi}\left(\frac{1}{r_3} - \frac{1}{r_4}\right) \tag{3.20}$$

The potential difference between points P_1 and P_2 is hence,

$$\Delta V = \frac{I\rho_a}{2\pi}\left(\frac{1}{r_1} - \frac{1}{r_2} - \frac{1}{r_3} + \frac{1}{r_4}\right) \tag{3.21}$$

$$\rho_a = 2\pi\left[\frac{1}{\frac{1}{r_1} - \frac{1}{r_2} - \frac{1}{r_3} + \frac{1}{r_4}}\right]\frac{\Delta V}{I} \tag{3.22}$$

where the distances r_1, r_2, r_3 and r_4 are all in meters.

Therefore, after re-arranging the distances between the current and potential electrodes according to the well-known configurations, we can determine the resistivity of the homogenous ground.

The Apparent Resistivity and True Resistivity

The resistivity calculated from equation (3.22) should be constant and be independent of both electrode spacing and surface location. But since the subsurface is inhomogeneous, the resistivity will vary with the relative positions of the electrodes. Any computed value is then known as the ***apparentresistivity*** (ρ_a) and will be a function of the form of the inhomogeneity. Equation (3.22) is the basic equation for calculating the apparent resistivity for any electrode configuration. By using curve matching or inversion techniques, this apparent resistivity has to be interpreted to find estimated resistivity and depth of the subsurface.

Since the geometric factor for different array types varies, the apparent resistivity also varies. For Schlumberger configuration in VES surveys (Figure 3.5), the potential electrodes (MN) remain fixed and the current electrodes (AB) are expanded symmetrically about the center of the spread. With very large values of *L* (AB distance), it may, however, be necessary to increase *l* (MN distance) also to maintain a measurable potential.

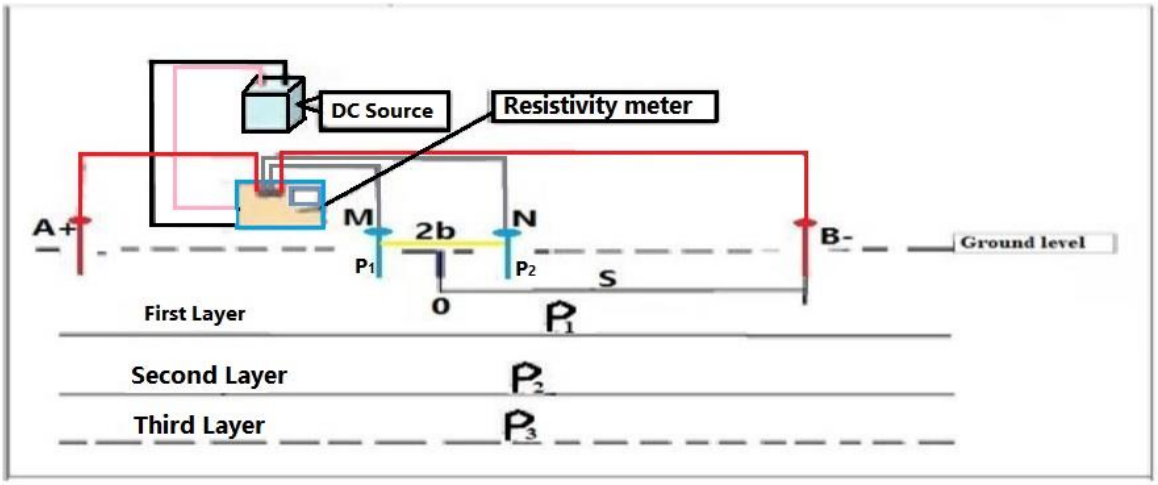

Figure 3.5: The Schlumberger electrode configuration.

where r_1=s-b, r_2=s+b, r_3=s+b, r_4=s-b and 'O' is the center of the array (the sounding point). The potential difference ΔV using equation (3.22) is given by

$$\rho_a = 2\pi\left[\frac{1}{\frac{1}{s-b_1}-\frac{1}{s+b}-\frac{1}{s+b}+\frac{1}{s-b}}\right]\frac{\Delta V}{I} \tag{3.23}$$

$$\rho_a = \pi\left[\frac{1}{s^2-b^2}\right]\frac{\Delta V}{I} \tag{3.24}$$

where, $\pi\left(\frac{1}{(s^2-b^2)}\right)$ is the geometric factor of the array**.**

3.2.3 Interpretation of VES Data

The interpretation of electrical resistivity sounding data is the process of **deriving the values of true resistivities (ρ) and thicknesses (t)** of various subsurface strata from the values of recorded resistance (R) or apparent resistivity (ρ_a) at electrode separations. There are several interpretation techniques for evaluating the true resistivity and thickness of each of the stratum. VES field curves can be interpreted qualitatively using simple curve shapes, semi-quantitatively with graphical model curves, or quantitatively with computer modeling (Reynolds, 1997).

In resistivity prospecting, for the case of theoretical deductions, the Earth is assumed to have several homogenous layers of differing resistivities bounded by sharp vertical and horizontal contacts. The purpose of interpretation of geoelectric sections namely the resistivity and

thickness of the formations is to subsequently correlate to the geology as well as hydrogeology of the area. There are various stages and ways of interpretation of resistivity data (Kearey et al., 2002).

Qualitative Interpretation: it is useful to make a rapid qualitative study of the field curves before a detailed quantitative interpretation. Qualitative interpretation is done by merely observing the shape of the VES curves and noting the changes in resistivity with increasing electrode separations. This qualitative analysis gives the number of layers and the order of resistivities.

Semi-Quantitative Interpretation: this method is useful in crystalline terrain when the bottom-most layer is infinitely resistive, which manifests on the VES curve in the form of a straight line making an angle of about 45^0 with the x-axis (known as S-line), at the extreme right-hand part of the VES curve. This method is usually adopted to determine the depth of the basement/hardrock.

Quantitative Interpretation: quantitative interpretation of the VES data can be done by the conventional curve matching techniques using the master curves or with the aid of software such as RESIST, etc.

Curve matching: graphical interpretation can be performed by using master curves and utilizing the curve matching technique. It is a quantitative interpretation of the vertical electrical soundings (VES) that aims principally, to determine the thickness (or depth) and true resistivity of the interpreted geoelectric layers.

Inversion: the calculated apparent resistivity values from the various electrode spacings are compiled and inverted using 1D inversion software based on the initial data curves and available constraining datasets. Inversion of the data is run over multiple iterations to determine the best-fit models of the acquired dataset.

3.3 The Magnetic Method

The Earth's magnetic field, as measured by a magnetic sensor on or above the Earth's surface, is the sum of magnetic fields generated by a variety of sources. In the magnetic method, the measured anomalous magnetic field results from the presence of sub-surface geological structures or buried targets. The anomaly overlies the background geomagnetic field and its amplitude and shapes depend on the sub-surface geological structure/buried targets susceptibility, shape, and orientation. The difference in the magnetic susceptibility of Earth

materials is recorded (the sum of Earth's field and fields induced in magnetic materials) by conducting a magnetic survey by measuring the magnetic field data in the air, on/under the ground, and on/under the ocean. To know the anomalous field (the local magnetic field that is superimposed on the main field), the main (earth's) field is removed from the observed magnetic field, then the interpretation is possible to have the location, shape, and susceptibility of the body based on the results from presented maps, profiles, and/or 3D models. The type and quantity of magnetic minerals; such as magnetite, iron oxide, Titanium oxide) of a given rock unit determines its magnetic susceptibility (Reynolds, 1997).

Magnetic surveys are used for delineating and locating magnetic iron ore deposits, metallic ore deposits which may have either magnetite or pyrrhotite associated with them, and geological structures such as contacts, faults, dykes, etc. In groundwater studies, the method is used for mapping the depth to basement rock, and also it provides a valuable aid to lithological mapping based on the magnetic anomaly. Moreover, it can also be applied in mapping structural features, which often provide a conduit or barrier for the accumulation of groundwater (Reynolds, 1997).

3.3.1 Principle of the Magnetic Method

Magnetic Force and Magnetic Field

Magnetic surveys make use of the variation in the magnetization of rocks. Rocks owe their magnetic properties to minor constituents, which can be very variable in their distribution, and thus less diagnostic of the formation (Griffiths and King, 1981).

The magnetic force is given by Columbo's law for magnetic poles, symbolically analogous to point masses of gravitational force (Telford et al., 1990). According to Coulomb's law, if two magnetic poles of strength p_1 and p_2 are separated by a distance "r", a magnetic force (Fm) exists between them and the force is expressed as:

$$F_m = \frac{1}{\mu}\frac{p_1 p_2}{r^2} \tag{3.25}$$

where "μ" is the constant of proportionality known as the ***magnetic permeability*** of the medium.

The convectional current in the outer core is the main source of the magnetic field; as all magnetic fields come up from current. A magnetic dipole is a magnetic field of the Earth that resembles a large bar magnet. This magnetic dipole (Earth's magnetic field) has two poles,

negative and positive, in the northern and southern hemispheres respectively. This Earth's magnetic field is described in terms of vectors that represent the Earth's magnetic field (magnitude-B), the angle between **B** and the horizontal (inclination-I), and the angle that *H* makes with geographic north (declination-D), (Figure 3.6).

Permeability and susceptibility

The magnetization intensity (I) is related to the strength of the magnetic force (F_m) via a proportional constant, K, and is given by;

$$I = KF_m \tag{3.26}$$

where K is the magnetic susceptibility.

According to Telford et al., (1990), the force associated with the magnetic field strength (F_m) is characterized by the magnetic induction (B) and is given as;

$$B = \mu F_m \tag{3.27}$$

where μ is the permeability of the medium and is defined as the product of relative permeability (μ_r) and permeability of the free space (μ_0), i.e. $\mu=\mu_o\mu_r$.

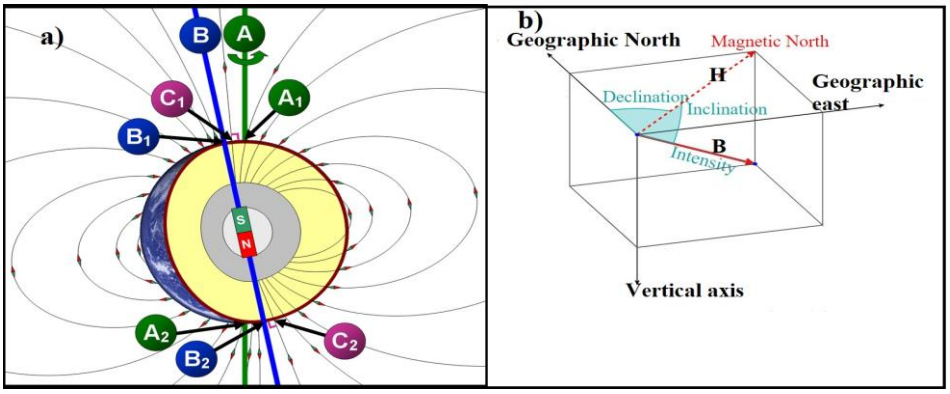

Figure 3.6: Earth's magnetic field components and description

(A1 and A2 are the geographic poles; B1 and B2 are the geomagnetic poles; C1 (south) and C2 (north) are the magnetic poles; image credit https://en.wikipedia.org).

Thus, equation (3.27) can be written as

$$B = \mu_0 (1+k) F_m \tag{3.28}$$

By introducing K= μ_r-1 and rearranging we have

$$B = \mu_0 (F_m + 1) \tag{3.29}$$

Magnetization and Magnetic Response

Earth's materials become magnetized when the source field is applied to them, thus resulting secondary field or anomalous field of magnetization. Looking for anomalous magnetization is the main task in the magnetic method of prospecting to process and interpret the data for geophysical, hydrogeological, geological, and engineering problems. However, during the field survey, the measured data (observed magnetic field) is not only the anomalous field, but it is the sum of the anomalous field and other magnetic fields.

$$B_{obs} = B_{ext} + B_{\text{int}} = B_{ext} + B_D + B_{rm} \tag{3.30}$$

where; B_{obs} is measured data (observed magnetic field), B_{ext} is the external magnetic field and B_{int} is the internal magnetic field.

3.3.2 Noise, Correction and Interpretation of Magnetic Data

As described earlier the observed or measured magnetic field data from the field contains other magnetic field signals irrelevant to the task. One of those fields is the noisy data caused by different sources such as electric power cable, railway, keys and other metallic materials which may cause magnetic noise, so they should be kept away from the sensor. On the other hand, magnetic fields raised due to currents within the Earth's ionosphere (diurnal part) can affect the data. This is caused by interactions of currents mainly with plasma connected with solar winds. The time variations of this field portion are much more rapid than that for the main field. For this type of increment on the reading, it is advisable to stop the survey and start it later (Telford et al., 1990).

Therefore, data correction is the beginning of magnetic data processing in which all noisy data are eliminated from the raw data and diurnal and IGRF corrections are applied. Base station readings are taken over a survey period to facilitate the compilation of diurnal correction.

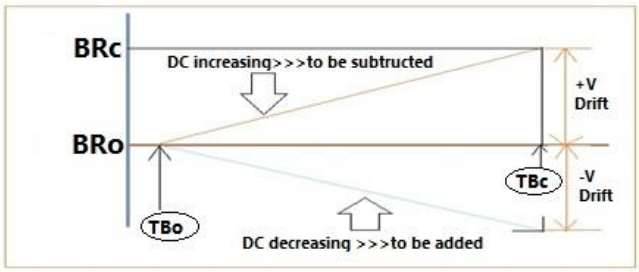

Figure 3.7: Drift Correction using readings at a base station modified from different sources.

Drift correction, for example, can be calculated as (Figure 3.7)

$$DC = \left[\frac{BR_c - BR_o}{TB_c - TB_o} \right] * T_i \tag{3.31}$$

where; DC=Diurnal Correction.

BR_c - the final reading at 'Base Station' (when the loop is closed)

BR_o - the first reading at 'Base Station' (when the loop is opened)

TB_c - the final Observation time at Base Station (when the loop is closed)

TB_o - the first Observation time at Base Station (when the loop is opened)

T_i - The time difference of observation at 'Base station' and each measuring point or station in minutes.

To produce a magnetic anomaly, the data have to be corrected to take into account the effect of latitude and, to a lesser extent, longitude. As the Earth's magnetic field strength varies from 25000nT at the magnetic equator to 69000nT at the poles, the increase in magnitude with latitude needs to be taken into account (Reynold, 1997). Survey data at any given point can be corrected by subtracting the theoretical field value obtained from IGRF, from the measured value.

After applying different corrections to the raw data, the next step is to interpret the anomaly qualitatively and quantitatively by preparing Profile Curves and different Contour Maps, to obtain information about the depth of a particular magnetic body, its shape, size and details about its magnetization. During interpretation, it is better to use an integrated approach and to include any other apriori information about the geology of a given study area to exact the result.

CHAPTER FOUR

4. DATA ACQUISITION AND PROCESSING

4.1 Survey Line Selection

Water supply is the key issue for the achievement of the goal set by Wolaita-Sodo University in a community-based service project to overcome the food insecurity problem in different parts of the Zone in collaboration with different stakeholders, governmental and non-governmental officials. So, detailed groundwater potential study becomes crucial due to lack of surface water for irrigation at Humbo-Larena and the surrounding rural Kebeles. In addition to utilizing previous geological, hydrogeological and geophysical studies available over the area VES and magnetic methods are chosen in this study. Accordingly, a detailed study of the lithology, groundwater potential of the area, geological structures related to the flow of groundwater and the characterization of subsurface rocks are planned to be done. The layout of the geophysical survey profile lines and observation points for the electrical and magnetic survey are as shown in Figure 4.1.

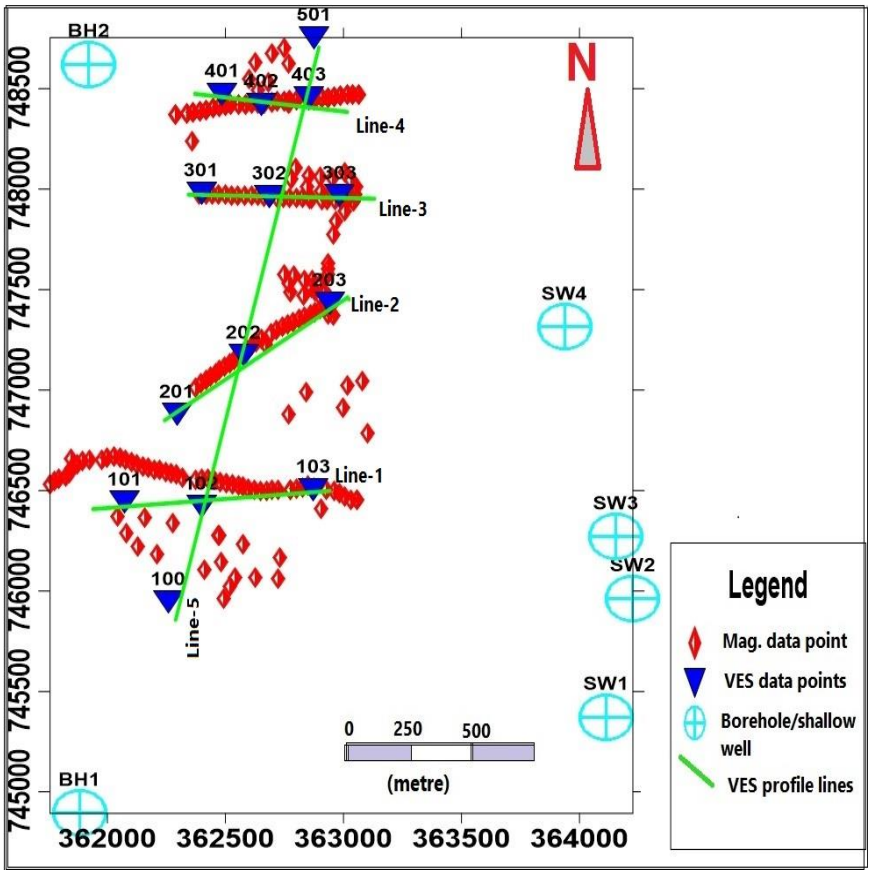

Figure 4.1: Distribution of VES points, magnetic profile line and location of boreholes over the study area.

A total of fourteen VES were conducted over five survey lines and an adequate number of magnetic data point readings were collected for mapping and analysis as well as profile plot and 2D modeling of the data. Additionally, six existing water well data from the vicinity of the study area are included to help the calibration of the electrical data and facilitate better interpretation.

4.2 Electrical Resistivity Survey Data Acquisition and Field Lines

The Vertical Electrical Sounding method was employed by using the Schlumberger configuration with half current electrode distance (AB/2=max of 500m) along five selected traverse lines that are oriented in near NE-SW and E-W directions. The instrument used for the survey is the PASI-16 GL Earth Resistivity unit along with the P100-3 Energizer. Stainless steel electrodes and specially designated cables on reels were used along with meter tape and hammers. Recording of the sounding point coordinates was done by using Handheld GPS. Additionally, short-range communication radios (walky-talkies) were used for ease of exchanging information during the survey. During the record of the VES point data, the data were plotted and examined at the same time on log-log paper to control data quality.

4.3 Data Reduction and Processing

4.3.1 Reduction and Processing of VES Data

During plotting of the VES data on the Log-Log paper, the curve is segmented due to overlap measurement at a time when the potential electrode distance (MN/2) is increased as the current electrode distance (AB/2) becomes longer. So, to have a smooth curve for better interpretation, the segmented curves were shifted to the small MN curve points (Reynolds, 1997; Frohlich et al., 1996). VES data are also pre-processed using the WinResist software by close visual examination, selection and removal of noisy data to obtain the model resistivity sections that give a better resolution.

Two approaches of interpretation, i.e. qualitative and quantitative were used to present the field data. The number of layers and their relative resistivity values were determined by observing the shape of the field data curve using the qualitative interpretation technique. Parameters resulting from the interpretation of VES data using ipi2WIN software were used to create the initial model layer parameters for the WinRESIST inversion software. Acceptable error values ranged between 2.0% to 5.0%. On the other hand, the quantitative method involves obtaining the geo-electric parameters, i.e. true resistivity and layer thickness

of the layers of the subsurface. For constructing the geo-electric sections, that use the true resistivity and thickness of the layers, the AutoCAD software was used.

To see how the apparent resistivity varies in the area with varying current electrode distance, slice and slice-stack maps for selected values of AB/2 were constructed (Figure 5.12). Pseudodepth section maps were constructed to know the variation of the apparent resistivity with position (electrode spacing, AB/2) and with an effective depth of penetration, rather than with true depth. Both slice-stack and pseudodepth section maps were constructed using the Surfer-13 Software. The geoelectric section reveals the subsurface variation in electrical resistivity and thickness and attempts to correlate the geoelectric sequence across the profiles. The outputs of the model parameters from WinResist inversion software are used to construct the geoelectric sections (both presented under section 5.3. and in Figures there).

4.3.2 Reduction and Processing of Magnetic Data

To remove the effect of external metallic materials, care was taken before the starting of the survey. After collection of the magnetic data, step by step data reduction and processing was done to remove signal and un-relevant noise from the raw data. The reduction process involved data checking and editing to remove the none genuine noisy high spike data that were potentially caused by nearby electric power lines and other spurious signal sources; the diurnal correction was done to carry out the drift and/or temporal variation of the Earth's field on the magnetic data by establishing a base station, and IGRF correction was done to remove the strong effect of the Earth's main field.

To determine the presence and depth of shallow geological structures, such as dikes, faults, fractured zones and layer contacts, different magnetic maps were constructed using the corrected data and then interpreted qualitatively. These maps include Reduced To Pole (RTP)-map, Regional Total Magnetic Anomaly (TMA)-map, Analytic signal (AS)-map, Residual Map, HD-TDR-map, Upward Continuation (UC) to 500m and 1000m maps and Euler-Deconvolution plots for depth to causative body/source mapping. Further, 2D modeling of the data for selected profiles were done. The analysis and processing of the magnetic data were done by a specialized computer program (Oasis Montaj V-7.0-1, 2007).

CHAPTER FIVE

5. RESULTS AND INTERPRETATIONS

5.1 General

For the determination and conclusion regarding the groundwater occurrence and potential in the study area, an integrated approach consisting of the geophysical methods of electrical resistivity (VES) and magnetic methods were used in combination with the existing borehole lithological data and geological information on the area were used to obtain better results. For the electrical data, different sections were produced from the apparent resistivity data and layer parameters of each sounding curve were determined that showed the contrast in the resistivity and depth of the underlying rock units. VES model results, constrained with the lithological logs, were used to produce the geoelectric sections. For the magnetic data, different magnetic anomaly and profile plots, such as regional residual separated anomaly plots, magnetic profile plots and 2D model sections were produced using the magnetic survey results showing the variation in the underlying lithology and the existence of possible geological structures over the study area.

5.2 Interpretation of the VES Curves

The interpretation of each VES data was carried out using the combination of ipi2WIN and WinRESIST inversion software that resulted in one dimensional (1-D) models of the VES data which were further integrated with the lithological logs to produce the geo-electric sections. The 1-D models of the VES data are compared with the field data curves plotted on a log-log paper are seen to show a good correlation between the two for all the sounding points with evidence of RMS error between 2% to 5%. Figure 5.1 illustrates four interpreted 1-D models of VES data curves taken from each survey line. Interpreted VES curves for the rest of the sounding points of all the survey lines are found in Annex-1.

5.3 Pseudo-depth section and geoelectric section of the profiles

After field data quality control and initial processing, the results are presented (interpreted) both qualitatively; to observe the shape of the VES curve as layer models and pseudodepth sections which give information about the number of layers of the subsurface, relative values of resistivity of subsurface layers and for information on relative values of thickness of the subsurface lithology that are component part of the initial information for identification of a

high potential zone of groundwater; and quantitatively; to know geoelectrical parameters (true resistivity and layer thickness) obtained from the geoelectric sections.

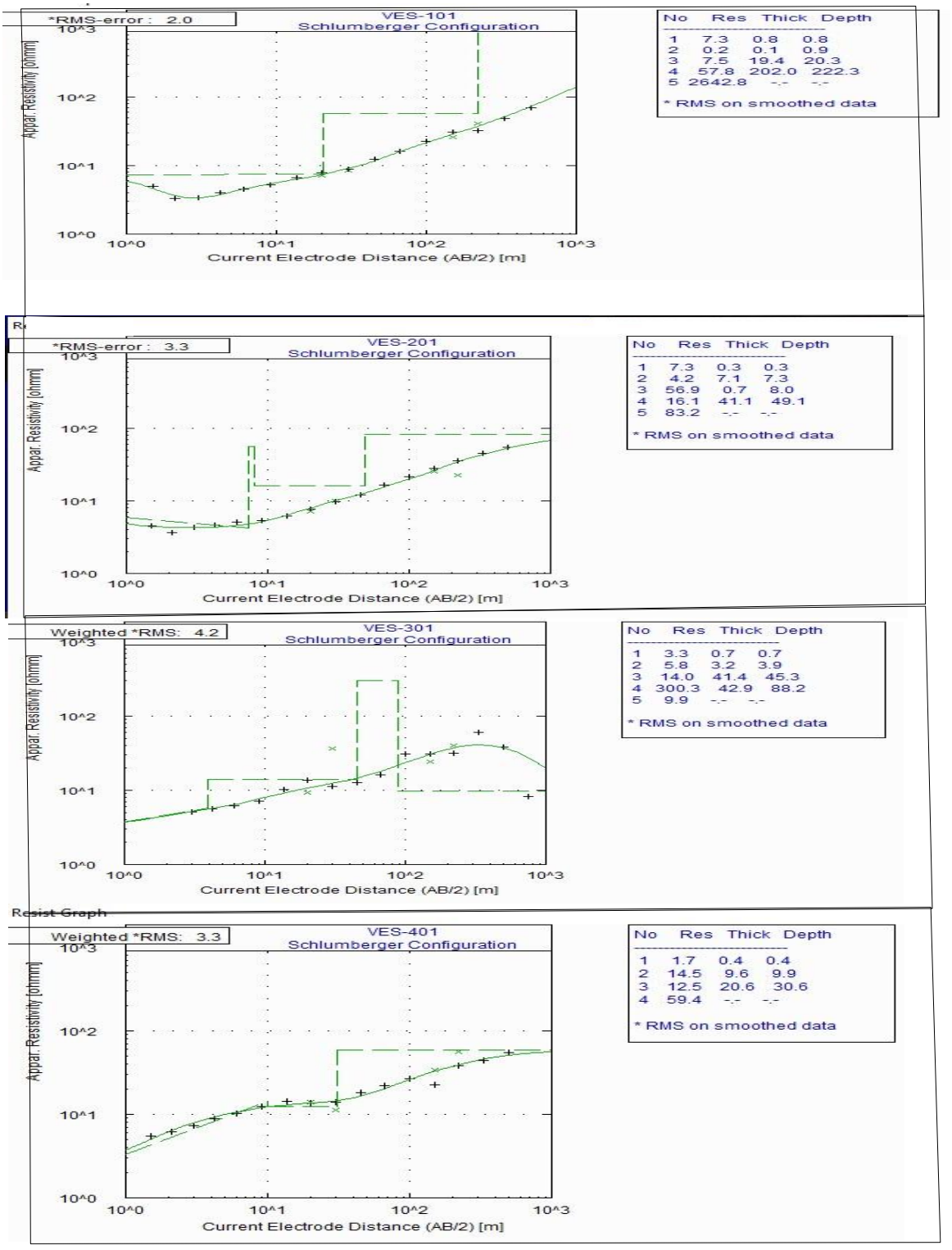

Figure 5.1: Illustration of four selected interpreted 1-D models of the VES data.

Pseudodepth sections were constructed using the Surfer software (Geotomo, V-13) whereas for the construction of the geoelectric sections, the VES data was processed using the ipi2WIN and WinResist software. Having initial model parameters through these processes is followed by construction of the geo-electric sections which were plotted using the AutoCAD-(Autocad, 2007) and the handy paint software.

The lithologic logs from boreholes that are found near a particular profile were used to fix the thickness of the layers by grouping the lithological units based on their type and degree of weathering and fracturing. The pseudodepth sections along the survey lines were examined to see the relative resistivity variations when preparing geoelectric sections.

5.3.1 Pseudodepth section and Geoelectric Section of Profile-1

a) Pseudodepth section of Profile-1

Three sounding points; V-101, V-102 and V-103; are aligned on this survey profile that is oriented in a near west to the east direction (Figure 4.1). Figure 5.2 shows a 2-D section of apparent resistivity response in which the upper part of all the three sounding points shows low resistivity values which range from 7.2 Ω-m to 20 Ω-m.

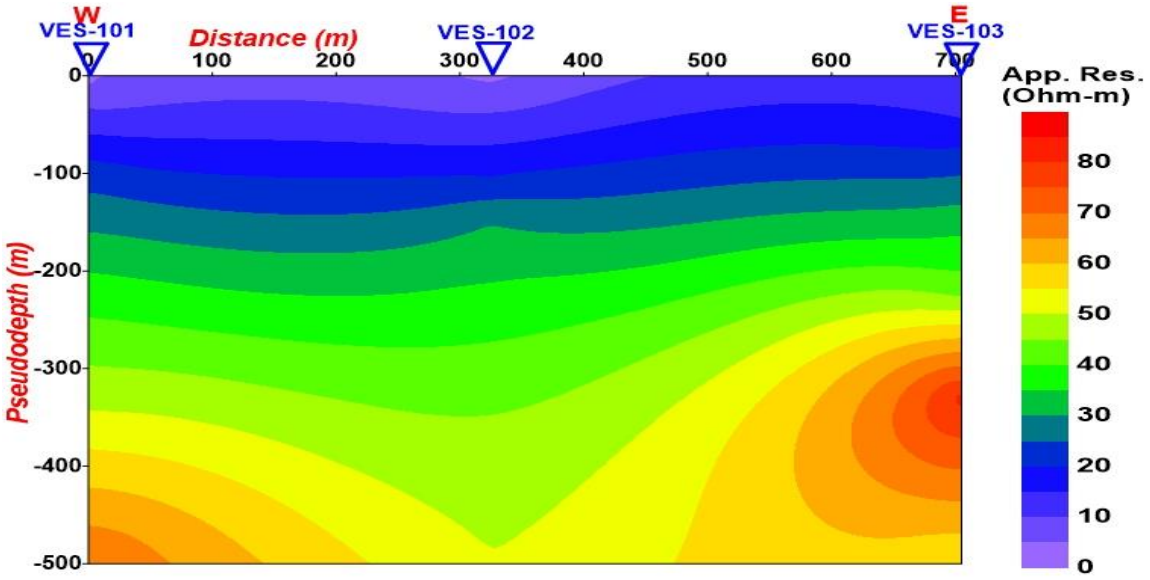

Figure 5.2: Apparent resistivity pseudodepth section along Profile-1.

This low resistivity value increases downward to some extent for VES-101 and VES-103 but, beneath VES-102, the low resistivity value goes to a deeper depth; which shows a horizontal variation of resistivity at the bottom, indicating the region of VES-102 is potentially water-saturated at depth relative to the others. The conductive zones below VES-101 and VES-103

are indicative of a variation in resistivity resulting from differences in weathering and the depth to the less weathered bottom units.

b) Geoelectric Section of Profile-1

The geoelectric section (shown in Figure 5.3) modeled to represent the subsurface lithology is constructed from the interpreted layer parameters (true resistivity and thickness) of each VES point along with the line and borehole data from nearby.

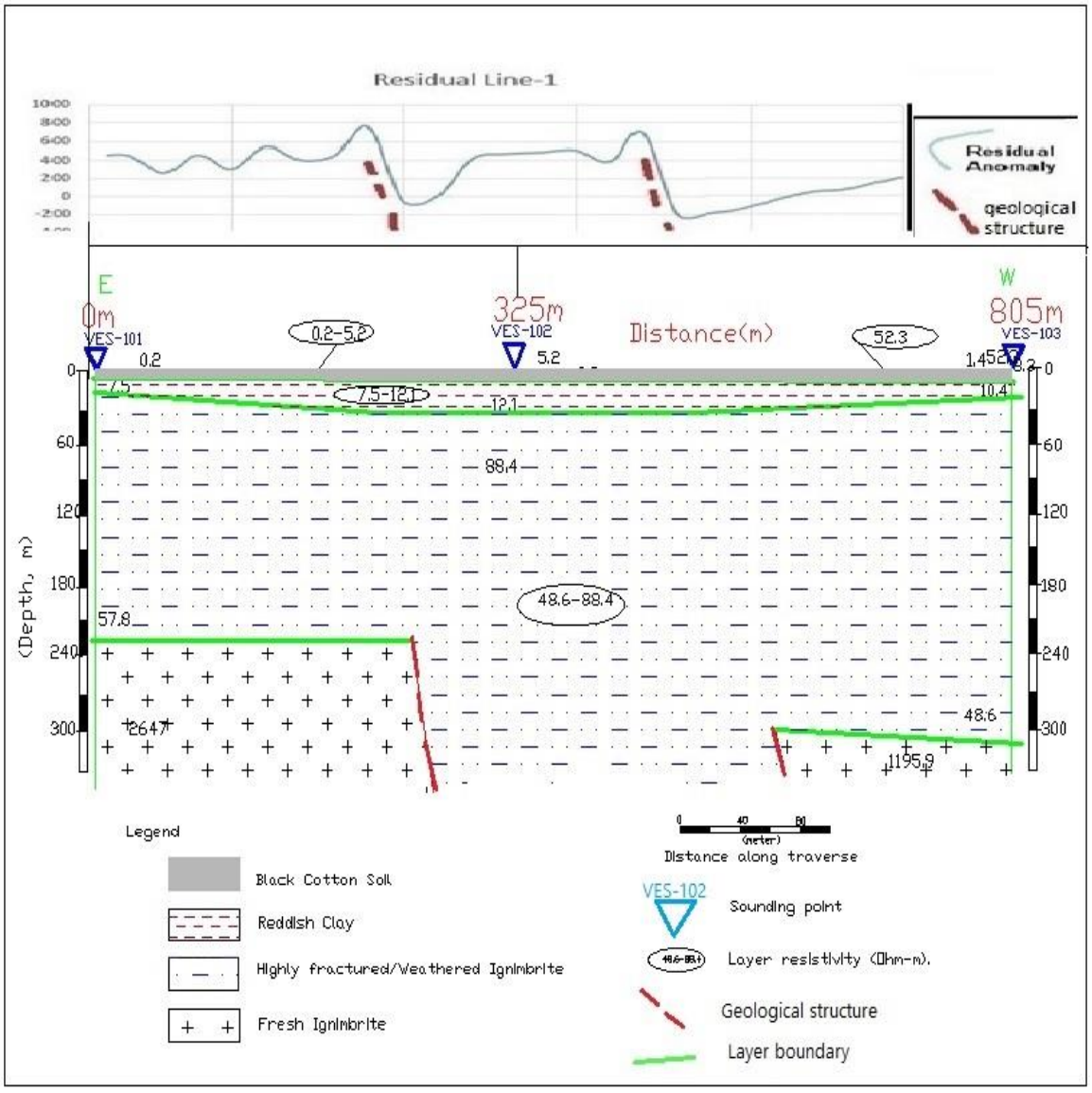

Figure 5.3: Geoelectric section along Profile-1 with magnetic profile plot for the same line.

The lithological description of BH-1 (called Shochoro-Pesho), SW-35.50 (Huletegna-Gututo_01), and SW-41.10 used for constraining the VES data are given in Annex-2A, Annex-2D, and Annex-2E respectively. VES-101 and VES-103 show the presence of four

geoelectric layers with the bottom layer having highest resistivity value while the subsurface beneath VES-102 shows the presence of three geoelectric layers.

The top layer has a very low resistivity value ranging from 0.2 Ω-m to 5.2 Ω-m indicating the presence of clay and silt as topsoil. The second layer has a relatively higher resistivity than the first one, but its value is low when compared to the bottom two. This geoelectric layer has a resistivity range from 7.5 Ω-m to 12.1 Ω-m and with a thickness of 0.1m to 1.1m. The geoelectric section possibly reflects a thin clay layer.

The geoelectric section below the second layer shows resistivity values ranging from 48.6Ω-m to 88.4 Ω-m. This layer likely indicates highly weathered ignimbrite and slightly to highly fractured ignimbrite which is a relatively good groundwater potential zone, especially beneath VES-102, having low resistivity and larger thickness. This layer has an average thickness of about 160m and the top of the potential water saturated zone/aquifer/ lies at a depth of 58m, 30m, and 48m below VES-101, VES-102, and VES-103 respectively. The bottom geoelectric layer is relatively conductive beneath VES-101 and VES-103 at a depth of 222m to 303m whose resistivity value is 2648 Ω-m and 1195.9 Ω-m respectively. This layer is most probably indicating the fresh ignimbrite.

5.3.2 Pseudodepth section and Geoelectric Section of Profile-2

a) Pseudodepth section of Profile-2

As can be seen from Figure 5.4, three VES points i.e. VES-201, VES-202, and VES-203; are aligned along this profile, which is oriented about a SW-NE direction.

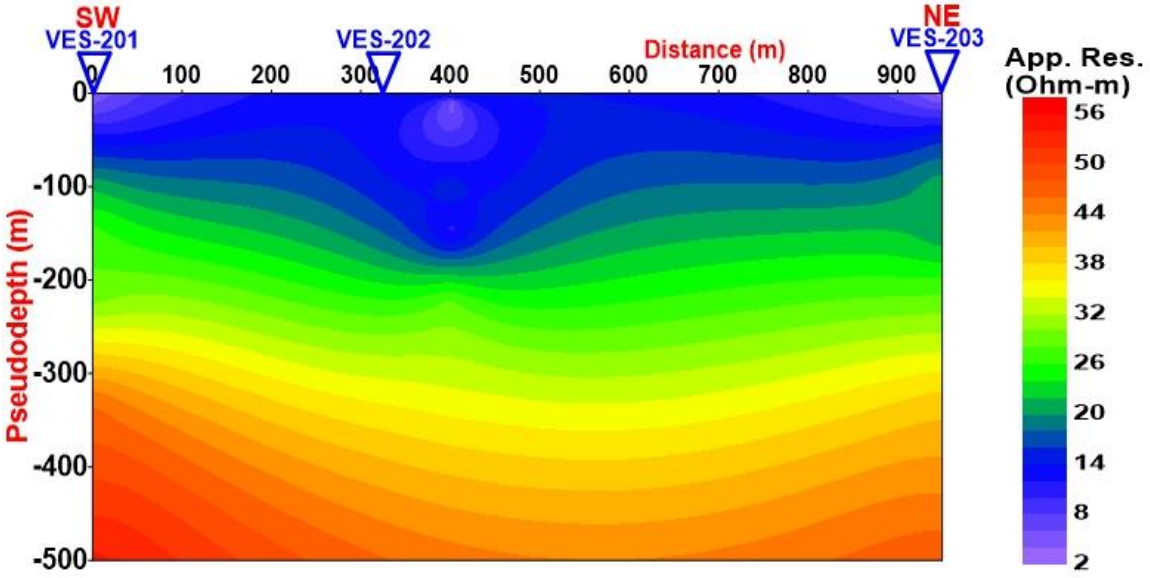

Figure 5.4: Apparent resistivity pseudo-depth section along Profile-2.

The apparent resistivity is very low in the upper region, within the range of 2Ω-m up to 20Ω-m and it increases downward. The resistivity values show smooth increment from the upper part to the lower part under all three VES points. However, the resistivity value is not showing an exaggerated increment even at the bottom of the three VES points. So, the vast region under this section generally shows a low resistivity range (2 Ω-m up to 60 Ω-m) that indicates potential water saturation or weathered stratum with less weathering at depth. It could possibly be the response of thick layer of soil with various sorting and composition.

b) Geoelectric Section of Profile-2

The geoelectric section (Figure 5.5) is constructed from the three VES points; VES-201, VES-202 and VES-203; in combination with some information from the nearby well data, i.e. from the lithological description of BH-1 (called Shochoro-Pesho) and SW-37.70 (Shochora-Ogadama), as given in Annex-2A and Annex-2C.

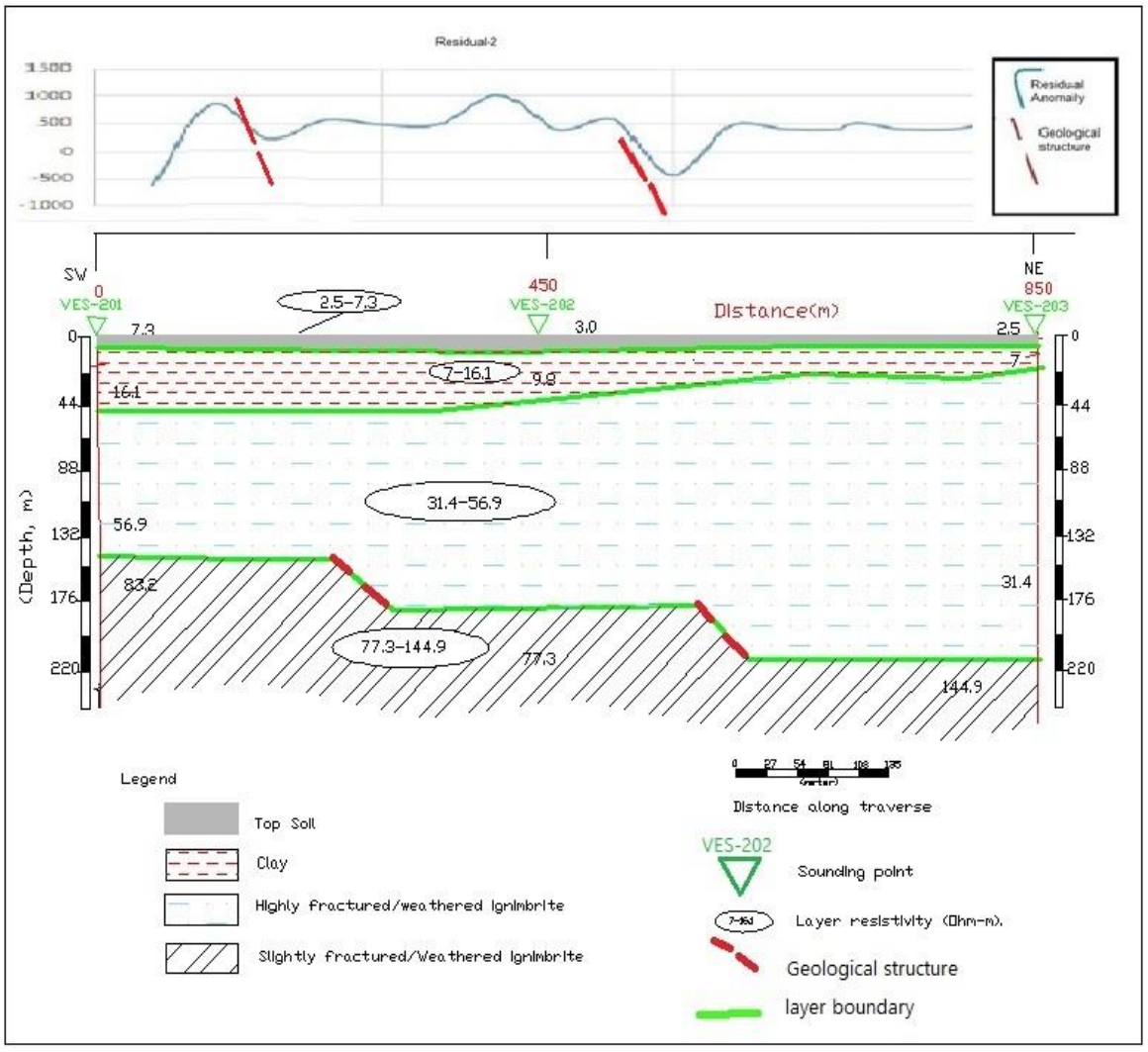

Figure 5.5: Geoelectric section along Profile-2 with magnetic profile plot for the same line.

The subsurface of profile two is represented by four different geoelectric sections. The top thin layer having a very low resistivity value (ranging from 2.5 Ω-m -7.3 Ω-m) represents the topsoil. Beneath this layer, another layer of low resistivity (7 Ω-m up to 16.1 Ω-m) with a thickness of 7.1m to 10.8m represents the reddish clay layer.

The layer underlying the second geoelectric section has a resistivity value between 31.4 Ω-m up to 56.9 Ω-m and with an average thickness of 93m. This geoelectric section represents highly fractured ignimbrite. Based on its low resistivity value and optimum thickness the layer could be a potential zone for groundwater accumulation. The top of this layer lies at an average depth of about 35m. The last layer with resistivity ranging from 77.3Ω-m up to 144.9Ω-m geologically represents a slightly fractured ignimbrite.

5.3.3 Pseudodepth section and Geoelectric Section of Profile-3

a) Pseudodepth section of Profile-3

The constructed pseudo-depth section of line-3 includes VES-301, VES-302, and VES-303 which lies in the west to the east direction along with the profile (Figure 5.6). The upper portion of the section shows low resistivity with no lateral variation under all three sounding points. But, the bottom portion of the section beneath VES-301 shows a higher resistivity value than the other two sounding points. The wide region beneath VES-302 and VES-303 is relatively conductive than VES-301 showing a lateral variation in resistivity at the bottom region. The low resistivity zone under VES-302 and VES-303 are indicative of good potential water saturation.

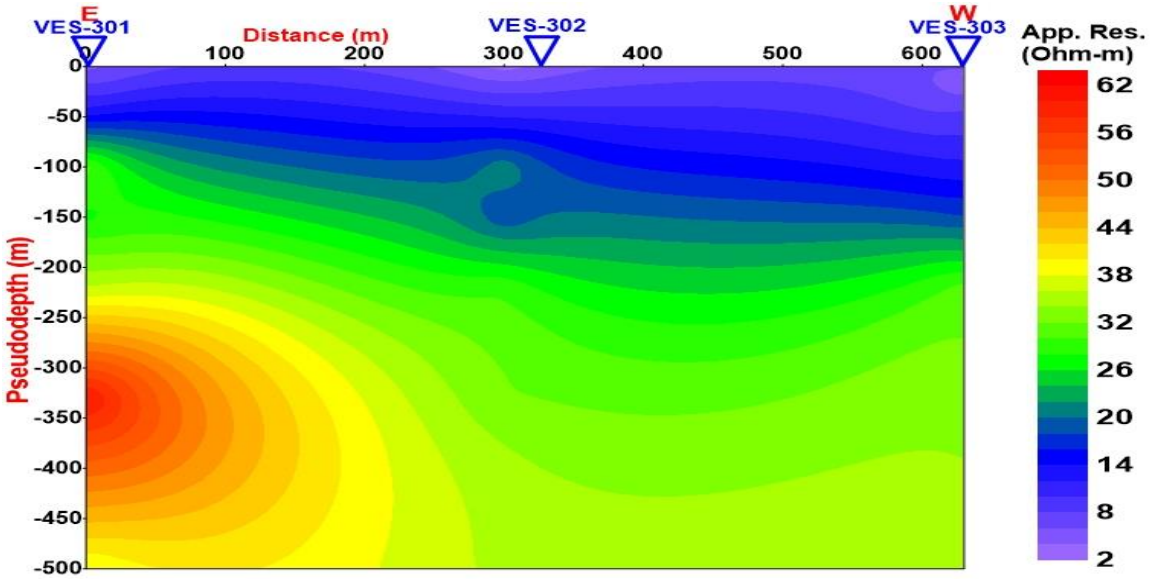

Figure 5.6: Apparent resistivity pseudodepth section along Profile-3

b) Geoelectric Section of Profile-3

The geoelectric section (Figure 5.7) of this line is constructed from the three VES points; VES-301, VES-302, and VES-303; by including the borehole data taken from nearby water well lithological description of BH-2 (called Gututo-Larena) and SW-37.70 (Shochora-Ogadama) as given in Annex-2B and Annex-2C.

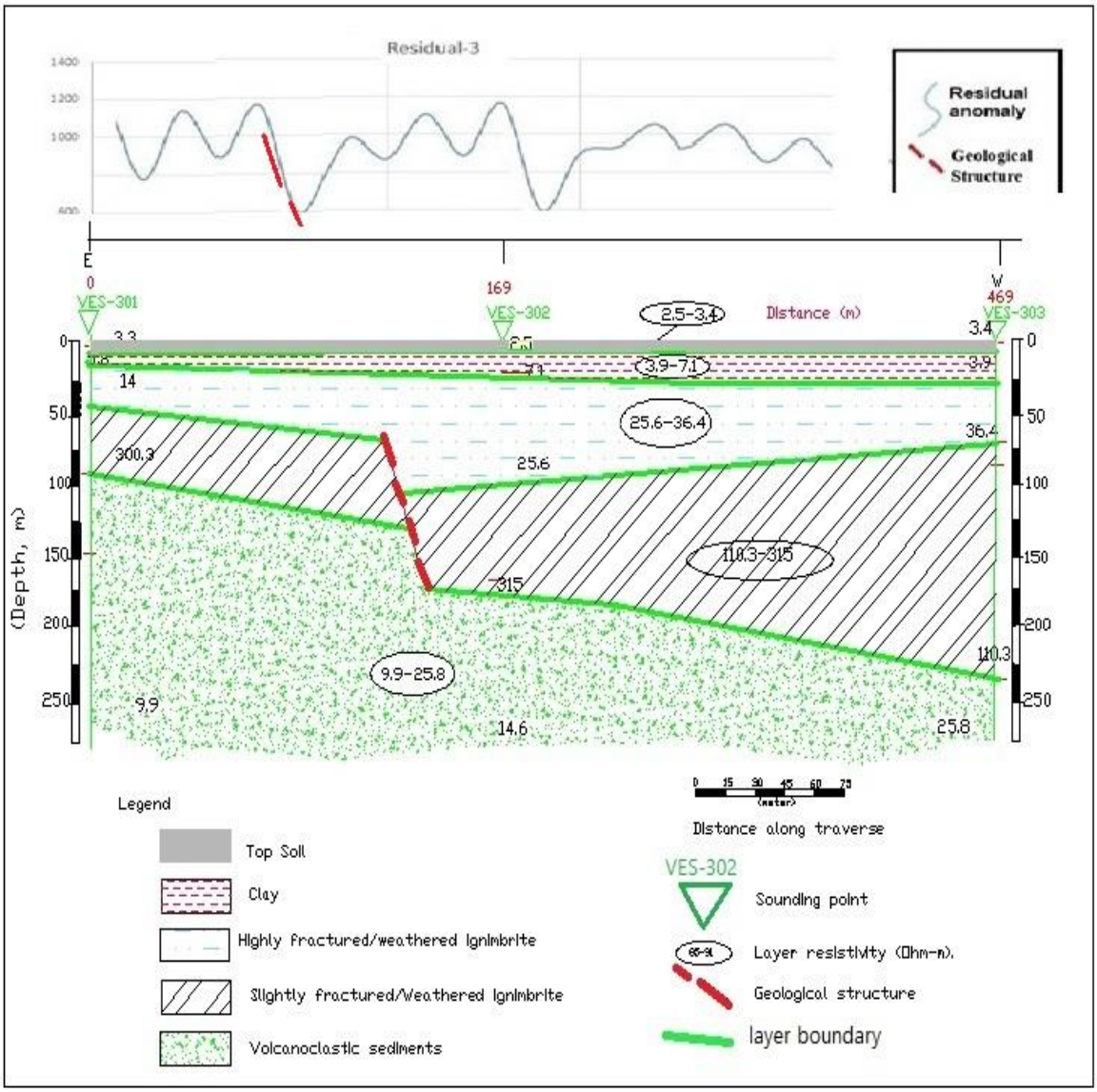

Figure 5.7: Geoelectric section along Profile-3 with magnetic profile plot for the same line.

Five geoelectric sections are representative of the subsurface of profile three. The very thin topmost layer that has a resistivity value ranging from 2.5 Ω-m 3.4 Ω-m is the topsoil or black cotton soil. Beneath this layer, another low resistive region (ranging from 3.9 Ω-m 7.1 Ω-m) is represented by tuff. The third layer has a relatively high resistivity value ranging

from 25.6 Ω-m 36.0 Ω-m with an average thickness of 70m represents the highly weathered and fractured ignimbrite. This layer could be good groundwater potential, where its top part lies at an average depth of about 22m. The fourth geoelectric layer of this line has a high resistivity value; ranging from 110 Ω-m up to 315 Ω-m which represents fresh ignimbrite. The final (fifth) geoelectric layer of line-3 has a resistivity value ranging from 9.9Ω-m up to 25.4 Ω-m which is a very low resistivity value. The top part of this layer lies at a depth of about 85m, 150m, and 220m below VES-301, VES-302, and VES-303 respectively, and this layer represents volcanoclastic sediments and/or volcanic sand/ash. Accordingly, the layer could be a potential zone for groundwater accumulation.

5.3.4 Pseudodepth section and Geoelectric Section of Profile-4

a) Pseudodepth section of Profile-4

Three sounding points; VES-401, VES-402, and VES-403; are lined along the west to the east direction of the profile used for the construction of the pseudo-depth section (Figure 5.8). The upper portion of the profile shows a low resistivity value under all three sounding points. The resistivity increases downward smoothly, but the increment in resistivity value varies under the three points. Beneath VES-401, and VES-402 the lower layer is relatively conductive than VES-403. So, there is some lateral variation of the resistivity at the bottom part of the section. The low resistive large region under VES-403 is indicative of potential groundwater.

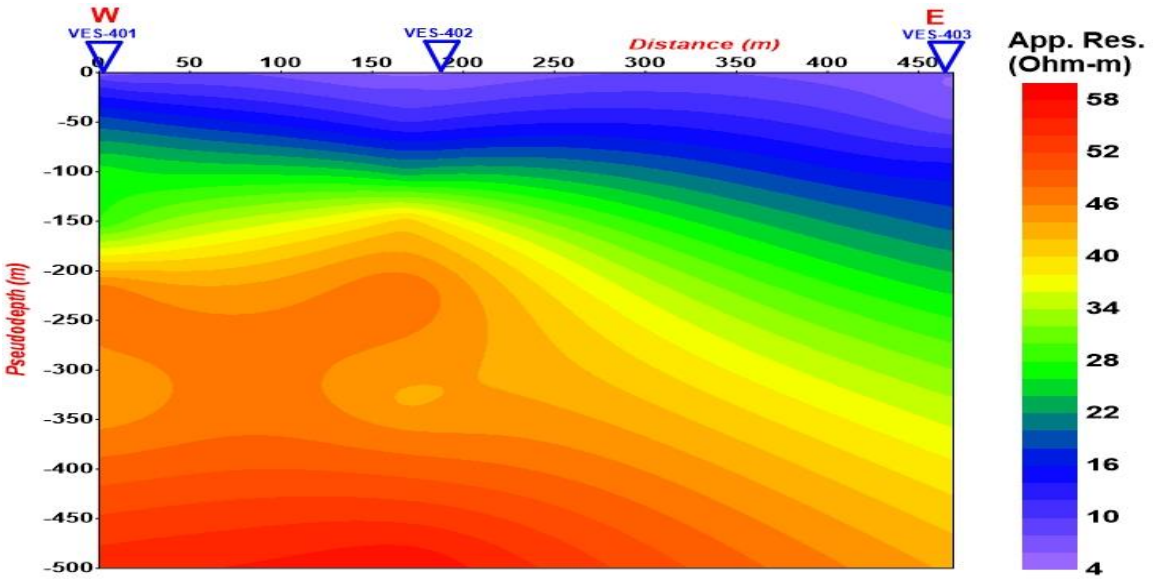

Figure 5.8: Apparent resistivity pseudodepth section along Profile-4.

b) Geoelectric Section of Profile-4

According to Figure 5.9, four geoelectric layers represent the profile. The geoelectric section is constructed by integrating the interpreted layer parameters of the sounding points; VES-401, VES-402, and VES-403; and the lithological log of nearby water wells, BH-2 (called Gututo-Larena) and SW-37.70 (Shochora-Ogadama) as given in Annex-2B and Annex-2C.

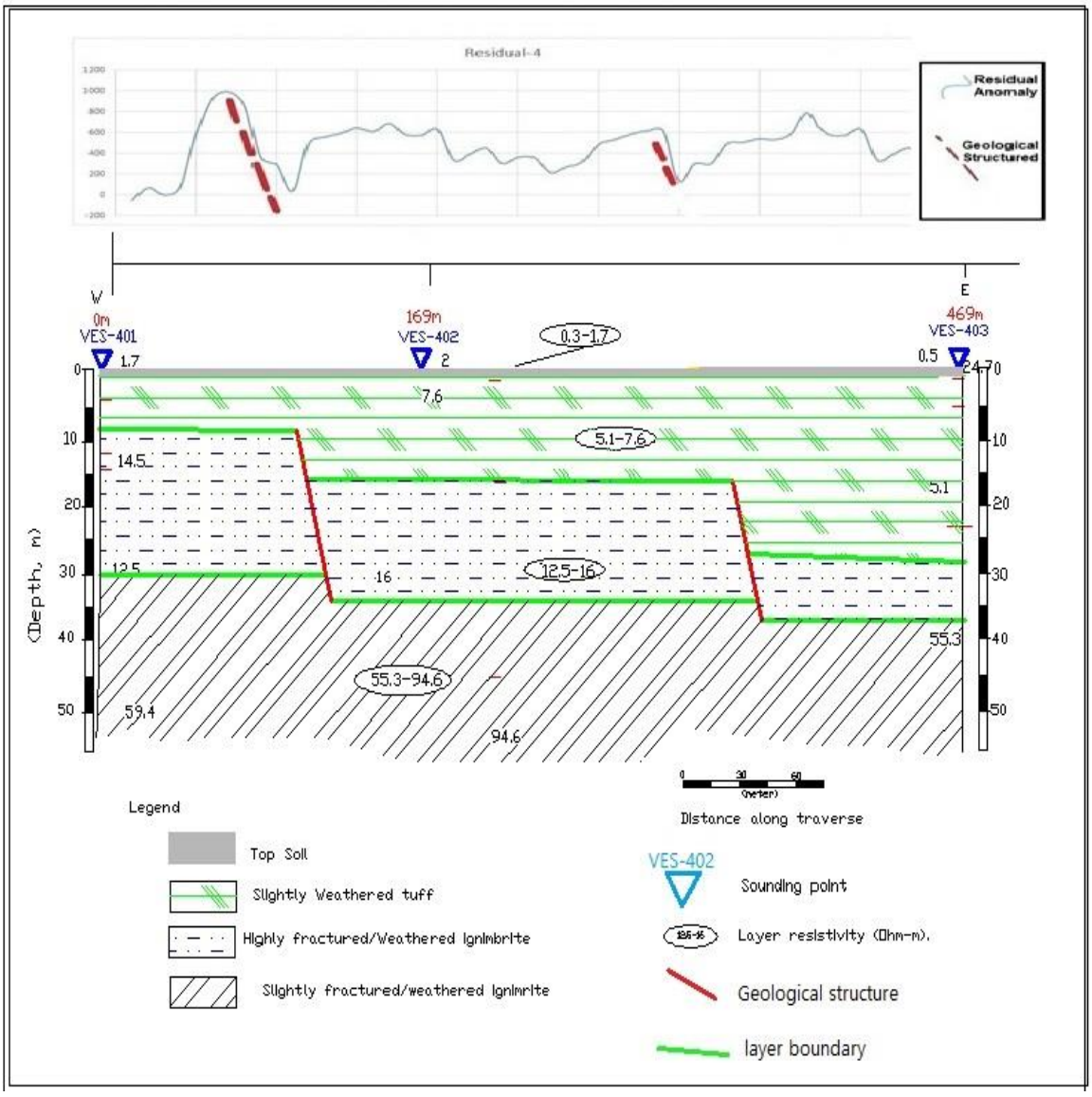

Figure 5.9: Geoelectric section along Profile-4 with magnetic profile plot for the same line.

The top thin layer having a resistivity value ranging from 0.5 Ω-m up to 1.7 Ω-m represents the topsoil. Beneath this layer, the second layer with a resistivity value from 5.1 Ω-m up to 7.6 Ω-m represents the slightly fractured and weathered tuff. The third layer has a resistivity value ranging from 12.5 Ω-m up to 16 Ω-m and with a thickness from 10m up to 25m represent highly fractured and weathered ignimbrite. This layer due to its low resistivity and moderate thickness it could be a good potential zone for groundwater accumulation.

The bottom layer has a resistivity value ranging from 55.3Ω-m up to 91.6Ω-m. this layer represents a slightly fractured and weathered ignimbrite. The inferred geological structure (fault) is correctly aligned with the regional fault system.

5.3.5 Pseudodepth section and Geoelectric Section of Profile-5

a) Pseudodepth section of Profile-5

Six strategically selected VES points; VES-100, VES-102, VES-202, VES-302, VES-402, and VES-501; constructed the pseudo-depth section of Profile-5 as shown in figure-5.10.

Taking the longest direction of the study area, this plan of action is intended to accomplish how the resistivity of the subsurface looks in different azimuth. This line is more or less perpendicular to all the previous four profiles (see Figure 4.1) and its direction is NNE to SSW. The upper layer of the profile shows a low resistivity region under all the sounding points and this low resistivity value smoothly increases downward. The bottom part of the profile shows a lateral variation of resistivity in which the region under VES-100, VES-102, VES-202, and VES-501 are relatively conductive. The wide region beneath the other sounding points; VES-302, and VES-402; shows low resistivity nature which could be a potential zone for groundwater accumulation

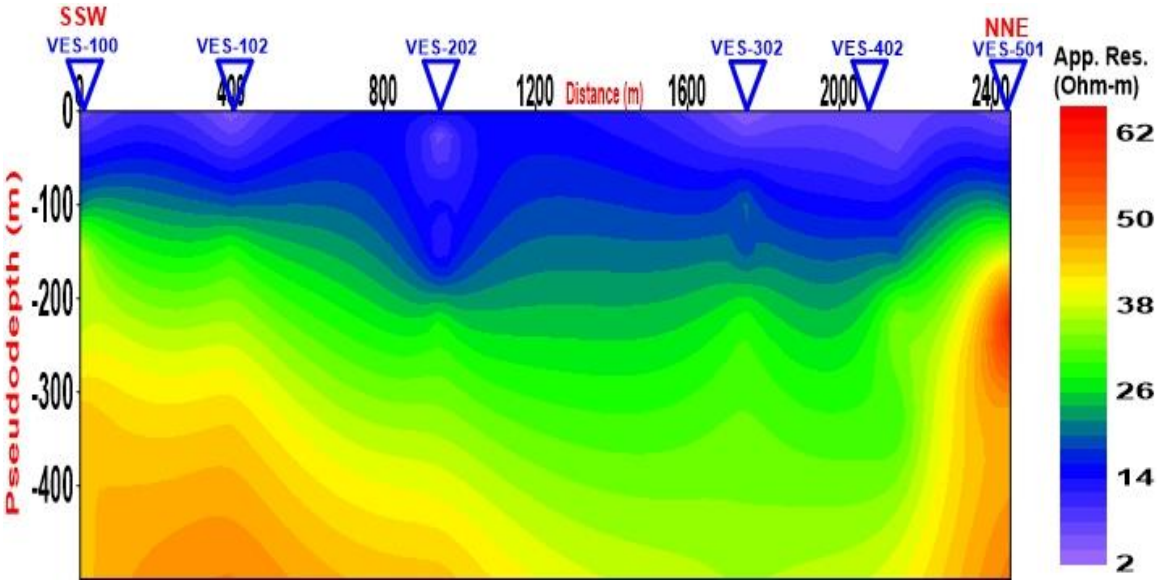

Figure 5.10: Apparent resistivity pseudodepth section along Profile-5.

b) Geoelectric Section of Profile-5

The geoelectric section of this profile (Figure 5.11) is constructed from the interpreted layer parameters of six strategically selected VES points; VES-100, VES-102, VES-202, VES-302, VES-402 and VES-501, in integration with the lithological logs of nearby water wells; two

boreholes and four shallow well data. The lithological description and correlation of the wells are given in Annex-2A up to Annex-2G.

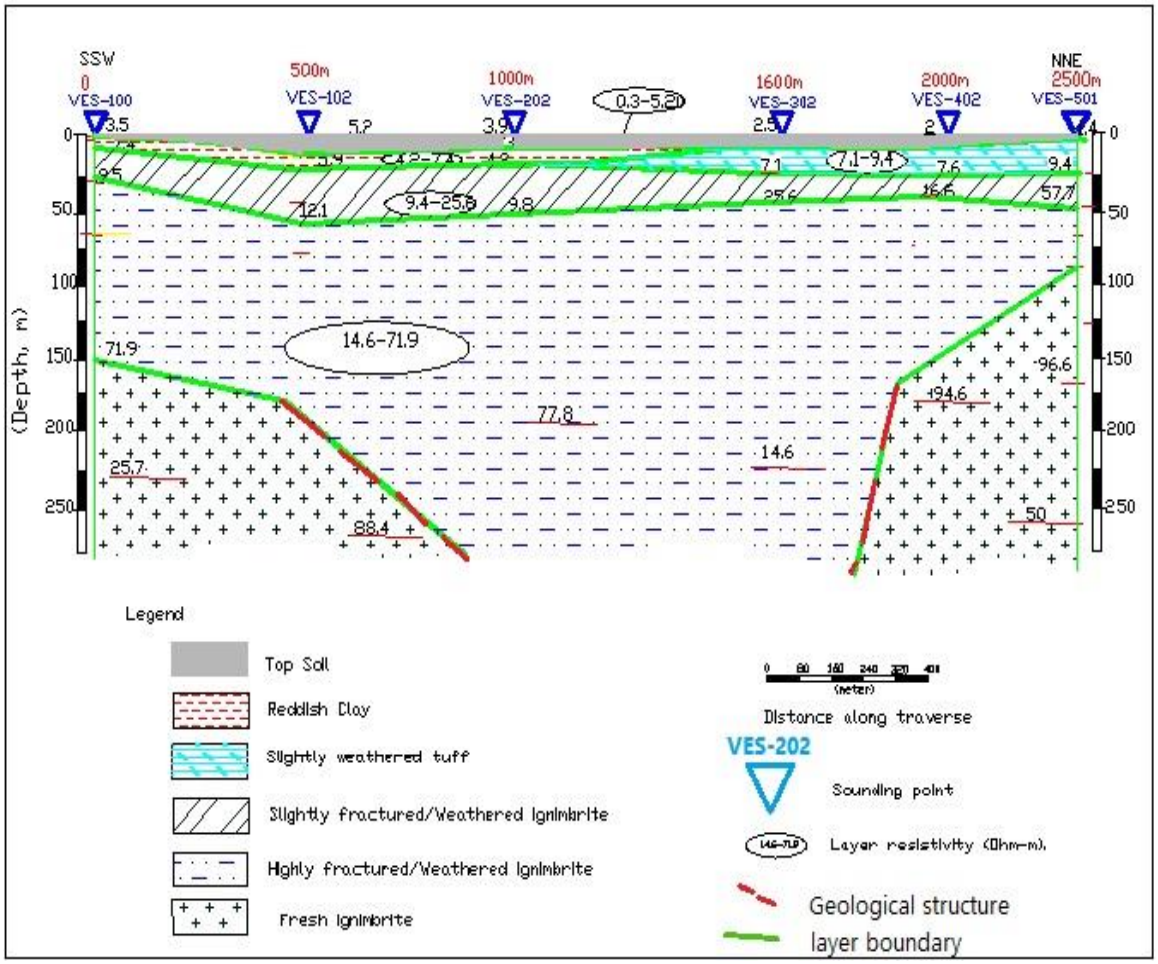

Figure 5.11: Geoelectric section along Profile-5.

The geoelectric section has four to five layers. The top layer of the profile is a very low resistive layer with resistivity ranging from 0.3 Ω-m up to 5.2 Ω-m and it represents the topsoil. The geoelectric layer beneath this layer has two different parts. The second layer below the three sounding points to the south direction of the profile has a resistivity from 4.2 Ω-m up to 7.2 Ω-m with an average thickness of 5m and this layer represents the reddish clay, whereas the second geoelectric layer under the three sounding points to the north direction of the profile has a resistivity ranging from 7.1 Ω-m up to 9.4 Ω-m and is 5m up to 8m thick that represents tuff. The third geoelectric layer of profile-5 has a resistivity value ranging from 9.4 Ω-m up to 25.6 Ω-m with an average thickness of 21m represents the slightly fractured ignimbrite. Beneath this layer, the fourth geoelectric layer with a resistivity value ranging from 14.6 Ω-m up to 71.8 Ω-m and having an average thickness of 78m represents the highly fractured and weathered ignimbrite.

5.4 Sliced-Stacked Section for different AB/2

Great attention is given to the vertical and horizontal variation in the relative apparent resistivity value of the area to locate the borehole site. A Sliced-stack map (shown in figure 5.12) better demonstrates this variation of resistivity value in the area that has been constructed by selecting different AB/2 distances depending on the variability between them, AB/2= 1.5m, 45m. 150m, 220m, 330m, and 550m. It is found that the resistivity value varies from 2-82 Ω-m.

As can be seen from Figure 5.12 although almost all parts of the area are low in their apparent resistivity value (<100Ω-m), the central region of all half current electrode spacing (AB/2) is dominated by a very low resistivity value (<50 Ω-m). In addition, almost all regions at AB/2=1.5m, AB/2=45m, AB/2=150m, and AB/2=220m show low resistivity value (<40 Ohm-m). Relatively higher apparent resistivity regions (>50 Ω-m) are revealed at SE-parts of AB/2=330m and South West, Northern, and Northeastern parts of AB/2=500m. Accordingly, potential productive boreholes could be proposed at the central, western end, and/or at the northwestern part of the study area.

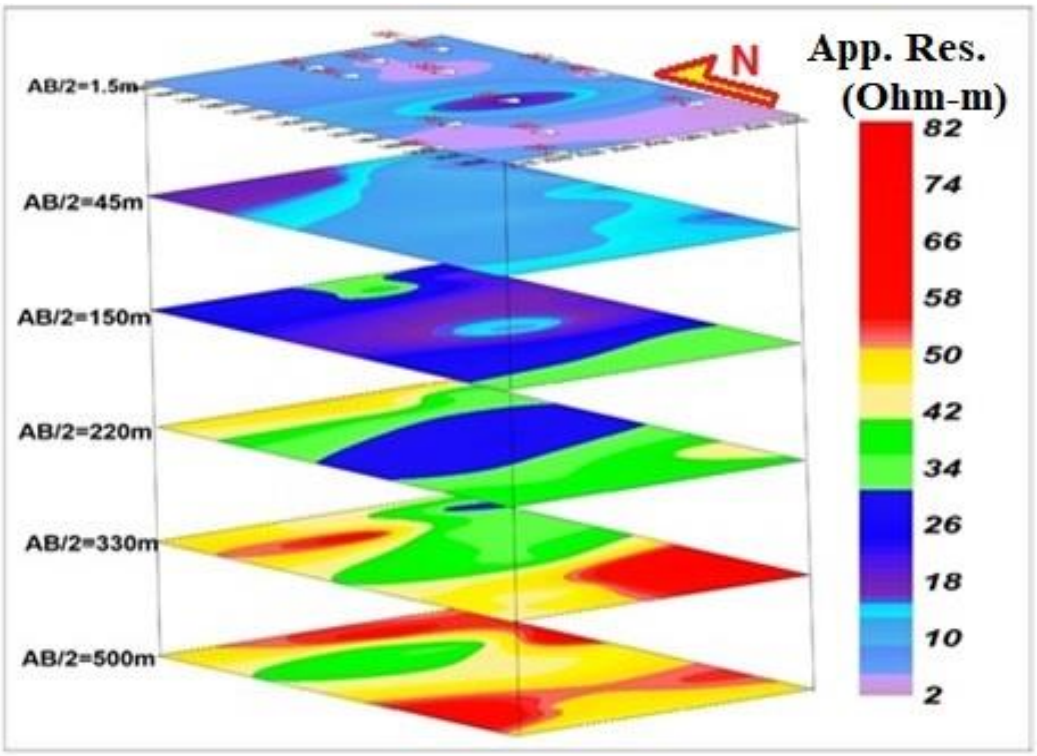

Figure 5.12: Sliced-Stacked Section map for different AB/2.

5.5 Interpretations of Magnetics

5.5.1 General

After correcting the effects or noises from a wide variety of sources (natural and man-made surface features, as well as instrumental; from observed data to eliminate or at least to minimize these effects) and IGRF correction (by subtracting the main geomagnetic field from the diurnal corrected observed data) the product of this processing is the magnetic anomaly. The results were further processed and analyzed using 2D gridding, contouring, and mapping software Oasis Montaj (V-7.0.1). For effective interpretation of the magnetic data, further enhancements were carried out using various transformations such as analytical signal, horizontal/vertical derivative and gradient, RTP, and tilt angle derivative. Different anomaly maps were then produced to show the contrast in the susceptibility, magnetization direction, and remanence of the subsurface rocks as shown in the coming sections.

5.5.2 Total Magnetic Field Anomaly (TMA) Map

This map (Figure 5.13) resulted after applying the diurnal and IGRF corrections to the collected field data.

Accordingly, the Northern, SW, and SE parts of the map show very low magnetic anomaly, whereas higher magnetic anomaly values are generally displayed on the central parts of the study area.

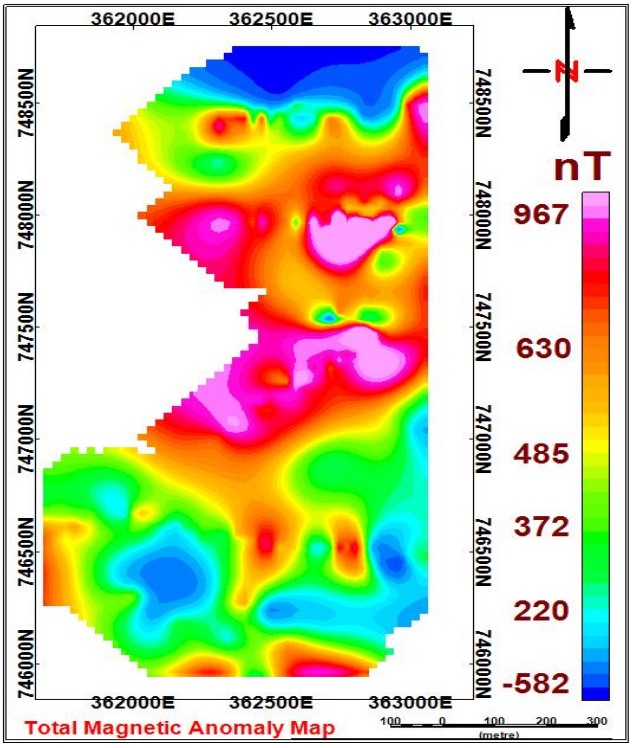

Figure 5.13: Total Magnetic Field Anomaly Map of the study area.

Reduced to Magnetic Pole (RTP) Map of TMA

When the magnetic survey takes place in areas besides the magnetic poles, especially in the lower magnetic poles, their anomalies will be affected due to the earth's magnetic inclination and declination. The map shows asymmetric and distorted nature, so when RTP-filter is introduced to Total Magnetic Field Anomaly (TMA) data it will provide a map that is more closely related to the rock magnetization and locates anomalies exactly above their sources. In this way, the pattern of magnetic anomalous data is simplified for interpretation (Figure 5.14) using the RTP method that modified its field location to that it would be in the vertical direction.

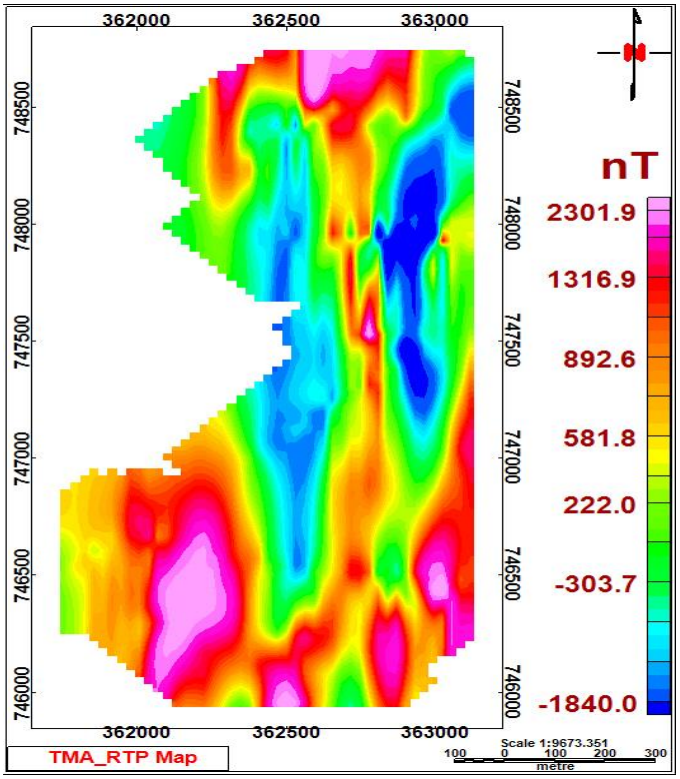

Figure 5.14: Reduced to Magnetic Pole (RTP) map of the study area

Accordingly, the Northern, South western, South Eastern and some central parts of the study area show very high magnetic anomaly informs about the presence of fresh unit beneath the surface, and the large parts of the study area show a low magnetic anomaly value that reveals the presence of thick soil cover and/or the presence of weak zones filled with weathered material which is related with the geological map of the area.

5.5.3 Separation of the Regional and Residual Magnetic Anomalies

The sum of magnetic fields produced due to the sub-surface sources (regional field from the deep-seated target objects and residual field from shallow target objects) are recorded in the magnetic data during the field survey. Since the residual anomaly is assimilated or incorporated in the regional field, it is required to separate these two fields by correctly estimating the regional field and removing it from the TMA field to yield the residual anomaly field of the target source. This process; the removal of the regional field from TMA; can be done using different methods including graphical, least square, digital filter, and stripping methods (Li and Oldenburg, 1998). The extracted residual anomalies are usually useful for tasks such as structural mapping, or qualitative interpretation based on visual inspection of the data.

A. Regional Magnetic Anomaly Map

Accordingly, the removal of the regional field is done by digital filter method by applying a low pass filtering technique to the observed data (TMA) using Geosoft Oasis Montaj Software (V-7.0.1). The result revealed the distribution of the different rock types with varying magnetic susceptibility over the study area. The high magnetic anomaly zones observed over the study area are due to the response of deep-seated high susceptible volcanic rocks (Figure 5.15).

From the regional anomaly map of the study area; Figure 5.15; it is clear that the central and NE parts of the study regions are characterized by the very low magnetic anomaly and on the other hand the northern and SE and SW parts of the study area show very high magnetic anomaly.

B. Residual Magnetic Anomaly Map

The residual magnetic field was obtained after applying a high pass filtering technique to the observed data (TMA) using Geosoft Oasis Montaj Software (V-7.0.1). This magnetic anomaly is partly due to the magnetic inclination and/or partly due to the presence of any remnant magnetization (the inclinations of magnetization and locations of the target) that govern the shape and phase of the anomaly. It is difficult to interpret the residual magnetic anomaly without further enhancement of the data since these anomalies have positive and negative components (bipolar). Therefore, the residual magnetic anomaly field data are subjected to data enhancement to eliminating the difficulty with the residual anomaly. Accordingly, the analytical signal magnetic map, the tilt derivative magnetic map, and the

Euler-depth magnetic map were produced from values of the residual magnetic anomaly map that is compiled for this study. In figure (5.16) location 01 and 02 show maximum positive anomalies where location 03 shows maximum negative anomaly.

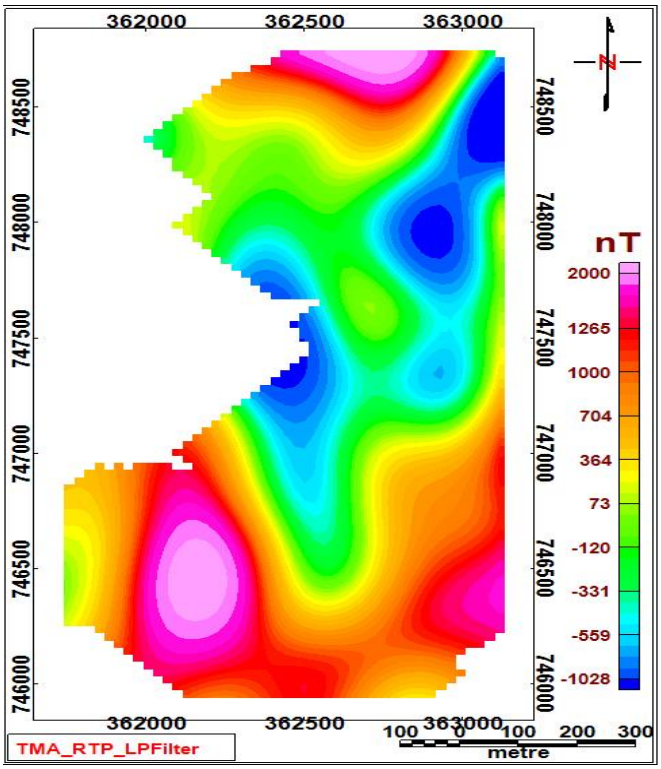

Figure 5.15: Regional Magnetic Anomaly map of the study area.

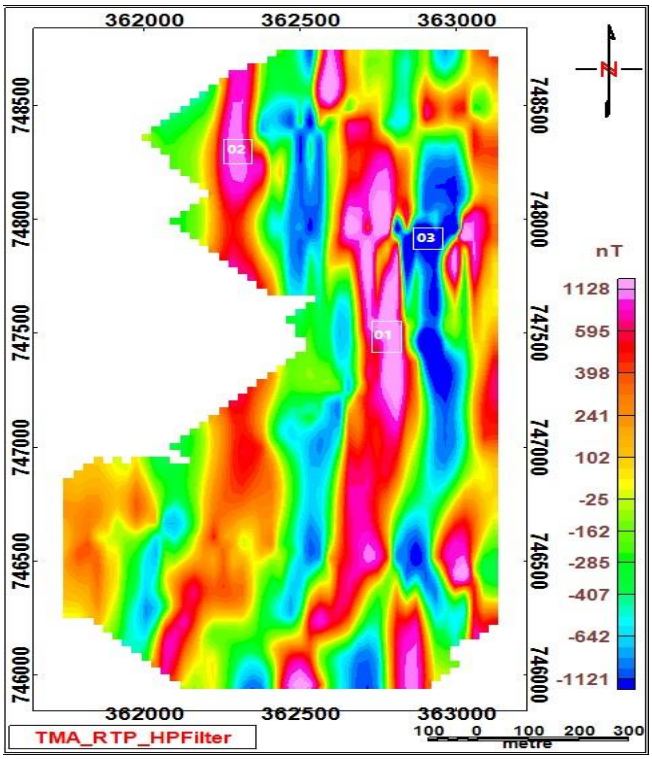

Figure 5.16: Residual Magnetic Anomaly map of the study area.

5.5.4 Data Enhancement Procedure

Different operations; such as the application of different filters; could be applied to the magnetic data to highlight field variations. Some of the data enhancement techniques applied in this work include Analytic signal, Upward Continuation, Tilt Derivative and Euler-Deconvolution depth method.

5.5.4.1 Analytic Signal (AS)

The Analytic Signal (AS) map is useful for locating the edge of the remnant magnetized body and in areas of low magnetic latitude. The shape of the analytic signal of geological bodies is not influenced by the directions of magnetization and the local geomagnetic field (Keating, P. and Sailhac, 2004). Different studies reveal that if the analytic signal calculations are performed to "Reduced to Pole" anomalies, it produces better results. So, in this research work, the analytic signal algorithm was applied to RTP data of the residual magnetic anomaly.

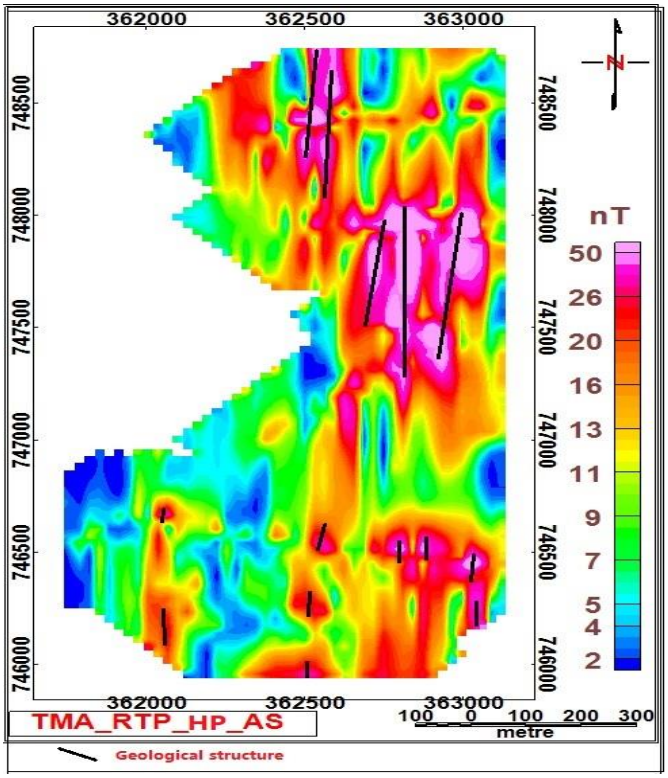

Figure 5.17: Analytic Signal map of the study area

The analytical signal map (Figure 5.17) represents the shallow subsurface conditions because it indicates the impulse response of the target body from the top part. Besides, the highest amplitude value perfectly take-up on the top of magnetic contact. It is also known that the

maximum amplitude is exactly located over a magnetic contact which depends on the location of the body (horizontal coordinate and depth) but not on the inclinations of magnetization.

From the analytic signal map (Figure 5.17) very high amplitude of the magnetic signal is observed in the central, northern, and some southern parts of the study area which has a good correlation with the points of the highest magnetic anomaly observed in the residual magnetic anomaly map. This indicates the presence of a high anomalous subsurface body or magnetic causative body location which is generally aligned in NE to SW direction. Also, networks of magnetic discontinuities are observed on the southern part of the map trending NE- SW that indicates geological structures in the study area.

5.5.4.2 Upward continuation (UC)

When the Fast Fourier Transform (FFT) filter is applied to the magnetic field data to recompute it at an elevation higher than the data is acquired, it emphasizes the field since the amplitude of a magnetic field above a source varies with elevation as an exponential function of wavelength. Upward continuation is inherently stable and acts as a smoothing filter and is beneficial for diminishing the field strengths from shallow magnetizations (residual anomaly) to focus only on deeper sources (regional anomaly) as the effect of the filter can be properly compensated by changing the elevation.

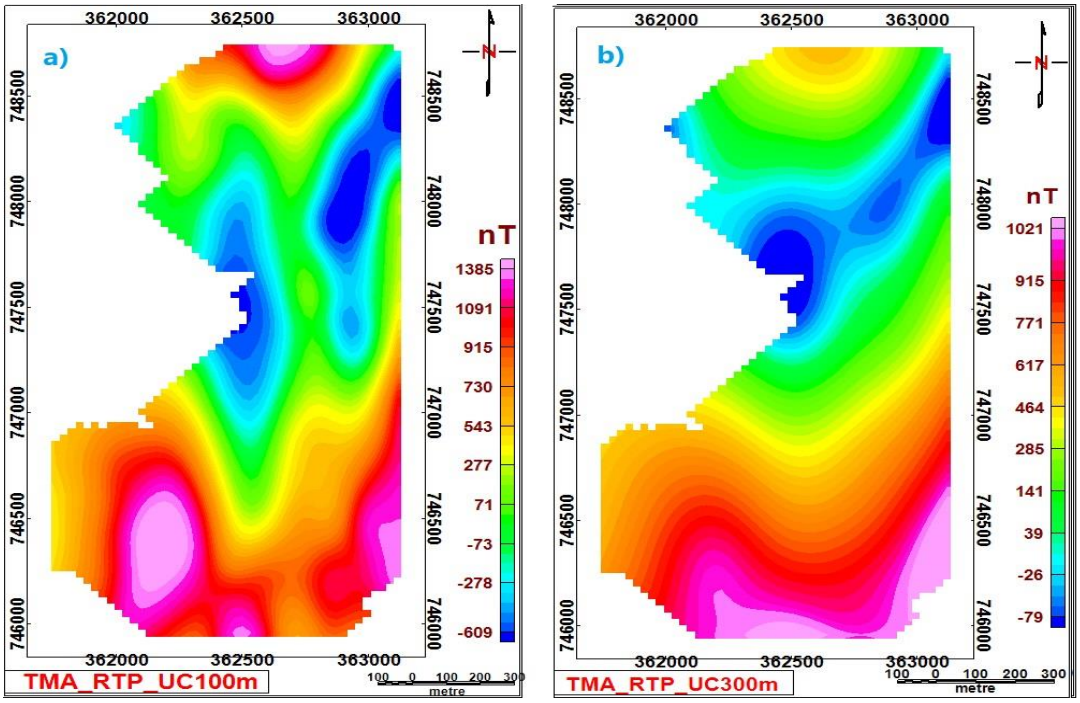

Figure 5.18: UC map of the Study Area; with 100m (a) and with 300m (b)

5.5.4.3 Tilt Derivative (TDR)

Edge detection of a magnetic structure is one of the most important tasks in the interpretation of magnetic data. Accordingly, two-phase filters; namely Tilt Derivative (TDR) and Horizontal Derivative of Tilt Derivative (HD_TDR) or Total Gradient of Tilt angle; are used for this task. The tilt angle depends on the inclination of the magnetic field and the peaks of its amplitude placed over the center of the source and its zeros over the edges. Since the tilt angle filter relatively less sensitive to the depth of the source, so it can resolve shallow and deep sources as well (Figure 5.19).

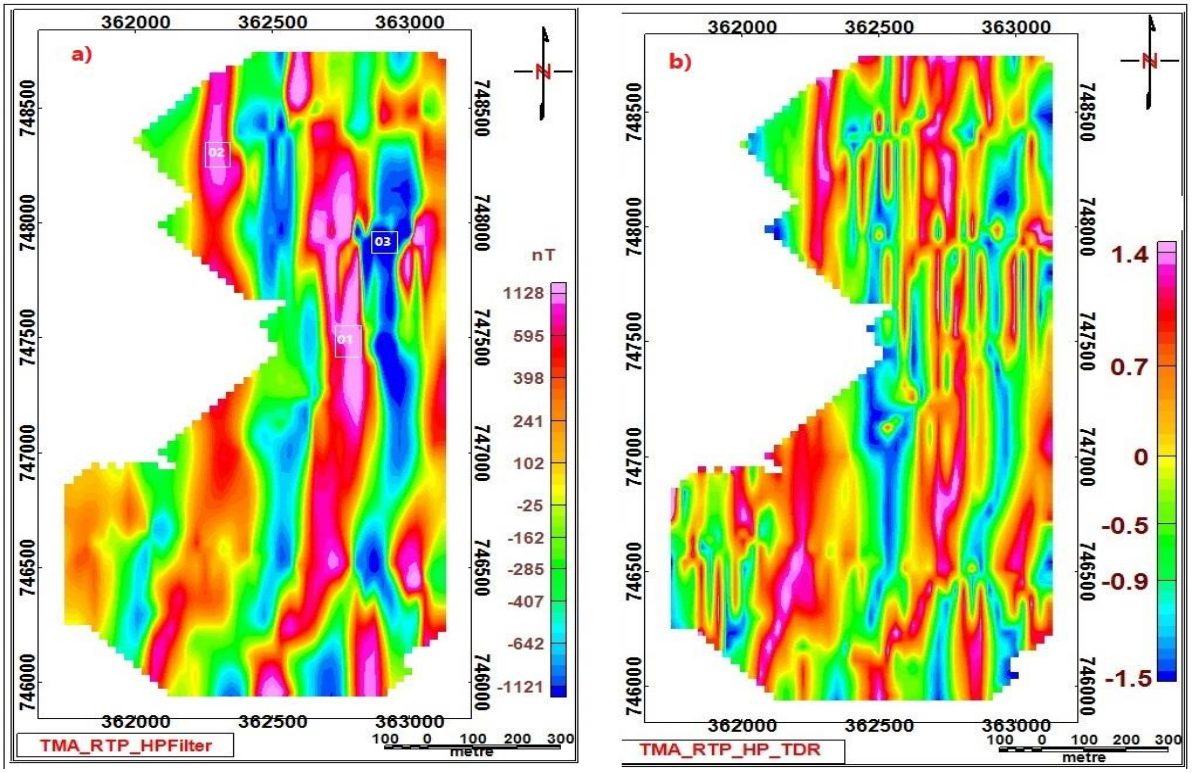

Figure 5.19: Tilt Derivative (TDR) map (b) produced from Residual data (a)

Another enhancement method is Horizontal Derivative of Tilt Derivative (HD_TDR). It is defined by taking the arctangent of the vertical derivative of the horizontal gradient, divided by the modulus of the horizontal gradient (Figure 5.20). The tilt angle of the horizontal gradient (TAHG) equalizes the signals obtained from shallow and deep sources. Its notable features are that it produces amplitude maxima over the source's edges, gives suitable resolution, and is less dependent on the depth of structures. Like the TDR, this method depends on the inclination of magnetic field (Stewart and David, 2018).

Applying this method in the residual magnetic data it revealed different structures/contacts oriented generally in the N-S direction.

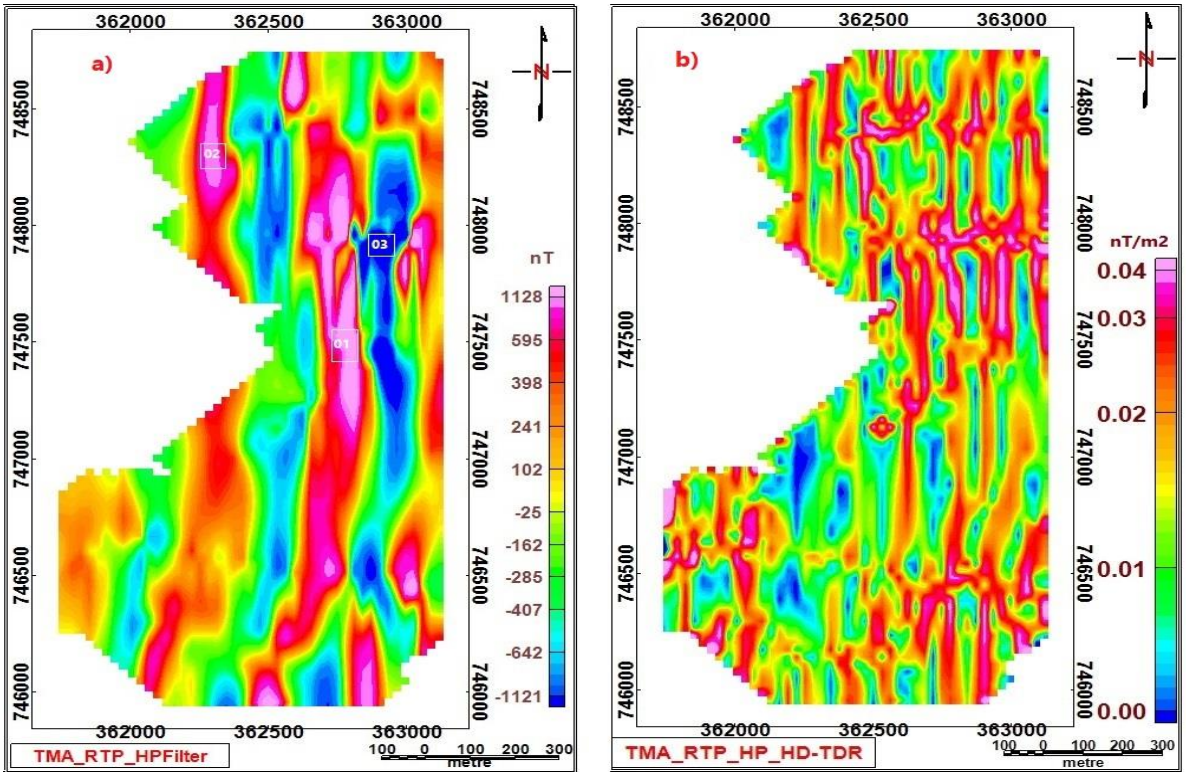

Figure 5.20: Horizontal Derivative (HD_TDR) map (b) produced from Residual data (a)

5.5.4.4 Euler-depth Deconvolution

To determine the location and estimate the depth of causative anomalous bodies for various magnetic sources in the study area, Euler deconvolution technique was employed on the residual data of the study area using the Oasis Montaj Software. Euler-depth calculated the horizontal and vertical gradients of the field and pole-reduced fields. The Euler method's homogeneity equation relates the magnetic field and its gradient components to the location of the source. The degree of homogeneity is expressed as a structural index (SI). The SI is a measure of the fall-off rate of the field with distance from the source and provides a way to discriminate between different source shapes. Different geological features are represented by varying SI values; i.e the SI=1, 2, and 3 for model geological features represented by contact, vertical pipe/horizontal cylinder, and sphere respectively.

Accordingly, to allow depth investigations for some individual units, solutions have been plotted as circles scaled for the depth magnitudes and subdivided into levels represented by different sizes (Figure 5.21). Most of the depth solutions are less than 1.0 km. This means

that most of the features mapped are shallow. Ranganai and Ebinger (2008) discussed that these shallow structures (particularly 150m) are considered important for regional groundwater exploration, and therefore the technique could be used to assess such structures and features.

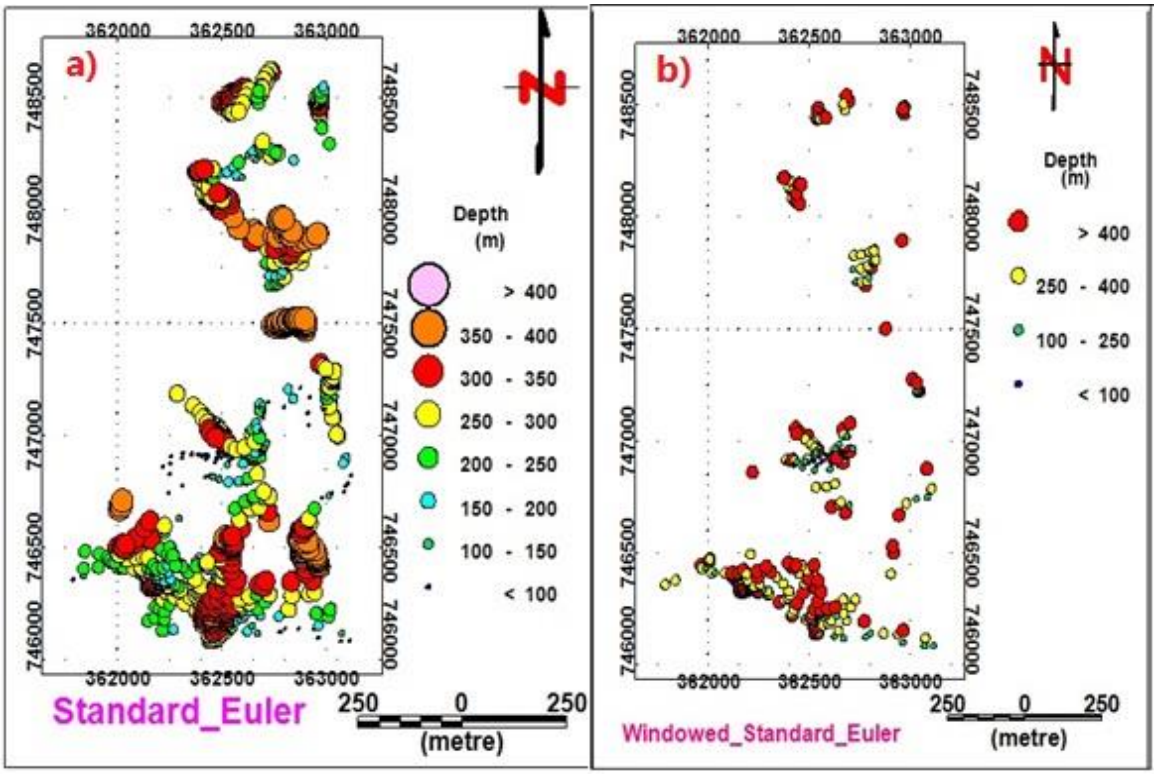

Figure 5.21: Euler deconvolution magnetic map of the study area with SI =1.

Using the various Euler solution maps, the magnetic sources in the southern and central parts of the area generally appear shallower than in the northern parts. The Euler solution maps presented (Figures 5.21) indicate several one-dimensional linear structures (fracture/fault), with a direct coincidence of clustering solutions with known regional features such as the MER.

5.5.5 2D Magnetic Modeling

For the magnetic 2D forward modeling the point data were imported to the modeling software, GM-SYS. The 2D magnetic forward models are not meant to constitute exact and very accurately detailed rock models, but the aim is to support the deformation zone modeling with indications mainly regarding the dip and width of low magnetic zones. It is very essential to estimate the physical properties of the subsurface geological units. Any difference between the model response and the observed magnetic field is reduced by refinement of the model structure.

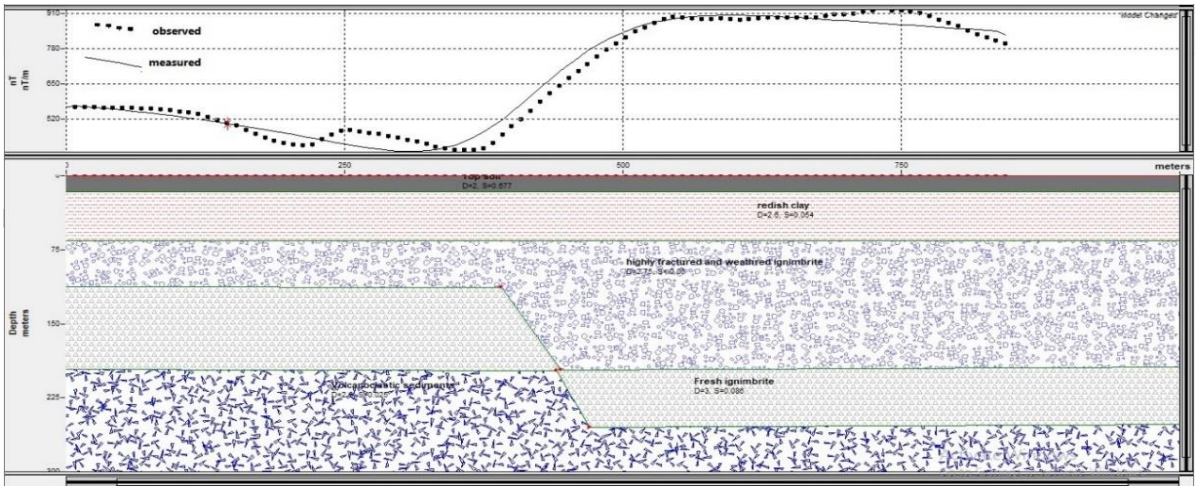

Figure 5.22: 2D Modeling of Magnetic data along Line-3.

As shown in Figure 5.22 the model reflects the existence of a weak zone (fracture/fault) at 325m horizontal profile distance and below a depth of 70m that extends to 250m depth for line-3, whereas for line-4 (Figure 5.23) the weak zone found at a horizontal profile distance of 62m (below a depth of 20m that extends to 130m), and 374m (below a depth of 70m that extends to 170m depth). The Lithologic units that are described for magnetic 2D model of line-3 (Figure 5.22) include top soil, reddish clay, fresh ignimbrite, and volcanoclastic sediments, and the units of line-4 (Figure 5.23) include topsoil, tuff, highly fractured and weathered ignimbrite, slightly fractured ignimbrite. The Geoelectric section along with these profiles as shown in section 5.3.3 and section 5.3.4 and figures there reflects the same lithologic units and geological structures except for slight variation in thickness.

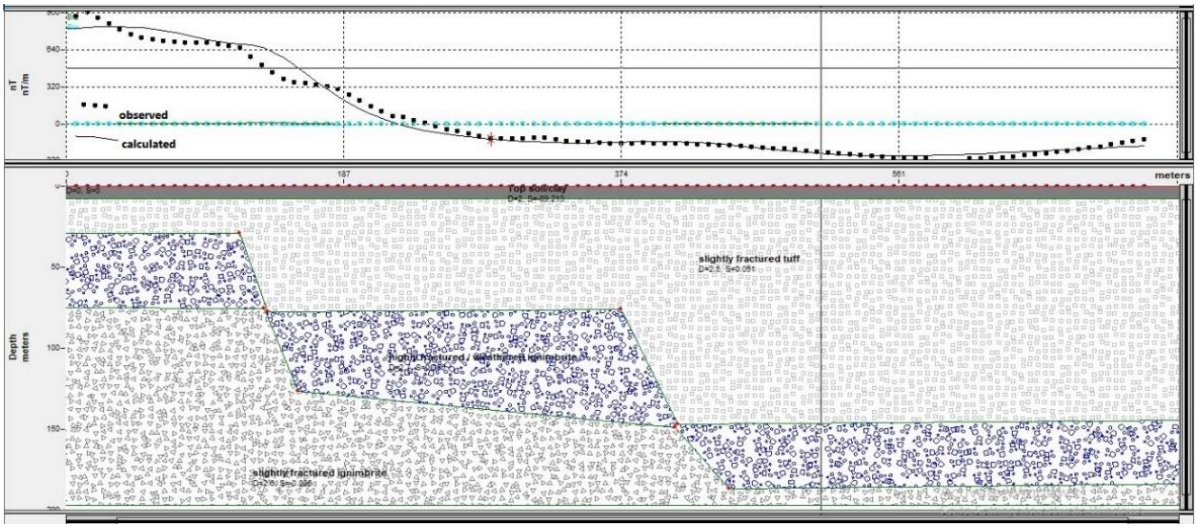

Figure 5.23: 2D Modeling of Magnetic data along Line-4.

CHAPTER SIX

6. CONCLUSIONS AND RECOMMENDATIONS

6.1 CONCLUSION

This study demonstrates the value of integrated geophysical techniques in groundwater investigations of the fractured and weathered aquifer.

The investigations were done in the "Larena plain" by collecting the VES and Magnetic Survey data. Fourteen VES-point measurements were conducted through five traverse lines with a maximum half electrode distance (AB/2) of 500m and a total of 245 magnetic data reading points with a separation distance of 30m between the points were also collected following the VES-profile lines and at random stations. Various ways for presentations of resistivity data were followed, such as VES-interpretation curves, pseudo-depth sections, and Geoelectric sections. After correction of the raw magnetic data, different magnetic maps; such as TMI-Map, Regional and Residual map, AS-map, TDR-Map, UC, and Euler-deconvolution map; were constructed to present the data.

Low resistivity horizons at various depths revealed the existence of aquifer beds based on the apparent resistivity pseudo-depth section, sliced-stacked map, and geoelectric sections, and their physical suitability. According to the investigation outputs, there are two-stage aquifers in the study area, the deeper fractured ignimbrite and volcanoclastic-sediment aquifer covered by the shallow weathered ignimbrite aquifer. Slightly-to-highly weathered ignimbrite, and volcanoclastic sediments are identified as the major subsurface geological units that are considered as the main water-bearing horizons, especially under VES-102, VES-201, VES-202, and VES-302, with a thickness ranging from 20m up to 94m. As can be seen from the Sliced-Stacked Section map for different AB/2, highly conductive (saturated) zones are present in the central part of the study area.

The geological structures that play a great role in the accumulation and flow of groundwater were revealed from the geoelectrical section and 2D-magnetic maps. These structures are more concentrated in the central and southern parts of the study area. The exactness of geophysical results is assured by comparing them with the apriori information from the borehole log data in and around the study area.

6.2 RECOMMENDATIONS

The results from this study were used to identify the major subsurface geological units and map possible water-saturated horizons, infer areas of maximum groundwater reservoir potential site to drill a borehole for a sufficient and sustainable yield of groundwater, and determine the depth of the groundwater table and to locate potential drilling sites for the extraction of groundwater This study can therefore be used to develop a much broader understanding of the nature of groundwater potential in the area and their relationship with the local geology. Hence, it is hoped that findings from this work will offer reliable background information for the future development of groundwater resources and their management in 'Humbo-Larena' Plain. Accordingly, the following recommendation points are forwarded:

- Four well-drilling sites; VES-102, VES-201, VES-202, and VES-302; are recommended in the study area with their UTM coordinate of (362398m E, 746419m N), (362295m E, 746877m N), (362577m E, 747170mN), and (362687m E, 747964m N) respectively.
- Additional geophysical surveys are highly recommended in the western, northern, and southern directions of the existing traverse lines for detailed investigation for the extension of low resistivity zones.
- For further study and mapping of the orientation of faults, fractures, and weak zones as well as their natures, detailed structural geological investigations are recommended.
- Further regional hydrological and hydrogeological investigations are highly recommended to understand the basin and the water balance of the basin.
- Environmental and Social Impact Assessment (ESIA) is highly recommended before the commencement of any groundwater-related projects in the area especially irrigation projects.

References

- **Abbate E., Bruni P., and Sagri M. (2015).** Geology of Ethiopia: A Review and Geomorphological Perspectives. In: Billi P. (eds) Landscapes and Landforms of Ethiopia. World Geomorphological Landscapes. Springer, Dordrecht. https://doi.org/10.1007/978-94-017-8026-1_2 **15;** 11-29

- **Abriham Asha (2006).** Integrated Hydrogeological Investigation in Hamessa catchment in wolaita zone, unpublished MSc. Thesis. 36-47

- **Ahmad, S.H (2017)**. Assessment of Groundwater Potentiality Using Geophysical Techniques in Wadi Allaqi Basin, Eastern Desert- Egypt–Case study: ELSEVIER/NRIAG Journal of Astronomy and Geophysics. **6;** 408-421

- **Adugna Eneyew and Wagayehu Bekele (2011).** Cause of Household Food Insecurity in Wolaita, Southern Ethiopia. MSc. Thesis Report. Journal of Stored Products and Postharvest Research **3(3)**; 8-11.

- **Almaz Balta, Ayele Tessema and Debebe H/Wold (2015).** Assessment of Household Food Security and Coping Strategies in Wolaita Zone: The Case of Sodo Zuria Woreda. Journal of Poverty, Investment and Development ISSN 2422-846X An International Peer-reviewed Journal www.iiste.org, **18**;11-16.

- **Ayele Almaw, Addis Kifle, Tesfamichael Gebreyohannes and Gebrerufael Hailu (2014).** Spatial Analysis of Groundwater Potential Using Remote Sensing and GIS-based Multi-criteria Evaluation in Raya Valley, Ethiopia, Hydrogeology Journal **23**; 6-11.

- **Bagnara, G. (2017).** Agricultural Production and Market of Wolaita Rural Area. CEFA, Bologna.**118**; 42-57.

- **Bernard, J. (2003).** Short Notes on Depth Investigation of Electrical Methods-In Relation with Groundwater Investigations. Unpublished technical note URL http://www.iris-instruments.com. pp8; 1-4

- **Bernard, J., Vachette, C. and Valla, P. (2003).** Deep groundwater survey with audio magneto-telluric soundings: Annual Meeting Abstracts, Society of Exploration *Geophysics*, **52**; 31-85.

- **Bogale Gebeyehu, Guta R. and Mesfin Tebeje (2014).** Rural households food security and livelihood strategies: the case of Offa Woreda, in Wolaita Sodo Zuria, Southern Nations, Nationalities and Peoples Regional State, Ethiopia. IJRESS. **4(7)**; 91-104.

- **Bonini, M., Corti, G., Innocenti, F., Manetti, P., Mazzarini, F., Tsegaye Abebe and Pecskay, Z. (2005).** Evolution of the Main Ethiopian Rift in the frame of Afar and Kenya Rifts Propagation. Tectonics, TC1007, doi:10.1029/2004TC001680. **24**; 2-7.

- **CSA-Central Statistical Agency (2012).** Statistical Report on The 2012 Urban Unemployment Survey. Unpublished technical report. Central Statistical Agency, Addis Ababa, Ethiopia. URL: -http://adapt.it/adapt-indice-a-z/wp-content/uploads/2015/01/survey-unemployment.pdf pp243; 39-69

- **Daniel Gamachu (1977).** Aspects of Climate and Water Budget in Ethiopia. Addis Ababa University Press. Addis Ababa. pp71; 12-27

- **Fathy, A. (**2012**).** Mapping of Groundwater Prospective Zones Using Remote sensing and GIS techniques: A case study from the Central Eastern Desert, Egypt. Academic Publishing and Press, King Saud University, Riyadh, Saudi Arabia, **8**; 4-9.

- **Fetter, C.W (2001).** Applied Hydrogeology; Fourth Edition. Prentice Hall, Inc. Upper Saddle River, New Jersey, ISBN-013-088239-9, pp615; 112-186

- **Francis and Taylor (2008).** Groundwater for Sustainable Development: Problems, Perspectives and Challenges. Library of Congress Cataloging-in-Publication Datawww.taylorandfrancis.co.uk/engineering, www.crcpress.com pp485; 93-121

- **Frohlich, R.K., Fisher, J.J. and Summerly, E. (1996).** Electric-hydraulic conductivity correlation in fractured crystalline bedrock: Central Landfill, Rhode Island, USA. J Appl. Geophy 1996; **35**;249-59.

- **Griffiths, D.H. and King, R.F. (1981).** Applied Geophysics for Geologists and Engineers. The Elements of Geophysical Prospecting-Second Edition. Pergamon Press. Oxford-New York-Beijing-Frankfurt. pp236;106-143

- **GSE-Geological Survey of Ethiopia (1996).** The 1:2 000 000 Scale Geological Map of Ethiopia. GSE. Addis Ababa Ethiopia.

- **Habtamu Eshetu and Rapprich, V. (2014).** Geological Hazards and Engineering Geology Maps of Dila, Explanatory Note. Czech Geological Survey Czech Republic First edition. pp140. 51-69

- **Haleh N., Biswajeet P. and Mohammad A. (**2014). Application of GIS Based Data Driven Evidential Belief Function Model to Predict Groundwater Potential Ponation. Elsevier B.V. Journal of Hydrology.**11**; 3-9.

- **Haile Arefayne and Semir Abdi (2016).** Groundwater Exploration for Water Well Site Locations Using Geophysical Survey Methods. Hydrology Current Research doi:10.4172/2157-7587.1000226. **7**; 226-234.

- **HDR-Human Development-Index Report (2019).** Inequalities in Human Development in the 21st Century Briefing Note for countries on the 2019 Human Development Report-the case of Ethiopia. Unpublished technical report. pp10; 4-9

- **Hyndman R.D. and Shearer P.M. (1998).** water in the Lower Continental Crust: Modelling MT and Seismic-Reflection Results: Geophysics Journal Int. **98**; 343-365.

- **IMF-International Monetry Fund (2020)**. World Economic Outlook Database, April 2020.URL: https://www.imf.org/en/Publications/WEO/weo-database/2020/October

- **Jackson, P.N., Taylor, S.D. and Stanford, P.N. (1978)**. Resistivity, porosity and particle shape relationships for marine sands, Geophysics, **43**;1250-1268.

- **Kearey, P. and Brooks, M. (1991).** An Introduction to Geophysical Exploration (second ed.), Blackwell Scientific, Oxford Publishing House. pp712; 115-142.

- **Kearey, P., Brooks, M., and Hill, I. (2002).** An Introduction to Geophysical Exploration-Third Edition. Blackwell Science Ltd, USA. pp281; 183-208.

- **Keating, P. and Sailhac, P. (2004).** Use of the Analytic Signal to Identify Magnetic Anomalies Due to Kimberlite Pipes. Society of Exploration Geophysicists. **69**(1);180–190.

- **Kirsch, R. (2006).** Groundwater Geophysics-A Tool for Hydrogeology, Second Edition. Springer-Verlag Berlin Heidelberg-Library of Congress: 2008936482, pp556; 85-116

- **Li, Y. and Oldenburg, D. (1998).** Separation of Regional and Residual Magnetic Field Data. Society of Exploration Geophysicists **63**(2); 431-439.

- **Loke, M.H. (2001).** Electrical Imaging Survey for Environmental and Engineering Studies: A practical guide to 2D and 3D surveys in Germany using near surface geophysics, Journal of Applied Geophysics, **84**; 77–85.

- **Mattsson, H (2011).** 2D and 3D Modelling of Magnetic and Resistivity Data from Äspö. Swedish Nuclear Fuel and Waste Management Co. GeoVista AB. Technical Report. 5-17

- **Mepaiyeda, S. Madi, K. Gwavava, O. Baiyegunhi, C. and Sigabi, L. (2019).** Contaminant Delineation of a Landfill Site Using ER and IP Methods in Alice Eastern Cape, South Africa.: Hindawi International Journal of Geophysic.**19**; 5-8.

- **Metwaly, G., El-Qady, U., Massoud, A., El-Kenawy, J., Matsushima, N. and Al-Arifi (2009).** Integrated geoelectrical survey for groundwater and shallow subsurface evaluation: El-Fayoum, Egypt Int. J. Earth Sci., **99**; 1427-1436.

- **Milsom, J. (2003).** Field Geophysics-The Geological Field Guide Series, Third Edition. The Atrium, Southern Gate, W.Sussex, England: John Wiley & Sons Ltd. pp249; 97-113

- **MoANRM-Ministry of Agriculture and Natural Resource Managnent (2011)**. Small-Scale Irrigation Situation Analysis and Capacity Need Assessment. MoANRM-Ethiopia. Unpublished Technical Report. URL:https://nrmdblog.wordpress.com/2017/02/22/small-scale-irrigation-situation-analysis-and-capacity-needs-assessment/

- **Mohamed S. E. Juanah and Sharharin Ibrahim (2013).** Groundwater Resources Assessment Using Integrated Geophysical Techniques in the Southwestern region of Peninsular Malaysia, Arabian Journal of Geosciences. **7**;4-9.

- **Mohr, P. and Zanettin, B. (1988).** The Ethiopian Flood Basalt Province. In: Macdougall J.D. (eds) Continental Flood Basalts. Petrology and Structural Geology,Springer, Dordrecht. https://doi.org/10.1007/978-94-015-7805-9_3. **(3);** 63-110

- **Oha, H.J., Jong, S.K., Eungy, K.C and Lee, P.S. (2011).** GIS mapping of regional probabilistic groundwater potential in the area of Pohang City, Korea. Journal of Hydrology. **399**;158-172.

- **Ranganai, R. and Ebinger, C. J. (2008).** Aeromagnetic and Landsat TM structural interpretation for identifying regional groundwater exploration targets, south-central Zimbabwe. Journal of Applied Geophysics. **65;** 3-12

- **Reynolds, J. (1997).** An Introduction to Applied and Environmental Geophysics – Second Edition. The Atrium, Southern Gate, West Sussex: Wiley-Blackwell. pp712; 289-346

- **Samuel Tessema, Admasu Adamu and Zenebe Yirgu (2017).** Climate Variability Impacts on the Small-Scale Farmers and Their Adaptations in Humbo and Duguna Fango Woredas of Wolaita Zone-Ethiopia. Journal of Environment and Earth Science ISSN 2224-3216. ISSN 2225-0948. **7**; 4-9.

- **Sandberga, S.K., Slaterb, L.D. and Versteegc, R. (2002).** An Integrated Geophysical Investigation of the Hydrogeology of Anisotropic Unconfined Aquifer: ELSEVIER, Journal of Hydrology pp267; 227–243.

- **Shahverdi, M. and Namaki, L. (2017).** Interpretation of magnetic data based on Tilt derivative methods and enhancement of total horizontal gradient, a case study: Zanjan Depression. Journal of the Earth and Space Physics **43**(1); 101-113.

- **Sharma, P. (1997).** Environmental and Engineering Geophysics. Cambridge University Press-UK. pp500; 123-145

- **Sikakwe, G.U. (2018)**. GIS-based model of groundwater occurrence using geological and hydrogeological data in Precambrian Oban Massif southeastern Nigeria. Springer; Applied Water Science. **8**; 4-12.

- **Stewart, C.F. and David T.M (2018).** Directional tilt derivatives to enhance structural trends in aeromagnetic grids. Journal of Applied Geophysics. **159**; 553–563.

- **Suleyman, Y.V. (2017).** Groundwater Potential Assessment Using Geographic Information System (GIS) Methods in the Province of Batman, Turkey. Batman University. International Journal of Scientific and Technological. **17;** 5-11

- **Svizzero Serge (2016).** Global Journal of Human Social Science: History, Archaeology & Anthropology, Double-Blind Peer Reviewed International Research Journal. USA: Global Journals Inc.**16**; 4-12

- **Tadewos Chernet (2011).** Geology and Hydrothermal Resources in the Northern Lake Abaya area-Ethiopia. Journal of African Earth Sciences **61**(2);129-141.

- **Taylor and Francis Group (2008).** Groundwater for Sustainable Development: Problems, Perspectives, and Challenges. Taylor & Francis Group, London, pp485; 246-321

- **Telford, W.M., Geldart, L.P. and Sheriff, R.E. (1990).** Applied Geophysics. Second Edition, Cambridge University Press, Cambridge.pp760**;** 283-335

- **Tenalem Ayenew, Molla Demlie, Stefan Wohnlich (2008).** Application of Numerical Modeling for Groundwater Flow System Analysis in the Akaki Catchment, Central Ethiopia. *Math Geosci* https://doi.org/10.1007/s11004-008-9144-x **40;** 887–906.

- **Tesfaye, S., Harding, D.J., Kusky, T.M. (2003).** Early Continental Breakup Boundary and Migration of the Afar Triple Junction, Ethiopia Geological Society of America Bulletin **115/9**; 1053–1067.

- **Tibebe Mengistu (2006).** Integrated Geophysical Investigation for the Evaluation of Groundwater Resources at the Ada'a Plain-Near Debre Zeit: unpublished MSc. Thesis; Addis Ababa University-Ethiopia.

- **UN-United Nations (2020).** United Nations Economic Commission for Africa, The Sustainable Development Goals in Ethiopia. URL: https://ethiopia.un.org/en/sdgs. Accessed Nov 17, 2020.

- **UNESCO-United Nations Education, Social and Cultural Organization (1998).** UNESCO Handbook for groundwater investigations. Technical Report, ITC.

- **WeldeGabriel Giday, Aronson, J.L. and Walter, R.C. (1990).** Geology, Geochronology and Rift Basin Development in the Central Sector of the Main Ethiopian Rift, Geological Society of America, bulletin ; **102;** 439-458.

- **World-Bank (2020).** United Nations Population Division, World Population Prospects: 2019 Revision URL: https://data.worldbank.org/indicator/SP.POP.TOTL?locations=ET. Accessed Nov 19, 2020.

- **WFP-World Food Program (2014).** Achievements and history, corporate strategy, Funding and donors, Nutrition, Social Protection and Safety Nets. Annual Report. URL https://www.wfp.org/publications/wfp-2014. Accessed Nov 11, 2020.

- **WFP-World Food Program (2019).** Analyses assessments and case studies, Reports. Annual Performance Report. URL https://www.wfp.org/publications/annual-performance-report-2019. Accessed Nov 11, 2020.
- **World-meter (2020).** Elaboration of the Latest United Nations data. URL https://www.worldometers.info/world-population/ethiopia-population/.
- **Yadav, G.S. and Abolfazli, H. (1998).** Geoelectric soundings and their relationship to hydraulic parameters in semiarid regions of Jalore, northwestern India, J. Applied Geophysics. **39**:35-51.
- **Zanettin, B., Nicoleti, M. and Petruciani, C. (1978).** The Evolution of the Chencha Escarpment and the Ganjuli Graben (Lake Abaya) in the Southern Ethiopian Rift. Neues Jahrbuch fur Geologie and Palaontologie. **8;** 473-490
- **Zohdy A., Eaton, G. and Mabey, D. (1990).** Application of Surface Geophysics to Groundwater Investigations-In Techniques of Water Resource Investigations of the United States Geophysical Survey. USGS publications. pp116.

Appendices

Annex-1: interpreted 1-D models of VES data curves of each sounding point.

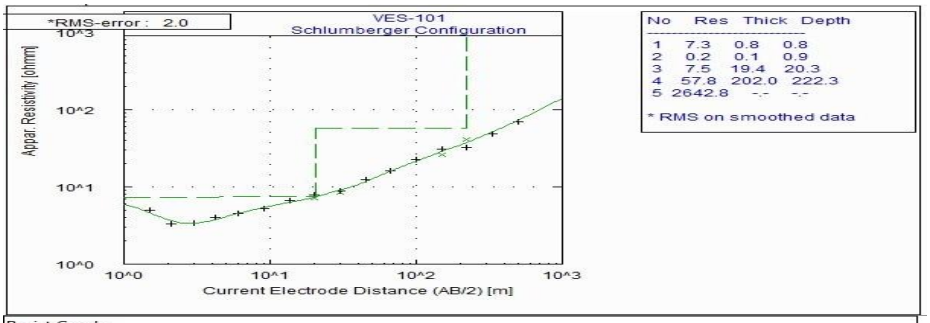

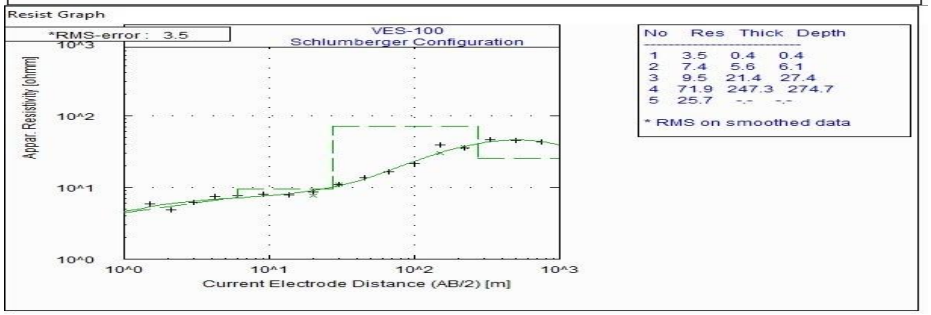

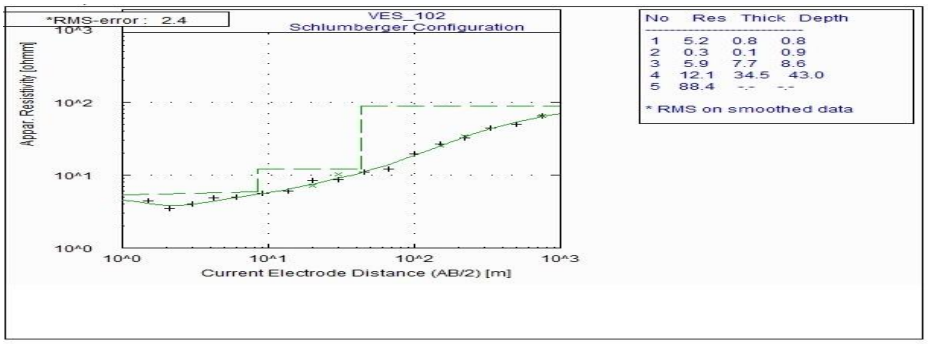

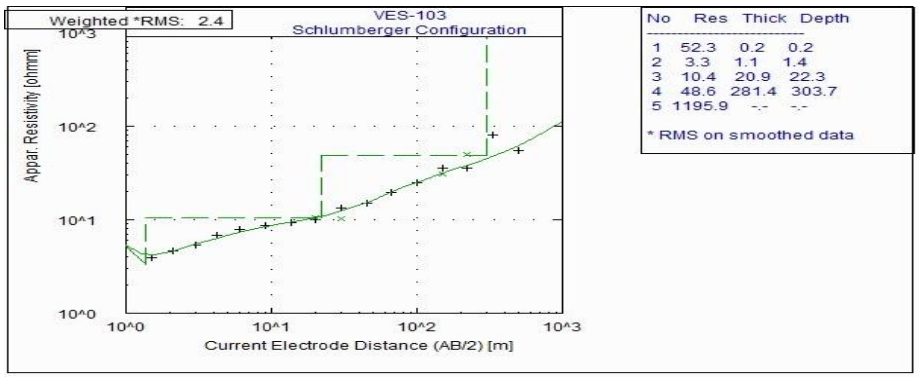

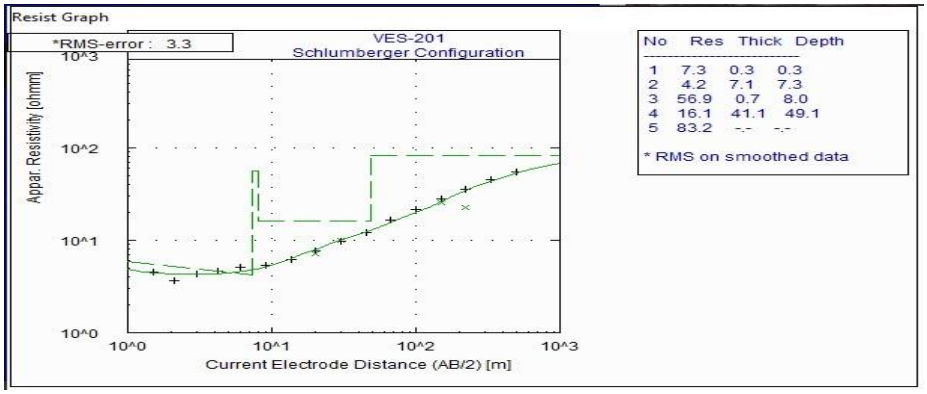
Resist Graph
*RMS-error : 3.3
VES-201
Schlumberger Configuration
Appar. Resistivity [ohmm]
10^3
10^2
10^1
10^0
10^0
10^1
10^2
10^3
Current Electrode Distance (AB/2) [m]
No Res Thick Depth
1 7.3 0.3 0.3
2 4.2 7.1 7.3
3 56.9 0.7 8.0
4 16.1 41.1 49.1
5 83.2 -.- -.-
* RMS on smoothed data

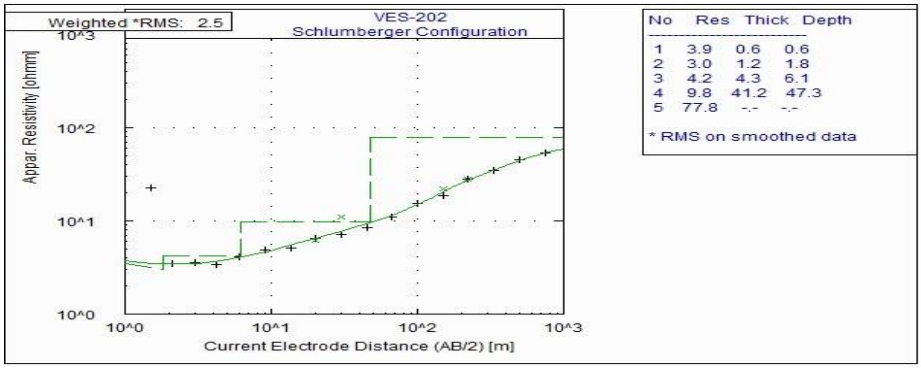
Weighted *RMS: 2.5
VES-202
Schlumberger Configuration
Appar. Resistivity [ohmm]
10^3
10^2
10^1
10^0
10^0
10^1
10^2
10^3
Current Electrode Distance (AB/2) [m]
No Res Thick Depth
1 3.9 0.6 0.6
2 3.0 1.2 1.8
3 4.2 4.3 6.1
4 9.8 41.2 47.3
5 77.8 -.- -.-
* RMS on smoothed data

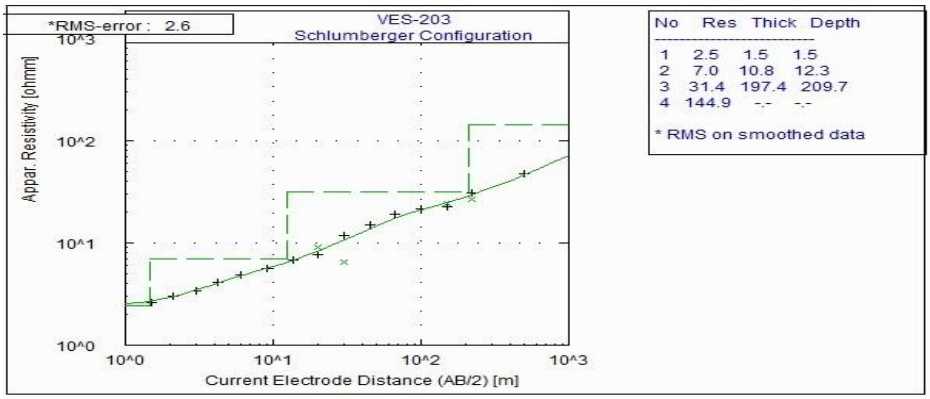
*RMS-error : 2.6
VES-203
Schlumberger Configuration
Appar. Resistivity [ohmm]
10^3
10^2
10^1
10^0
10^0
10^1
10^2
10^3
Current Electrode Distance (AB/2) [m]
No Res Thick Depth
1 2.5 1.5 1.5
2 7.0 10.8 12.3
3 31.4 197.4 209.7
4 144.9 -.- -.-
* RMS on smoothed data

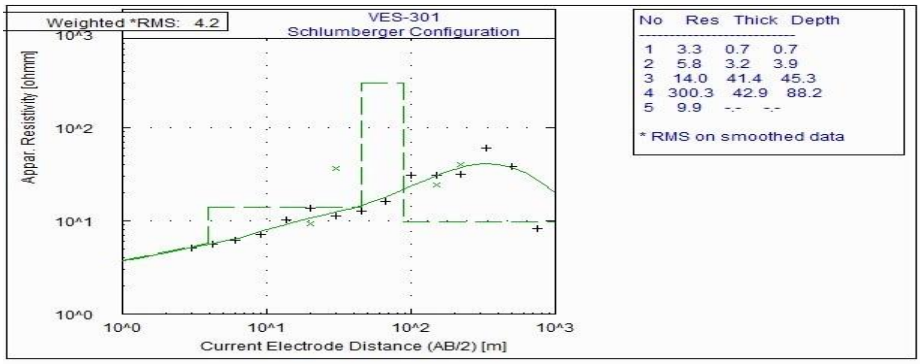
Weighted *RMS: 4.2
VES-301
Schlumberger Configuration
Appar. Resistivity [ohmm]
10^3
10^2
10^1
10^0
10^0
10^1
10^2
10^3
Current Electrode Distance (AB/2) [m]
No Res Thick Depth
1 3.3 0.7 0.7
2 5.8 3.2 3.9
3 14.0 41.4 45.3
4 300.3 42.9 88.2
5 9.9 -.- -.-
* RMS on smoothed data

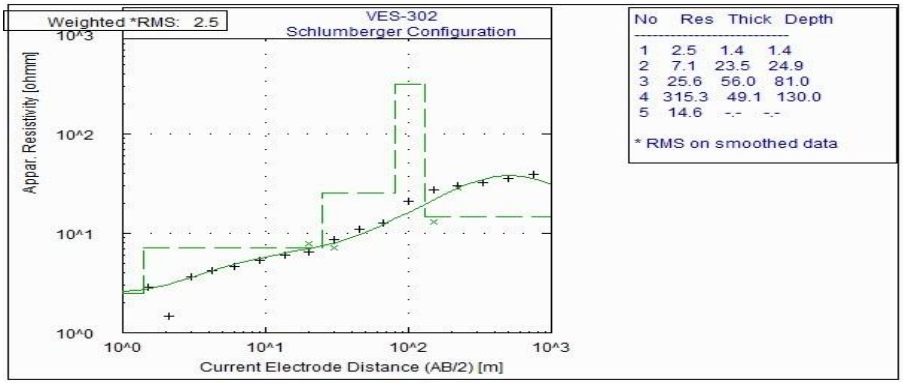
Weighted *RMS: 2.5
VES-302
Schlumberger Configuration
Appar. Resistivity [ohmm]
10^3
10^2
10^1
10^0
10^0
10^1
10^2
10^3
Current Electrode Distance (AB/2) [m]
No Res Thick Depth
1 2.5 1.4 1.4
2 7.1 23.5 24.9
3 25.6 56.0 81.0
4 315.3 49.1 130.0
5 14.6 -.- -.-
* RMS on smoothed data

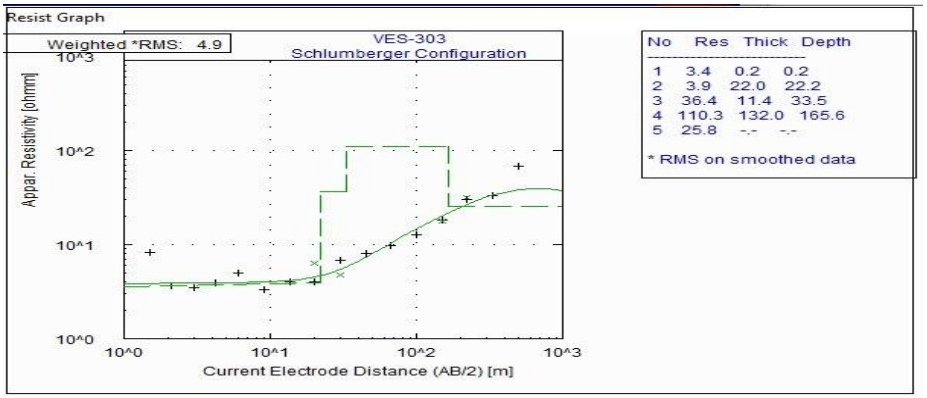
Resist Graph
Weighted *RMS: 4.9
VES-303
Schlumberger Configuration
Appar. Resistivity [ohmm]
10^3
10^2
10^1
10^0
10^0
10^1
10^2
10^3
Current Electrode Distance (AB/2) [m]
No Res Thick Depth
1 3.4 0.2 0.2
2 3.9 22.0 22.2
3 36.4 11.4 33.5
4 110.3 132.0 165.6
5 25.8 -.- -.-
* RMS on smoothed data

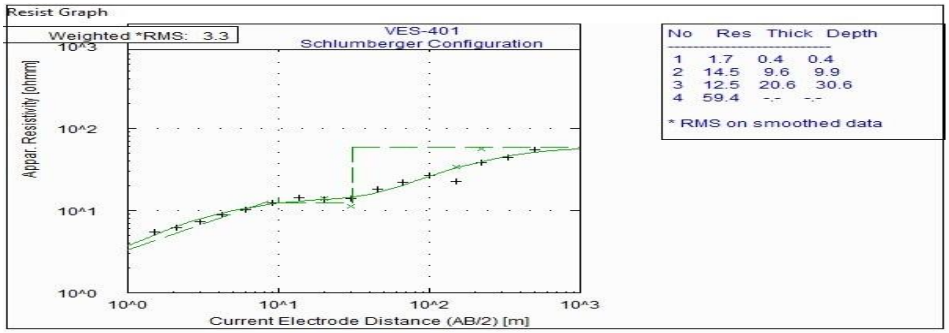
Resist Graph
Weighted *RMS: 3.3
VES-401
Schlumberger Configuration
Appar. Resistivity [ohmm]
10^3
10^2
10^1
10^0
10^0
10^1
10^2
10^3
Current Electrode Distance (AB/2) [m]
No Res Thick Depth
1 1.7 0.4 0.4
2 14.5 9.6 9.9
3 12.5 20.6 30.6
4 59.4 -.- -.-
* RMS on smoothed data

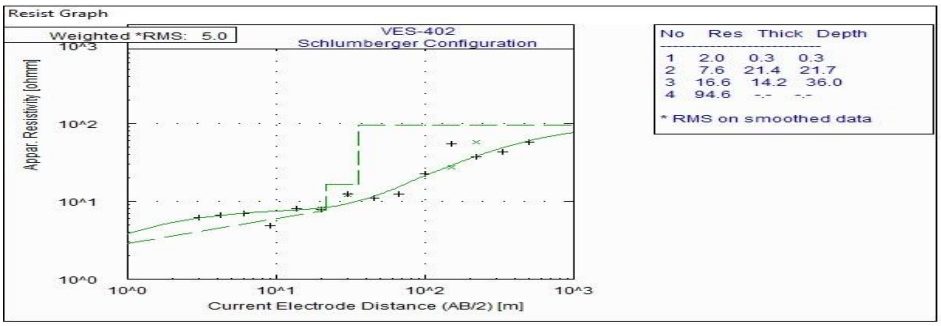
Resist Graph
Weighted *RMS: 5.0
VES-402
Schlumberger Configuration
Appar. Resistivity [ohmm]
10^3
10^2
10^1
10^0
10^0
10^1
10^2
10^3
Current Electrode Distance (AB/2) [m]
No Res Thick Depth
1 2.0 0.3 0.3
2 7.6 21.4 21.7
3 16.6 14.2 36.0
4 94.6 -.- -.-
* RMS on smoothed data

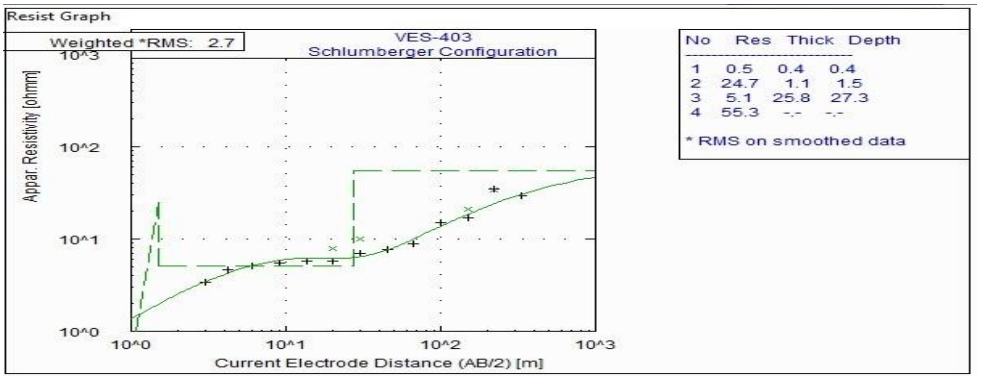

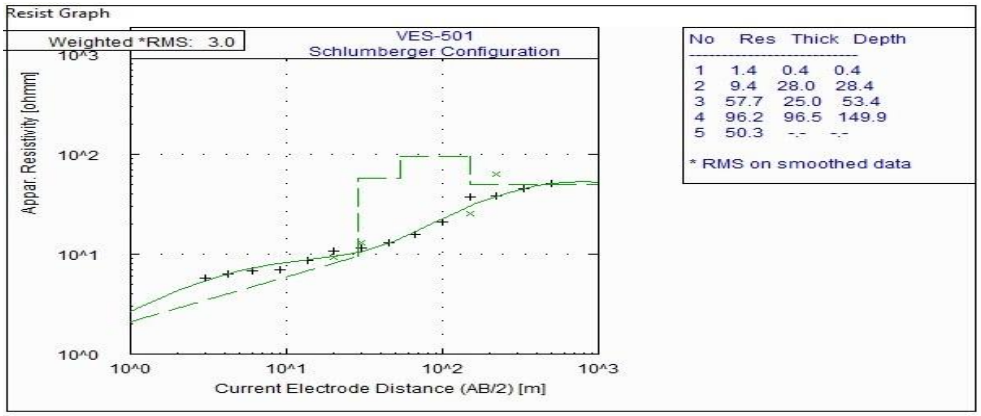

- **Annex-2A: Shochoro-Pesho-BH-1 (**361883-**E** and 744893-N**)**

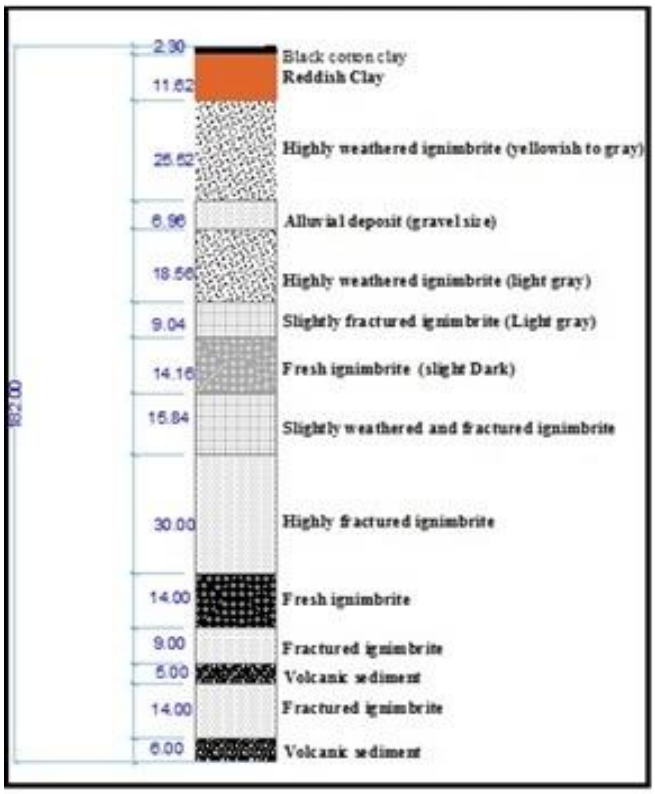

- **Annex-2B: Gututo Larena Borehole_BH-2 (**361922-**E** and 748621-**N)**

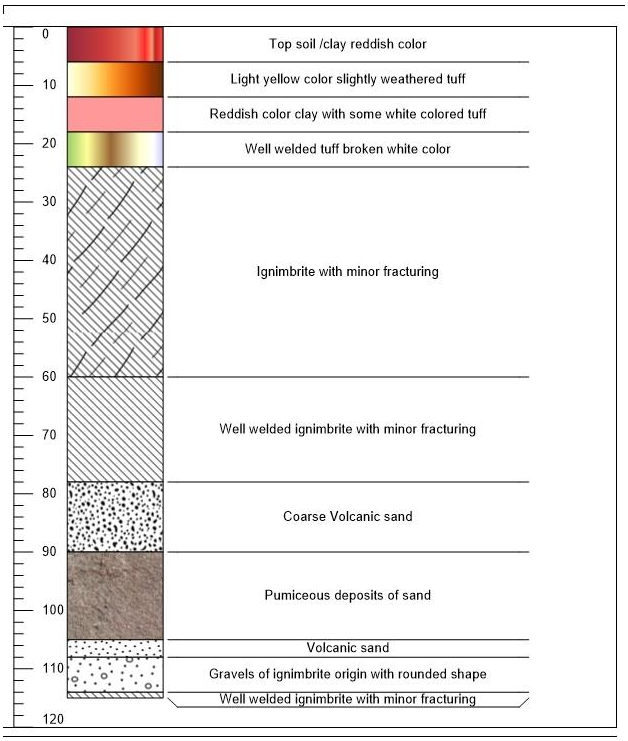

- **Annex-2C: Shochora Ogodama_SWL-37.70 (**363937-**E** and 747313-**N)**

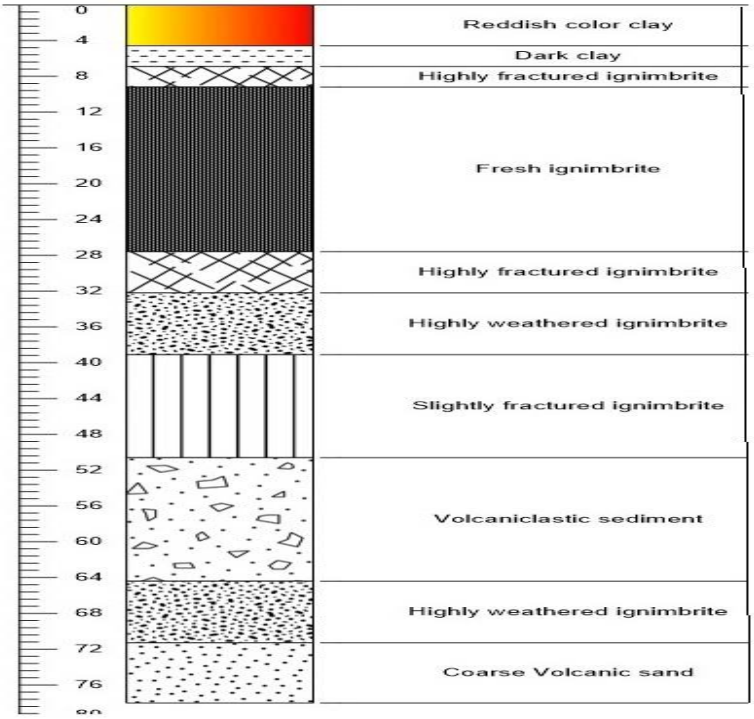

- **Annex-2D: Huletegna-Gututo01_SWL-35.50 (**364226-**E** and 745962-**N)**

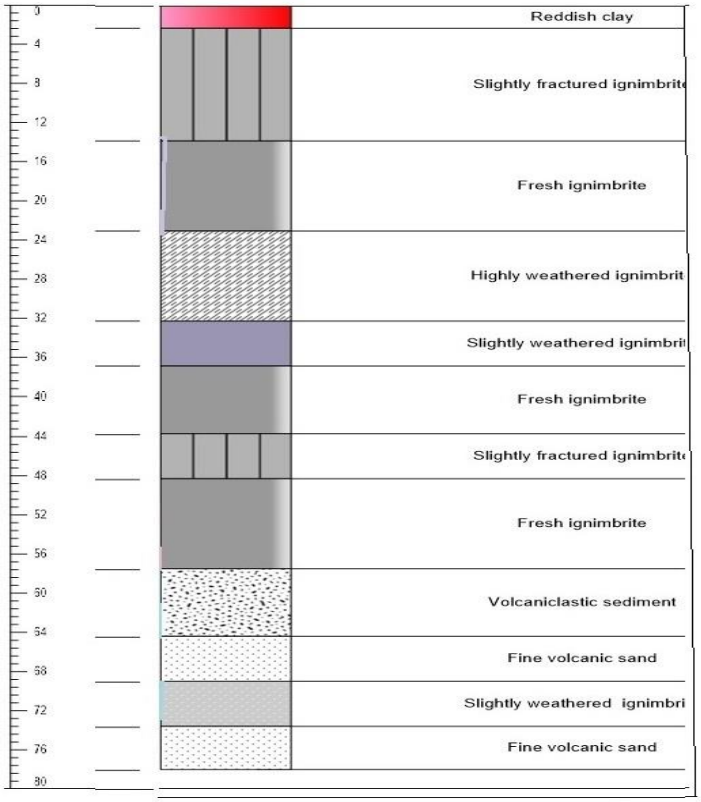

- **Annex-2E: Huletegna-Gututo02_SWL-35.50 (**364155-**E** and 746269-**N)**

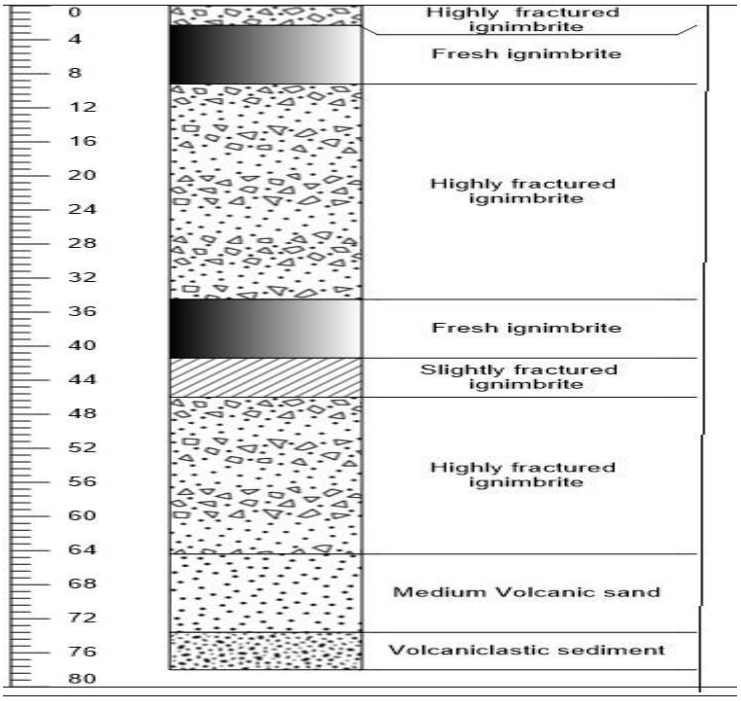

- **Annex-2F: Mino-Koysha_SWL-35.50 (**364114-**E** and 745372-**N)**

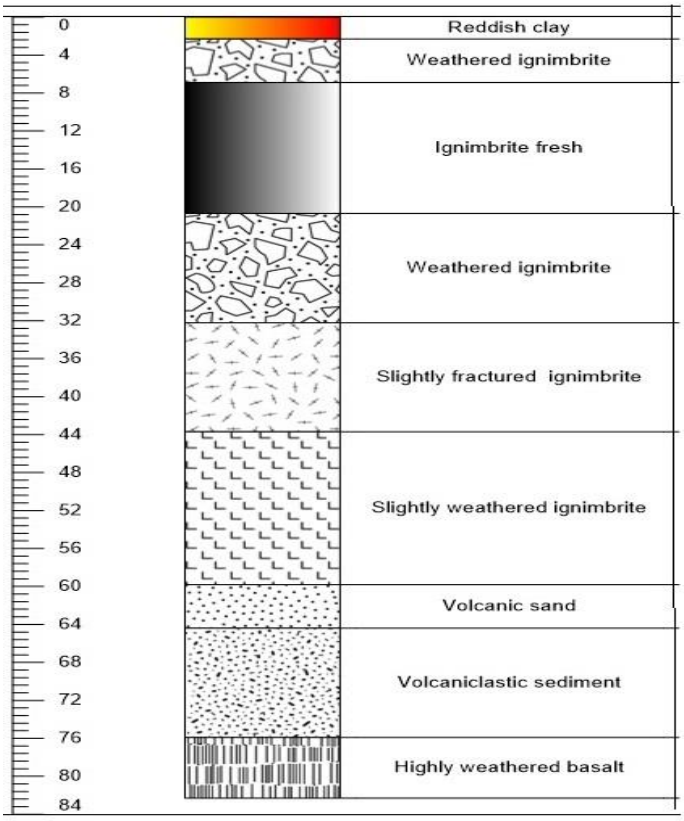

- **Annex-2G: Correlation of the water wells near the study area**